OCS Study
BOEM 2024-057

SCRAM 2: Transparent Modeling of Collision Risk for Three Federally Listed Bird Species in Relation to Offshore Wind Energy Development

U.S. Department of the Interior
Bureau of Ocean Energy Management
Office of Renewable Energy Programs
Sterling, VA

BOEM
BUREAU OF OCEAN ENERGY MANAGEMENT

OCS Study
BOEM 2024-057

SCRAM 2: Transparent Modeling of Collision Risk for Three Federally Listed Bird Species in Relation to Offshore Wind Energy Development

July 2024

Authors:
Holly Goyert, Evan Adams, Andrew Gilbert, Julia Gulka, Pamela Loring, Julia Stepanuk, and Kate Williams

Prepared under BOEM Intra-Agency Agreement No. M19PG00023

by

Biodiversity Research Institute
276 Canco Rd., Portland, Maine 04103

U.S. Fish and Wildlife Service
Division of Migratory Birds
Northeast Region
50 Bend Rd, Charlestown, Rhode Island 02813

U.S. Department of the Interior
Bureau of Ocean Energy Management
Office of Renewable Energy Programs
Sterling, VA

BOEM
BUREAU OF OCEAN ENERGY MANAGEMENT

DISCLAIMER

This study was funded, in part, by the U.S. Department of the Interior, Bureau of Ocean Energy Management (BOEM), Office of Renewable Energy Program, Washington, DC, through Intra-Agency Agreement Number M19PG00023 with the Fish and Wildlife Service (USFWS). This report has been technically reviewed by BOEM, and it has been approved for publication. The views and conclusions contained in this document are those of the authors and should not be interpreted as representing the opinions or policies of BOEM or USFWS, nor does mention of trade names or commercial products constitute endorsement or recommendation for use.

REPORT AVAILABILITY

Download a PDF file of this report at https://espis.boem.gov/Final%20Reports/BOEM_2024-057.pdf.

To search for other Environmental Studies Program ongoing and completed studies, visit https://www.boem.gov/environment/environmental-studies/environmental-studies-information/.

CITATION

Goyert HF, Adams EM, Gilbert A, Gulka J, Loring PH, Stepanuk JEF, Williams, KA (Biodiversity Research Institute, Portland, ME; U.S. Fish and Wildlife Service, Charlestown, RI). 2024. SCRAM 2: transparent modeling of collision risk for three federally listed bird species in relation to offshore wind energy development. Sterling (VA): U.S. Department of the Interior, Bureau of Ocean Energy Management, Sterling, VA. 80 p Obligation No.: M19PG00023. Report No.: BOEM 2024-057. Also available at https://briwildlife.org/SCRAM/.

ABOUT THE COVER

SCRAM logo credit: Iain Stenhouse/BRI.

ACKNOWLEDGMENTS

We would like to thank Wendy Walsh and Anne Hecht of the USFWS for their input on regional population size estimates for inclusion in the models, and David Bigger (BOEM) for his review of the models, user interface, and user manual. We would also like to thank five reviewers from the U.S. Geological Survey for their input on an earlier version of SCRAM. We thank the funders and Principal Investigators of the red knot studies that collected satellite telemetry data used in SCRAM, including Stephanie Feign and Larry Niles (Wildlife Restoration Partnerships), Paul Smith (Environment and Climate Change Canada), Scott Lawton and Matt Overton (Dominion Energy, Coastal Virginia Offshore Wind Project), Candice Cook-Ohryn (Shell, Atlantic Shores Offshore Wind), and Kim Peters and Liz Gowell (Orsted, Ocean Wind). SCRAM builds on significant intellectual and analytical contributions from earlier collision risk models, including models by Band (2012), Masden (2015), McGregor et al. (2018), as well as the current implementation of stochCRM in the stochLAB R package (Caneco et al. 2022).

FOR MORE INFORMATION

SCRAM 2 is available online[1]. For more information on the tool or to provide comments, contact Andrew Gilbert at the Biodiversity Research Institute (mailto:Andrew.Gilbert@briwildlife.org). The R code for SCRAM is provided at the SCRAM GitHub repository[2]. Update requests and bugs can be posted at the SCRAM GitHub repository[3].

The originally published version of SCRAM (v. 1.0.3) is described in this 2022 BOEM report:

Adams EM, Gilbert A, Loring P, Williams, KA (Biodiversity Research Institute, Portland, ME and U.S. Fish and Wildlife Service, Charlestown, RI). 2022. Transparent modeling of collision risk for three federally listed bird species in relation to offshore wind energy development: final report. Sterling (VA): U.S. Department of the Interior, Bureau of Ocean Energy Management. 79 p. Obligation No.: M19PG00023. Report No.: OCS Study BOEM 2022-071.

[1] https://briloon.shinyapps.io/SCRAM2/

[2] https://github.com/Biodiversity-ResearchInstitute/SCRAM2

[3] https://github.com/BiodiversityResearch-Institute/SCRAM2/issues.

Contents

List of Figures

List of Tables

List of Abbreviations and Acronyms

BOEM	Bureau of Ocean Energy Management
BRI	Biodiversity Research Institute
COP	Construction and Operations Plan
CRC	cyclic redundancy check
CRM	Collision Risk Model
GPS	global positioning system
QA/QC	Quality Assurance/Quality Control
NCSA	Northern Coast of South America
NES	United States Northeastern Continental Shelf Ecosystem
OCS	Outer Continental Shelf
PTT	platform transmitter terminal
RPM	rotations per minute
SCRAM	Stochastic Collison Risk Assessment for Movement
SEC	Southeast U.S./Caribbean
USFWS	U.S. Fish and Wildlife Service
YOY	young of the year

Glossary

Term	Explanation
Avoidance	Behavior in which birds choose to avoid coming into proximity with an offshore wind turbine. Can occur at a range of spatial scales; the avoidance metric commonly used in collision risk models typically incorporates meso- to micro-avoidance (e.g., avoidance of turbines within a wind farm or avoidance of turbine blades when in their immediate proximity), but does not include macro-avoidance, in which birds may choose to avoid entering a wind farm altogether.
Collision risk model	A model that predicts risk of avian collisions with offshore wind turbines. Most collision risk models combine an estimate of the number of birds available to collide with a turbine with the probability of a collision occurring; as reviewed in Masden and Cook (2016), this is "generally based on the probability of a turbine blade occupying the same space as the bird during the time that the bird takes to pass through the rotor." Collision risk models thus typically include some type of bird density value, as well as a variety of parameters describing both bird behavior and turbine characteristics. The earliest collision risk model was developed in the 1980's; more recent iterations for offshore use are often based on the Band (2012) model.
Cumulative use	Cumulative daily occupancy (per month): the proportion of individuals in a grid cell each day, summed across days within each month.
Cumulative impacts	Effects of multiple offshore wind farms on the same species or population, including effects throughout the lifespan of the wind farms. In the context of this report, cumulative risk of collisions is assumed to be additive across offshore wind farms.
Monthly population size	Estimate for each grid cell of the number of birds present in that grid cell during that month. Derived by multiplying the estimated cumulative use (i.e., daily occupancy) for the grid cell by the monthly regional population size.
Effects determination	Assessment by federal agencies as to whether an action affects species listed under the U.S. Endangered Species Act (ESA; 16 U.S.C. §§1531-1544). Typical findings are "no effect", "not likely to adversely affect", or "likely to adversely affect".
Exposed population	Number of individuals estimated to be present in a grid cell and transit a wind turbine (and thus are available to collide with the turbine blades). Estimated from the cumulative daily population size estimate for a grid cell (by month), as well as factors such as the number and size of turbines. The "exposed population" can be larger than the monthly regional population size if enough birds are estimated to be exposed to collision risk on multiple days within that month.
Flight height model	Model for estimating altitude of birds based on flight height data collected from 1) GPS and PTT satellite tags (for locations over water and >50 m from the nearest coastline), or 2) Motus position estimates from previous work (Loring et al. 2019) for birds located over federal waters (e.g., >3 miles from shore) that were moving quickly enough to be flying (based on timing of sequential locations).
Hatch year	Bird born within the same calendar year as the time period of interest. Birds born in previous calendar years are "after hatch year" individuals.
Morphometrics	Body measurements of birds, such as wing length.
Motus Wildlife Tracking System	Also "Motus". An international automated radio telemetry network on coordinated frequencies (Taylor et al. 2017)[4]. Automated radio telemetry systems consist of radio tags (small transmitters

[4] The Motus Wildlife Tracking System: www.motus.org.

Term	Explanation
	attached to birds, bats, or insects) and stations (receivers with antennas that record signals from "tagged" organisms). When tagged animals are within detection range of a station, the receiver automatically records transmitter ID number, date, time stamp, antenna (defined by monitoring station and bearing), and signal strength value of each detection. All Motus data currently used in SCRAM were obtained from previous studies (Loring et al. 2018; Loring et al. 2019; Loring et al. 2021).
Movement model	A correlated random walk (CRW) model that uses either Motus or satellite-based tracking data to estimate two-dimensional (X,Y) position estimates for tagged animals. These models have two major components: a correlated random walk process (movement) model and an observation model that describes measurement error. Used to estimate cumulative use (i.e., daily occupancy) rates.
Occupancy	Presence of a species in a grid cell. Estimated in this report by the proportion of individuals found within a grid cell per day or month. Cumulative use (i.e., daily occupancy) rates per month within each grid cell are calculated by summing the proportion of individuals in a grid cell each day. This is multiplied by the monthly regional population size to predict monthly population use for each grid cell. Probability of daily occupancy within all grid cells across the study area sums to one.
Regional population size	Also "monthly regional population size". The number of individuals of a given species that are estimated to be present within the study area during a given month of the annual cycle.
Sampled population	Also "tagged population". Subpopulation of birds that were tagged with transmitters and that contributed data to the development of movement and flight height models.
Station	Also "tracking station". Motus equipment is designed to detect animals tagged with coded radio transmitters. Detection range of stations varies with the height of the receiving antennas (meters above sea level: m asl), altitude of the tagged animal, and the signal gain properties of the transmitter and receiver, among other factors. Most land-based stations included in this study had a 12.2-m radio antenna mast supporting six 9-element (3.3 m) Yagi antennas, which were mounted in a radial configuration at 60° intervals and connected via coaxial cables to a receiving unit (Lotek SRX).
Telemetry array	Network of Motus stations used to detect tagged animals.
Transit	Movement of an animal through the rotor-swept zone of a turbine. In the current version of SCRAM, can occur no more than once per day per individual.
Transmitters	Also "tags". Transmitters used in this study included 0.67 g and 1.1-g Motus models (brand name "nanotag"; Lotek Wireless, Ontario, Canada). All Motus transmitters were programmed to emit signals at fixed burst intervals on a shared frequency of 166.380 MHz from activation through the end of battery life. Burst intervals were unique to each transmitter and ranged from 4 to 6 s. GPS tags used in this study were 4.1 g Lotek PinPoint GPS-Argos 75 tags; Argos PTT tags were 2 g Lotek Sunbird Solar Argos Transmitters and 2 g Microwave Telemetry Solar Satellite Transmitters (Microwave Telemetry, Columbia, MD, USA).
Wintering population	Number of birds estimated to be present on the non-breeding grounds during the boreal winter. Can include specific subpopulations of birds that winter in different locations. For the three species discussed in this report, wintering grounds range from the southeastern United States to southern South America.

1 Introduction

This document describes the products of Phase 2 of funding under the Bureau of Ocean Energy Management (BOEM) Contract No. M19PG00023, "Transparent modeling of collision risk for three federally listed bird species in relation to offshore wind energy development" (Adams et al. 2022). This report accompanies release of an update to the SCRAM model (Stochastic Collision Risk Assessment for Movement), a collision risk decision support tool for the Northeastern Continental Shelf Ecosystem (NES). SCRAM includes (1) a stochastic collision risk model, which uses avian movement data from telemetry studies to estimate risk of bird collisions with offshore wind turbines planned for construction in the U.S. Atlantic, as well as (2) a web application to implement the model. SCRAM currently estimates collision risk for three federally protected bird species: the roseate tern (*Sterna dougallii*), piping plover (*Charadrius melodus*), and red knot (*Calidris canutus rufa*).

SCRAM Version 2, released in 2024, includes a range of updates from the version of the model and web application that was discussed in Adams et al. (2022; Version 1.0.3). All changes from the initial release of Version 1.0.3 to Version 2.1.6 are discussed in this report. Further updates to the SCRAM web application from the time of this report publication will be documented on the project GitHub page[5].

2 SCRAM 2 Updates

The major components of SCRAM are outlined in Figure 1 (below), including:

- Data inputs, such as movement data, species data, and wind turbine data,
- Three main models, including movement models, flight height models, and stochastic collision risk models, and
- The open-source web application that implements the models and produces fully documented estimates of collision risk based on data inputs.

SCRAM 2 includes changes to most of these components, summarized in Table 1, along with an assessment of the estimated impact of each change on resulting collision risk estimates. Additional details for each update are provided in the text below. Additional summarization of key changes is included in Appendix A (Frequently Asked Questions for SCRAM 2).

[5] See https://github.com/Biodiversity-ResearchInstitute/SCRAM2. The updated SCRAM web application, model code, and user manual are available at https://briloon.shinyapps.io/SCRAM2/. All study products are also available via https://briwildlife.org/SCRAM/.

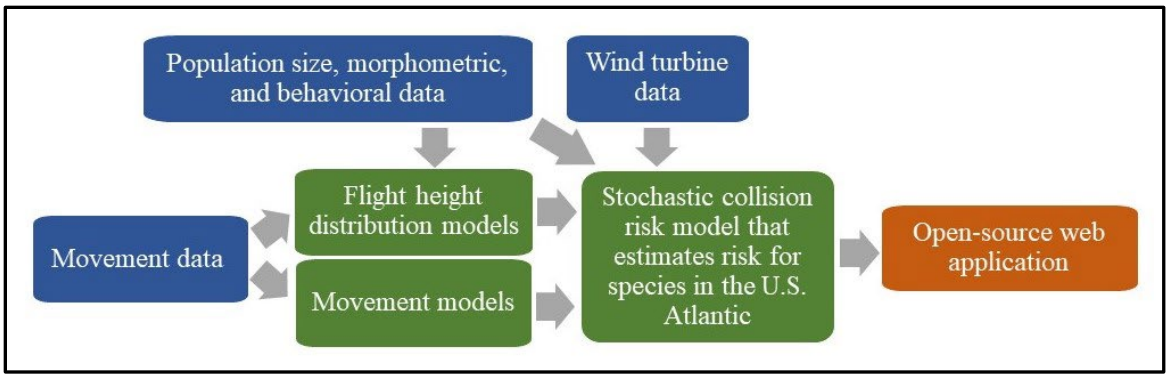

Figure 1. Stochastic Collision Risk Assessment for Movement (SCRAM) project components
Data inputs are shown in blue; models in green; and the web application for implementing the collision risk model in orange.

Table 1. Summary of changes implemented in SCRAM 2 along with their expected influence on resulting estimates of collision risk.

Component	Change Implemented in SCRAM 2	Influence on Collision Risk Estimates
Data inputs	*Increased the amount of Motus tracking data included for Red Knots and additional data filtering applied to Red Knots, Piping Plovers, and Roseate Terns.* SCRAM 1.0.3 used Motus tracking data for the three focal bird species that were collected in 2015-2017, as described in Loring et al. (2018) and Loring et al. (2019). SCRAM 2 incorporated additional Motus data, as described in Loring et al. (2021). Overall, the sample size of Red Knots increased in Loring et al. (2021), due to the inclusion of birds tagged by new projects. However, Loring et al. (2021) also excluded individuals with "ambiguous" detections that had not been identified in previous quality assurance and quality control procedures. SCRAM 2 also applied a more conservative filtering method for Piping Plovers and Roseate Terns to retain detections for each individual with greater than three consecutive bursts (within one minute of each other) per site (SCRAM 1.0.3 did not calculate burst length by site).	↑↓
Data inputs	*For Red Knots, SCRAM 2 incorporated GPS and PTT satellite-based data in addition to Motus data.* Red Knot occupancy models developed using GPS and Argos data were not constrained geographically as with Motus data used in SCRAM (see changes to Movement Models, below), and thus provided occupancy estimates for the entire NES.	↑↓
Data inputs	*Updated avoidance rates used in collision risk models based on values from Cook (2021) and Ozsanlav-Harris et al. (2023).* Previous avoidance rates were based solely on values from the Cook report and were lower than the averaged values from the two reports included in SCRAM 2.	↓
Data inputs	*Updated monthly regional population size estimates (e.g., the populations of individual birds that are estimated to be present in the study area and thus potentially available to collide with turbines) from U.S. Fish and Wildlife Service.* Generally, these values decreased from SCRAM 1.0.3 due to refined monthly estimates of when animals are expected to be present in the NES.	↓
Data inputs	*Changed the required user-provided parameters.* This update includes requiring average turbine rotational speed in rotations per minute (RPM), rather than estimating this value based on previously required wind speed data. This update aligned with the original Band (2012) inputs used in the current stochLAB stochCRM implementation (see changes to Stochastic Collision Risk Models, below). SCRAM 2 determined mean annual turbine rotational speed based only on the time that the turbine was expected to be operational, since non-operational time (due to maintenance downtime and low wind speeds) was accounted for elsewhere in the model.	N/A

Component	Change Implemented in SCRAM 2	Influence on Collision Risk Estimates
Movement Models	*Updated the structure of the Motus movement models: addressed changes to the tracking datasets (see changes to Data Inputs, above), improved model fit, and simplified the model structure.* The previous two-state models were converted to one-state models. Therefore, staging movements were no longer distinguishable from migratory movements. The SCRAM 2 model assumed equal risk across all movements, which smoothed out predictions, such that changes in the highest highs and lowest lows from SCRAM 1.0.3 tended towards the median in SCRAM 2.	↑↓
Movement Models	*Constrained the geographic region in which SCRAM occupancy estimates were used to inform collision risk models for the models that were based on Motus data only.* Geographic constraints were based on the latitudinal range of actively maintained Motus stations during the period of the Motus tracking study (Loring et al. 2018; Loring et al. 2019; Loring et al. 2021). In geographic regions (offshore areas located approximately from Massachusetts to Virginia) where both Motus-based and GPS/Argos-based occupancy estimates were available for Red Knots, SCRAM 2 equally weighted the two datasets to produce a single ensemble model of cumulative use (i.e., daily occupancy). Movement models for Roseate Terns and Piping Plovers remained purely based on Motus data due to a lack of sufficient GPS/Argos tracking data for these species.	N/A
Flight Height Models	*Developed new flight height models for Red Knots using altitude estimates derived from birds tagged with GPS transmitters.* Flight height models for Piping Plovers and Roseate Terns remained based on estimates of altitude from Motus data, due to a lack of sufficient GPS tracking data for these species.	↑↓
Stochastic Collision Risk Model	*Updated the model structure to fully align with stochLAB, the most up to date collision risk modeling environment developed as an R package by Caneco et al. (2022).* This updated the R implementation of Masden (2015) and included several relatively minor bug fixes as well as a substantial computational speed improvement. The calculations in this package were tested against outputs from Band (2012) to confirm computational equivalence (e.g., by comparing the deterministic answer produced by the original Band spreadsheet to the stochastic estimates produced by stochLAB).	↓
Stochastic Collision Risk Model	*Added the ability to estimate stochastic collision risk for migratory birds as laid out in Band (2012) Annex 6.* The underlying code calculated migratory flux by dividing the migratory population estimate, for the migratory corridor at the latitude of the wind farm, by the width (km) of that corridor. This estimate of flux assumed a uniform distribution of birds along the migratory front. Migratory front width was estimated throughout the range and varied by latitude.	N/A
Web Application	*Updated the options available to users.* Removed the sensitivity analysis button and output, as it was not being utilized, and a formal sensitivity analysis was planned for a later date. Since the improvements in computational efficiency (see changes to Stochastic Collision Risk Model, above) greatly reduced the time for the model to complete, the "cancel model" button was removed and the number of model iterations was increased. SCRAM 2 also changed the name of Model Option 1 to Model Option 2 to match the nomenclature used in Band (2012).	N/A
Web Application	*Updated the user interface to allow the Band (2012) Annex 6 model to be run via the SCRAM web application.* This allowed Band and SCRAM 2 collision risk modeling estimates to be produced using the same data inputs (e.g., regional population size, wind project data, etc.), and for similar PDF reports to be developed for each type of collision risk model. Note: Band and SCRAM have different spatial extents of their predictions and estimate collisions for different months. Care should be used when comparing results.	N/A

2.1 Input Data

Four sources of data inform SCRAM. Movement modeling relies on (1) animal telemetry data, whereas collision risk modeling relies on (2) morphometrics and behavioral (e.g., flight height) data, (3) population size data, and (4) wind turbine input data. For the movement modeling, SCRAM 2 used updated and new telemetry data for Red Knots (see Table 1 and "Telemetry Data," below). Most morphometrics and behavior data remained the same from SCRAM 1.0.3 to SCRAM 2, with the exception of avoidance rates and flight heights (which differed only for Red Knots; see "Morphometrics and Behavioral Data," below). Regional population size was updated for all species (see "Population Size Data" below), and wind turbine input data also changed to accommodate turbine rotor speed rather than wind speed (see "Wind Turbine Input Data," below).

2.1.1 Telemetry Data

2.1.1.1 Automated Radio Telemetry

SCRAM 2 movement models were fit to the best available individual tracking data for the three study species at the time of model development. All three species were tracked using coordinated automated radio telemetry data from the Motus Wildlife Tracking System ('Motus', Taylor et al. 2017). SCRAM 1.0.3 used Motus tracking data for the three focal bird species that were collected in 2015-2017, as described in Loring et al. (2018, 2019). SCRAM 2 incorporated additional Motus data, as described in Loring et al. (2021). Loring et al. (2021) also excluded individuals with "ambiguous" detections that had not been identified in previous QA/QC procedures. That report noted that "Ambiguous detections occur when multiple tags with the same properties (ID code, burst interval) are active in the Motus network at the same time and cannot be distinguished from each other. Through this process we found that some receiving stations were consistently associated with high rates of false positives during certain time periods, and we therefore removed all detections at those stations during those periods" (Loring et al. 2021). Altogether, and including quality assurance and quality control (QA/QC) procedures outlined below (in this section), the introduction of new data resulted in an increase of sample size from 125 (SCRAM 1.0.3) to 240 (SCRAM 2) Red Knots included in the movement models. Piping Plover and Roseate Tern sample sizes remained at 107 and 134, respectively (these sample sizes were stated incorrectly in Adams et al. 2022).

SCRAM 2 also refined the spatial and temporal extent of the Motus data to avoid incomplete sampling of northbound movements. Red Knots tagged in Delaware Bay, New Jersey, during their spring stopover (e.g., mid-migration), had already crossed the Atlantic Outer Continental Shelf. Following Loring et al (2021), we included only red knots detected after 21 June, which restricted movements to fall (southbound) migration. All detections from these individuals were included in the movement modeling to derive occupancy estimates across the NES. However, only occupancy predictions within a smaller study area were used to estimate collision risk; this study area was based on Motus station maintenance activity throughout the study period (2015–2017; Loring et al. 2018, 2019; see "Calculation of Habitat Use," below).

For the remaining Motus data, we developed a QA/QC procedure to verify correct processing of the detections. During this process, we designed alternative methods of data filtering and computation to compare to SCRAM 1.0.3. We found that the false positive filter for piping plovers and roseate terns distinguished false positive detections across sites, rather than within sites, as originally intended in SCRAM 1.0.3 ('false_pos_filter.R' , 'remove_false_pos.R'). It calculated 'burst length' as the number of detections for each individual within one minute of each other, across multiple sites. This was inconsistent with the conventional definition of 'run length': "the number of continuous detections of a unique code by a receiver" (Taylor et al. 2017). Therefore, we replaced this function ('false_pos_filter.R') with a calculation of burst length using the number of continuous detections for each individual *per site*,

within one minute of each other. We retained only detections with greater than three consecutive bursts, as in SCRAM 1.0.3 ('remove_false_pos.R'; Adams et al. 2022). The correction to the false positive filter resulted in more data being removed during the SCRAM 2 filtering process, particularly for roseate terns. However, because this filter applied only to near-simultaneous detections among multiple receivers (within one minute of each other), it minimally impacted the results.

Our QA/QC process also improved computing time in data processing. For example, following false positive data filtering, we removed duplicate bursts by retaining only the first detection within a time step (consistent with SCRAM 1.0.3). We implemented a method that generated identical results to the original calculations while greatly reducing computing time, which we used to replace the original function ('remove_dup_bursts.R'). We also corrected the function that calculated the number of hours or days since the first record of the data frame (serial_time.R). The hourly calculations erroneously assigned 21 days to January rather than 31. This correction had no effect on the daily models (as implemented in SCRAM 1.0.3). We used alternative methods that accounted for the leap year (2016) to corroborate the hourly results of the corrected function (serial_time.R). All adjustments to SCRAM 1.0.3 are accessible in the SCRAM 2 GitHub repository[6].

2.1.1.2 Satellite Telemetry

In addition to updated Motus data, new global positioning system (GPS) and Platform Transmitter Terminal (PTT) satellite tag data for red knots were incorporated into SCRAM 2. Between 13 August 2020 and 26 August 2023, a total of 239 GPS and satellite tracking devices were deployed on red knots across six research projects (see Appendix B for full tag deployment information). This included 178 GPS tags (4.1 g Lotek PinPoint GPS-Argos 75) and 61 Argos PTT tags (2 g Lotek Sunbirds and 2 g Microwave Telemetry solar satellite transmitters; Table 2). These tags were primarily deployed during fall staging in coastal regions of Massachusetts, New Jersey, and Delaware, with a small proportion of tags deployed during spring staging in these regions or on wintering grounds in South America. A subset of these tags (primarily those tagged during spring staging) did not last through fall migration and therefore only retained data on interior movements towards breeding grounds in the United States and Canada. These were therefore excluded from analysis for the purposes of calculating cumulative occupancy in the NES. This included all GPS tags deployed from the Environment and Climate Change Canada dataset, as well as a subset from the Massachusetts Migration study (Table 2; Appendix C).

The satellite-based telemetry data was used in the movement models and flight height models. Because spring migration through the area of interest was only available from 6 PTT tags, movement modeling focused on fall migration only (with data from July 22 – Dec 16). This was consistent with the Motus data, which were only included in movement modeling for fall staging and migratory periods. The refined GPS-PTT dataset included all GPS data from fall deployments (earliest fall deployment August 13). In the case of Argos PTT tags, data included in modeling was visually determined per individual based on location and timing (see Figure B-1). Initial overland movement from Arctic Canada breeding locations to coastal staging sites occurred in July-August, with fall staging and migratory movement to central and South America from July 22 to December 16.

To maximize sample size, both spring and fall GPS data (May–December) were used in flight height modeling (see "Flight Height Modeling for Red Knots," below). These data were not used to update the flight speed values for Red Knots (see "Morphometrics and Behavioral Data," above), because the duty

[6] See the SCRAM 2 GitHub repository: https://github.com/Biodiversity-ResearchInstitute/SCRAM2

cycles of the satellite tracking data varied (up to 24 hours), and this was judged to be too low a resolution to accurately estimate flight speeds based on these data.

Table 2. Summary of GPS and PTT satellite tags deployed on Red Knots from August 2020-August 2023 and included in movement modeling for SCRAM.

Additional project and deployment details are included in Appendix B.

-	GPS Tags	GPS Tags	PTT Tags	PTT Tags
Project	**Deployed**	**Included**	**Deployed**	**Included**
Atlantic Shores Offshore Wind	61	37	-	-
Coastal Virgina Offshore Wind	-	-	15	15
Environment and Climate Change Canada	30	0	46	10
Massachusetts Migration	10	6	-	-
Ocean Wind 1	61	38	-	-
USFWS Spring Migration	16	0	-	-
TOTAL	**178**	**81**	**61**	**25**

GPS and PTT tracking data were processed and cleaned using the following steps:

- Removed data prior to tag deployment as this represented tag testing data and not animal movement information.
- Removed locations marked as "Failed" in the error-detecting code, the cyclic redundancy check (CRC) by Lotek.
- Removed duplicate locations.
- Removed locations with a date in the future (> December 2023) as impossible given the timing of data retrieval.
- Removed impossible locations based on latitude and longitude (i.e. latitude must be between –90 and 90 degrees and longitude between –180 and 180 degrees).
- Implemented a speed filter using the R function ddfilter from the SDLfilter package (Shimada et al. 2012) that removed points if movement speed between subsequent locations was >100 km/hour.
- Implemented a distance filter to remove data from tags that were suspected to have fallen off. For this we removed tags (n=8) for individuals that did not move >150 m over the full tag deployment period, as this was deemed unrealistic for Red Knot movements.

This filtering resulted in the use of 81 GPS and 25 PTT tags included in movement modeling across six projects (Figure 2).

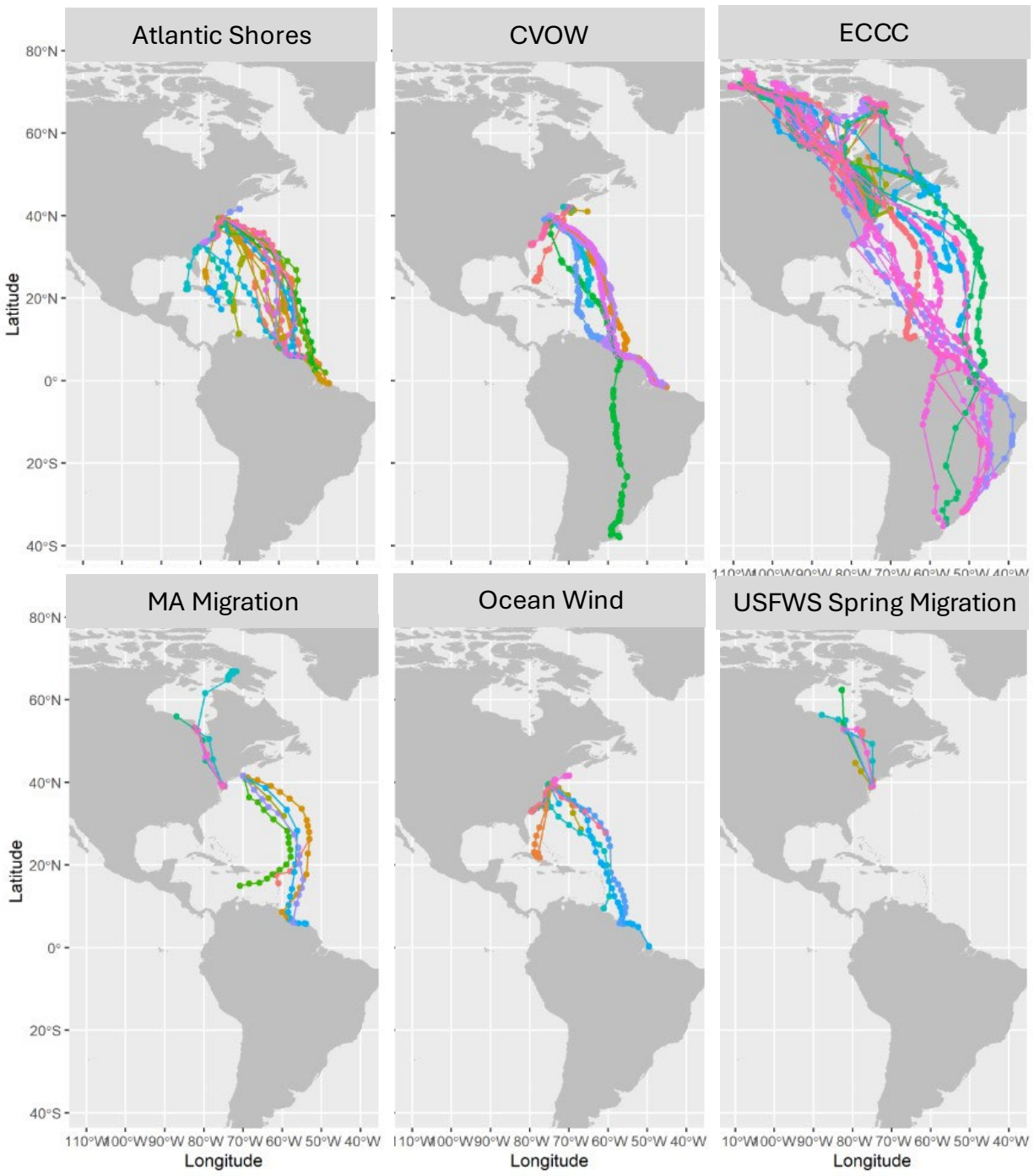

Figure 2. All GPS (n=178) and PTT (n=61) tracking data for Red Knot considered for inclusion in movement modeling for SCRAM 2 by project.
Colors represent individuals.

2.1.2 Morphometrics and Behavioral Data

Several species-specific morphometric and behavioral parameters informed estimates of collision risk at offshore wind turbines in SCRAM 2. These included avoidance rates, body length, wingspan, flight speed, and flight type (i.e., flapping or gliding; Adams et al. 2022). SCRAM 1.0.3 included a single set of

avoidance rates per species, whereas SCRAM 2 included different basic and extended avoidance rates depending on which option was selected for collision risk estimation (after Band 2012). The "extended" model (Option 3) option tabulates collision risk for different altitudes within the rotor swept zone, and thus better estimates collision risk relative to the patterns of flight altitude for a species of interest. The "basic" model (Option 2) is more simplistic and runs more quickly. SCRAM 1.0.3 used the extended avoidance rates for both options; SCRAM 2 used the basic avoidance values for Option 2 and the extended values for Option 3.

Additionally, SCRAM 1.0.3 avoidance values were based on the "all gull and tern" avoidance rates from Table A2 of Cook (2021). This avoidance rate was recommended by the study author for terns and was considered to be the best available and best supported avoidance rate available, even though it was for a different taxonomic group than the shorebird focal species for SCRAM. Another report was published in 2023 (Ozsanlav-Harris et al. 2023) that used a slightly different dataset to estimate avoidance rates. Upon review, neither analysis was a clear improvement over the other, and thus we chose to average the basic and extended avoidance rates from the two reports (Table 3).

Table 3. Avoidance rate estimates from recent reports and summary of how avoidance rates for SCRAM 2 were derived.

Source	Avoidance rate	Avoidance SD	Option	SCRAM Version	Derivation
Cook 2021	0.9295	0.0047	extended	SCRAM 1	"All gulls and terns" avoidance rate from Table A2 - recommended value for terns using extended sCRM model (also almost the exact same value used for Red Knots in Gordon and Nations 2016 collision risk model)
Cook 2021	0.9861	0.0005	basic		"All gulls and terns" basic sCRM avoidance rate from Table A2 - recommended value for terns using basic sCRM model
Ozsanlav-Harris et al. 2023	0.9907	0.0004	basic		"Gulls and terns" basic stochastic CRM avoidance rate from Table 4
Ozsanlav-Harris et al. 2023	0.95	0.0038	extended		"Gulls and terns" extended stochastic CRM avoidance rate from Table 5
Average of Cook and Ozsanlav-Harris et al. estimates	0.9884	0.0005	basic	SCRAM 2	Average of "gull and tern" rates from Cook 2021 and Ozsanlav et al. 2023. Avoidance rate is simple average of the two avoidance rate values; revised standard deviation is calculated using the Delta method, e.g., sqrt((A.sd2^2 + A.sd1^2)/2)
Average of Cook and Ozsanlav-Harris et al. estimates	0.9398	0.0043	extended	SCRAM 2	Average of "gull and tern" rates from Cook 2021 and Ozsanlav et al. 2023. Avoidance rate is simple average of the two avoidance rate values; revised standard deviation is calculated using the Delta method, e.g., sqrt((A.sd2^2 + A.sd1^2)/2)

Note: SD = standard deviation.

2.1.3 Population Size Data

For each species in SCRAM, monthly regional population size (defined as the maximum number of animals present within the Northeast U.S. Continental Shelf [NES] study area in each month) was estimated by USFWS staff using best available information. Monthly variation in regional population sizes resulted from migration to or through the study area, as well as annual breeding productivity.

The regional population size dataset used in SCRAM 2 included substantial updates to align with current values being used in the Band (2012) Annex 6 collision risk model. Band (2012) continues to be used by USFWS in conjunction with SCRAM to help estimate collision risk for wind projects in the NES. SCRAM 2 incorporated updates to overall population size estimates for these species, including the total number of northbound individuals during spring migration (NB), the total number of southbound

individuals during autumn migration (SB), and the number of young of the year (YOY), or birds hatched during a given calendar year that join the southward migration (and thus partially dictate SB; Table 4). These updates utilized the best available information (Table 4). For Red Knots, these updated calculations were summarized in the recent USFWS analysis, "Estimated Monthly Numbers of Rufa Red Knots Crossing 'Migration Fronts' in the Mid-Atlantic (Massachusetts to Virginia)" (Appendix C). The only monthly regional population size estimate that varies between Band and SCRAM implementations in SCRAM 2 is the estimate for Roseate Terns in July, as noted in a footnote below Table 4.

In addition to updating the overall population size estimates for these species, the proportion of individuals present in the NES were also calculated differently from SCRAM 1.0.3. Rather than allowing individuals to potentially linger in the study area for multiple months during migration, SCRAM 2 assumed that all individuals passed through the study area once during a given migration season, and that this passage occurred within a single month (as noted in Table 4). This led to lower estimated regional population sizes in months where only migrants were in the region, since only a percentage of the total population were thought to pass through the region.

For piping plovers, a further change was implemented to estimate regional population size on a state-by-state basis. This meant that all birds breeding north of a state were assumed to migrate through that state. This change did not affect estimates for roseate terns and red knots, since the entire populations of these species bred north of the NES (red knots) or at or above the northernmost state for which SCRAM 2 made predictions of collision risk for the species (roseate terns). This adjustment brought the SCRAM regional population size estimates for piping plovers in line with those being used by USFWS in the Band (2012) Annex 6 calculations of collision risk. As a result, reduced piping plover regional population size estimates occurred at wind projects in most locations, with those farthest north within the NES incurring the largest reductions. Changes to the regional population size estimates included in SCRAM 2 (Table 4; also used by USFWS in current Band (2012) Annex 6 collision risk models) as well as updates to state-by-state total population size estimates for piping plovers (Table 5) generally decreased collision risk estimates in SCRAM 2 as compared to SCRAM 1.0.3.

Table 4. Regional population size data inputs used in Band (2012) Annex 6 and SCRAM 2.

-	Piping Plover	*Rufa* Red Knot	Roseate Tern
Total northbound (NB)	4,589	59,782	10,866
Young of the year (YOY)	2,927	13,736	5,433
Total southbound (SB)	7,516	73,518	16,299
# of Jan crossings	0	0	0
# of Feb crossings	0	0	0
# of Mar crossings	State-specific (10% of NB)	0	0
# of Apr crossings	State-specific (60% of NB)	0	3,622 (33% of NB)
# of May crossings	State-specific (30% of NB)	59,782 (100% of NB)	3,622 (33% of NB)
# of Jun crossings	State-specific (10% of SB)	1,470 (2% of SB)	3,622 (33% of NB)
# of Jul crossings	State-specific (60% of SB)	11,028 (15% of SB)	10,746 (all U.S. breeders)
# of Aug crossings	State-specific (30% of SB)	29,407 (40% of SB)	5,433 (33% of SB)
# of Sep crossings	0	14,704 (20% of SB)	5,433 (33% of SB)
# of Oct crossings	0	11,028 (15% of SB)	5,433 (33% of SB)
# of Nov crossings	0	3,676 (5% of SB)	0
# of Dec crossings	0	2,206 (3% of SB)	0

Note: NB = the total number of northbound individuals during spring migration; SB = the total number of southbound individuals during autumn migration. YOY = young of the year, or birds born during a given calendar year that join the southward autumn migration.

Piping Plover estimates are state-specific, since the species breeds along the coast of the NES (e.g., only birds breeding north of a state are assumed to migrate through that state). For more information, see Table 5.

Piping Plover estimates were based on the following:

- Population data were based on 2021 estimates (USFWS 2021a) and represented the best available estimates from USFWS Ecosystem Services and Migratory Birds. Numbers excluded an unknown (but likely small) number of nonbreeding birds. Monthly numbers used in SCRAM and Band (2012) may have varied slightly from source documents due to rounding of monthly percentages.
- Because the piping plover breeding range overlapped with the NES, regional population size was estimated on a state-by-state basis, so only birds that were breeding or born north of a given state (or in that state) were included in the regional monthly population size estimates for that state. Thus, during southward fall migration, the entire population could theoretically be exposed to a wind project in South Carolina, while only birds from Maine and Eastern Canada could be exposed to a wind project off the coast of Maine. Estimates of monthly crossings (e.g., monthly regional population size estimates) were thus based on birds from [state at latitude of wind project] northward, including Atlantic Canada (Table 5). The southbound (SB) total included young of the year (YOY), calculated as the unweighted mean 20-year productivity rates (2002-2021) multiplied by the 2021 breeding pair estimate for each state and Atlantic Canada.
- The eastern edge of the migration corridor ran southwest parallel to the general orientation of the coast to account for major migration staging areas in North Carolina (Weithman et al. 2018). The eastern edge of the corridor south of Cape Hatteras, North Carolina was also constrained westward to account for much larger numbers of piping plovers wintering in the western Bahamas. Future tagging may reveal some migration pathways to the east of the corridor and/or concentrations within this corridor. The corridor delineated here was based on the limited available data.

Rufa red knot estimates were based on the calculations presented in Appendix C. USFWS expects to further update these population numbers in future iterations of SCRAM.

Roseate Tern estimates were based on:

- Migration numbers were generated based on 2021 breeding population numbers and productivity rates from the U.S. and Canada and represented the best available estimates from USFWS Ecosystem Services and

Migratory Birds. Monthly numbers used in SCRAM and Band (2012) may have varied slightly from source documents due to rounding of monthly percentages.

- Spring migration totals were calculated as the number of breeding pairs in each region multiplied by 2 adults per breeding pair.
- Fall migration totals included all adults from spring migration plus the approximate number of YOY.
- YOY totals were calculated by multiplying the number of breeding pairs in the U.S. and Canada by the average productivity of these pairs (approximately 1 YOY per pair).
- Migration months were determined based on peak migration during the spring and fall migration seasons, as reported by Gochfeld and Burger (2020).
- Number of spring and fall migrants were then assumed to be divided evenly across migration months.
- SCRAM 2 uses movement data collected during the breeding and post-breeding dispersal period (June to Sept) and assumes the July population of roseate terns is 10,746, which equals the total number of NB adults based on 2021 breeding population numbers, minus birds that breed in Canada and would not be expected to be present in the study area during the breeding and post-breeding period. The current implementation of Band (2012) Annex 6 is limited to assessing risk during northbound and southbound migration and assumes that no roseate terns are migrating during July, and thus uses a regional population size estimate of zero for this month.

Table 5. State-by-state population size estimates for Piping Plovers.

Young of the Year (YOY) were added to numbers of breeding adults in each state beginning in June to estimate total numbers of birds present in the state at the beginning of fall migration. Spring numbers included breeding adults only. Only birds that were breeding or born north of a given state (or in that state) were included in the regional monthly population size estimates for that state.

State and/or Location	YOY	Breeding Adults
Eastern Canada	274	360
Maine	204	250
New Hampshire	16	26
Massachusetts	1200	1934
Rhode Island	134	198
Connecticut	98	120
New York	554	878
New Jersey	146	274
Delaware	35	48
Maryland	25	44
Virginia	211	366
North Carolina	22	80
South Carolina	0	0
Total	**2,919**	**4,578**

2.1.4 Wind Turbine Input Data

Rather than estimating turbine RPMs (rotations per minute) based on wind speed data, as was done in SCRAM 1.0.3, SCRAM 2 now requires users to input RPMs directly. This change aligned SCRAM with stochLAB, the collision risk modeling (CRM) package used in the United Kingdom (see "Collision Risk Modeling," below). Thus, developers should submit RPM data rather than wind speed data for their wind

facilities as part of the Construction and Operations Plan (COP; Appendix D). Specifically, SCRAM 1.0.3 asked for the following inputs:

- WindSpeed_mps (mean wind speed at the proposed project in meters per second) for the periods during which wind speeds are between cut-in and cut-out speeds of the turbine (i.e., turbines could be spinning); or if not available, the rated wind speed of the turbines
- WindSpeedSD_mps (the standard deviation in wind speeds or wind speed rating in meters per second)

In SCRAM 2, the following turbine inputs are now required instead of wind speed data:

- RotorSpeed_rpm (mean number of turbine rotations per minute when active)
- RotorSpeedSD_rpm (the standard deviation of turbine rotations per minute)

We recommend setting RotorSpeedSD_rpm to 0 unless data can be obtained on the variation in RPMs due to wind speed or other environmental conditions. Mean annual turbine rotational speed (and standard deviation when possible) should be determined over the time that the turbine is expected to be operational only, since non-operational time (due to maintenance and low wind speeds) is accounted for elsewhere in the model.

This change is not expected to have a consistent influence on collision risk estimates as compared to SCRAM 1.0.3 (e.g., it's not expected to either increase or decrease collision risk estimates as compared with earlier versions of SCRAM).

2.2 Movement Modeling

SCRAM 2 updated the movement models implemented in SCRAM 1.0.3 (Adams et al. 2022), to include newly available telemetry data. We devised new models that described the satellite-based tracking data, and revised existing models (i.e., from SCRAM 1.0.3) that accommodated the updated automated radio telemetry (Motus) dataset. State-space movement models were implemented on both data sources to isolate model uncertainty from two types of error: ecological process and observation error. The models separated the process variance from the observation variance, rather than confounding these two sources of variation in a single source of error (Auger-Méthé et al. 2021). Variation among the estimated locations of individuals comprised process uncertainty. Variation among tags, for example due to measurement error from deployment, comprised observation error. Accounting for the observation error allowed users to focus on interpreting the movement process, offering greater utility to informing estimates of risk from offshore wind energy development.

In addition to variation between individuals, the state-space models captured within-individual variability in their behavioral state(s) across space. The SCRAM 1.0.3 two-state models (Adams et al. 2022) differentiated between different movement types (as proxies for behavior) based on characteristics of the Motus data. They separated migratory from staging movement rather than treating all movements or behaviors the same, as in a single-state model. However, the two-state movement models implemented in SCRAM 1.0.3 (Adams et al. 2022) failed on the updated Loring et al. (2021) Motus data. Though intended to better capture variance in the two different types of behaviors and improve model fit, the increased complexity instead resulted in model failure. Therefore, SCRAM 2 required the use of single state models (Table 1), which improved model fit and thereby reduced model uncertainty. For consistency, the single state models were also used with satellite-based data (see "Satellite-based Model Methods," below).

2.2.1 Motus Model Development and Structure

Originally modified from Baldwin et al. (2018), SCRAM 1.0.3 Motus movement models (Adams et al. 2022) were based on models designed for GPS data by Jonsen (2016) in the associated R package bsam (v. 1.1.3): hierarchical Discrete-time, Continuous-space, Correlated Random Walk models with a Spatial measurement-error observation model (hDCRWS). SCRAM 1.0.3 Motus movement models were designed to be "hierarchical": to estimate parameters across multiple individuals jointly with related submodels. Bird movements were estimated between the coordinates of radiotelemetry stations where individuals were detected, at regular time intervals through space, following a "Discrete-time, Continuous-space, Correlated Random Walk." The observation model accounted for spatial measurement error and incorporated behavioral state estimation. All these aspects of the SCRAM 1.0.3 movement models were retained within SCRAM 2. We developed a thorough QA/QC process on the movement model that compared SCRAM 1.0.3 line-by-line with the hDCRWS from bsam (Jonsen 2016) and Baldwin et al. (2018). SCRAM 2 incorporated simplified model parameters and a streamlined model structure, which included the reduced behavioral state specification (described in further detail below in "Motus Model Assessment").

2.2.1.1 Observation Error Model

The observation error component of the SCRAM 2 Motus movement model derived from Baldwin et al. (2018) to account for measurement error among individual tag deployments. Each observed location y_i corresponded to the coordinates (latitude and longitude) of the automated radiotelemetry receiver at which each tag was detected. Temporally irregular detections i occurred at the true location μ_i (otherwise referred to as $\hat{y}_i$; Baldwin et al. 2018).

$$y_i \sim N(\mu_i, \tau_{observation})$$

The measurement error around the true location was defined by the precision τ, or the inverse square of the standard deviation, which followed a uniform distribution:

$$\tau_{observation} = {}^{1}\!/_{\sigma^2_{observation}}$$

$$\sigma_{observation} \backsim U\,(0, 0.1)$$

This prior gave a low chance of detections at a longer range than 50 km, with the vast majority within 22 km of a Motus receiving station (as converted from decimal degrees using the average size of a grid cell).

2.2.1.2 Process Model

The process component of the SCRAM 2 Motus movement model explained variation among the estimated locations of tracked individuals. Each true location μ_i was derived from the estimated, unobserved location state x_t at regular time step t (Baldwin et al. 2018). The set of the estimated unobserved location state $\boldsymbol{X_t}$ was calculated from the displacement distance from the previous location $\boldsymbol{X_{t-1}}$, in both the X- and Y-planes (longitude and latitude, respectively). To calculate displacement from the previous location, each single time step $(\boldsymbol{X_{t-2}} - \boldsymbol{X_{t-1}})$ was multiplied by the autoregressive parameter γ and added to the previous location $\boldsymbol{X_{t-1}}$.

$$\boldsymbol{X_t} = \boldsymbol{X_{t-1}} + \gamma \times (\boldsymbol{X_{t-2}} - \boldsymbol{X_{t-1}})$$

$$\boldsymbol{X}_{t+1} \sim N(\boldsymbol{X}_t, \tau_{process})$$

$$\tau_{process} = {}^{1}\!/_{\sigma^2_{process}}$$

$$\sigma_{process} \backsim U\ (0, 0.1)$$

The autoregressive parameter γ described the correlation between subsequent movements, where

$$\gamma \backsim U\ (0, 1).$$

A high value for γ represented rapid, persistent migratory movements, whereas a low value represented more random turning (such as staging or foraging). Maximal displacement distance in a single timestep was constrained to less than the distance traveled if the bird were flying at a constant speed of approximately 46.25 km/h (12.8 m/s) without turning (Adams et al. 2022).

2.2.2 Motus Model Fit

SCRAM Motus movement models were fit within a Bayesian framework. In SCRAM 2, parameter estimates were sampled from three parallel chains and tested for convergence on a single solution. Using JAGS (v4.3.1) via package 'rjags' (Plummer 2023) in R, we ran 30,000 iterations of the three independent chains, following a burn-in of 30,000 iterations. Chains were thinned by increments of 10 to reduce the size of output files. We assessed model convergence through visual inspection and the Gelman-Rubin statistic ($\hat{r}$), which measured consistency among and within model chains, retaining models with $\hat{r} < 1.1$ (Gelman and Rubin 1992). Upon further assessment, we found that models did not converge due to either irregular data, inappropriate model assumptions and excessive complexity or structural rigidity (see "Motus Model Assessment," next).

2.2.3 Motus Model Assessment

Motus model assessment aimed to address updates to the Motus dataset and improve model fit for all species. We first assessed whether data characteristics contributed to model failure when applying SCRAM 1.0.3 models to the updated dataset (Loring et al. 2021; see "Automated Radio Telemetry," above). We examined patterns across individuals, including tagging year, total number of detections, number of stations at which the individual was detected, number of between-station detections, maximum distance between detections, necessary flight speed and number of days between station detections, and minimum and maximum latitude and longitude of detections. We found no consistent patterns in the data, or in data filtering, that resulted in sufficient convergence without further adjustments to the model. Testing the models on satellite-based data resulted in better convergence, suggesting that model failure was in part due to temporal irregularities inherent to Motus data.

Next, we adjusted model components systematically, which marginally improved convergence on a subset of model parameters, but did not resolve issues for all species. We tested modifications of many model parameters on a systematic trial-by-parameter basis, i.e. using a stepwise approach, one parameter at a time. For example, we reinserted a component from the Baldwin et al. (2018) and Jonsen (2016) hDCRWS, which had been erroneously removed from SCRAM 1.0.3. This "random deviate" was used to assign one behavior to rapid, persistent migratory movements and the second behavior to slower, more random turning movements (e.g., staging or foraging). Additionally, we modified a parameter from SCRAM 1.0.3 Motus movement models referred to as migratory "drift" (Baldwin et al. 2018). Drift allowed animals to move beyond their estimated locations in a given direction, for example southwesterly during fall migratory movements along the East coast (Baldwin et al. 2018). Whereas SCRAM 1.0.3 allowed for 360° drift (Adams et al. 2022), we tested westerly drift in SCRAM 2, given that active Motus stations during the study period were land-based, and therefore more likely to detect westerly-drifting movements over the NES. We also corrected the indexing of behavior and coordinates in the drift parameter for the two-state model. While the single state model converged for all three study species both with and without drift, the parameter contributed inconsistently and insignificantly to the model. Therefore, in the absence of strong justification to the contrary, we selected the simpler models without

drift. While these parameter adjustments in the Motus Movement models improved convergence, they did not resolve it.

Last, we proceeded to improve structural flexibility of the Motus movement models for increased transferability to broader data sources. To test whether the original hCDRWS model showed similar convergence issues on the SCRAM 2 data, we ran the Loring et al. (2021) data through the R (R Core Team 2023) package bsam (Jonsen 2016). For comparison, we also ran the data through the R package crawl (Johnson and London 2018) to fit continuous-time correlated random walk models. Similarly poor convergence revealed that the underlying error structure of the model required adjustment. We tested multiple covariance structures, including greater degrees of freedom in the Wishart prior (e.g., k=100 rather than k=2; Plummer 2017), to allow for independence among elements of the multivariate normal distribution. These also continued to fail, revealing a flawed assumption of covariance between uncertainty around the detected and estimated coordinates. The assumption of dependence among elements of this distribution (Jonsen 2016; Baldwin et al. 2018), originally applied to GPS tracking data, was apparently too rigid for the Motus data used in this study. We concluded that detection ranges of Motus stations should be allowed to vary differently in the X- and Y-dimensions, given inconsistencies in antenna orientation, station height above sea level, flight heights, and other factors (Loring et al. 2019). Therefore, we relaxed the assumption of covariance in error around position uncertainty, and allowed for independent normal variance around the observed and estimated locations. In other words, SCRAM 2 errors in latitude were allowed to vary independently from longitude rather than being required to covary (e.g., see sections 11.6.2-11.6.3 in Kéry and Royle 2016).

2.2.4 Motus Model Refinement

Once we obtained a converged single-state daily model, we tested finer temporal resolutions on the Motus detection data for SCRAM 2. We updated the model code to accommodate sub-daily movements and tested one, six, 12, and 24-hourly (i.e. daily) models. As with the daily models in SCRAM 1.0.3, we retained only the first detection within the time step (e.g., six-, 12-hourly). Consistent with the daily models, we fit the models to this sub-daily time step and predicted to the same time step (at regular intervals). Rather than fitting models to the observed detections, fitting to the time step avoided limitations in computing capacity (both processing and memory).

The single state model without drift was the best performing model in SCRAM 2 across all three study species (Table 6). The two-state model did not converge for any species, though it came closest for Red Knots. The one-hourly models failed due to computing capacity limitations, and the six-hourly one-state model converged only for Piping Plovers. The 12-hourly one-state model converged for Piping Plovers and Roseate Terns, whereas the 24-hour (daily) single-state model converged across all three species.

Table 6. Summary of Motus model convergence by species, behavioral state, and time step (6, 12, or 24 hrs).

"No" indicates that tested models failed to converge.

-	1-State	1-State	1-State	2-State	2-State
Species	**6 hr**	**12 hr**	**24 hr**	**12 hr**	**24 hr**
Red Knot	No	No	Yes	No	No
Piping Plover	Yes	Yes	Yes	No	No
Roseate Tern	No	Yes	Yes	No	No

2.2.5 Satellite-based Model Methods

The satellite-based datasets for red knots were used in continuous-time correlated random walk (CRCRW) models that allowed for the incorporation of uncertainty in the position estimation process and prediction to a consistent time step (duty cycles of individual tags varied from hourly to 24-hourly with variations in between). These models differed from the Motus movement models to account for fundamental differences in the underlying tag data, whereby the location information received from GPS and PTT transmitters was independent of receiving station infrastructure. These models were implemented using the 'crawl' R package version 2.3.0 (Johnson et al. 2008) to predict movements of individual red knots at a consistent 15-min time interval for calculation of cumulative occupancy (Figure 3). These models used a state-space version of the continuous-time stochastic movement process and included an observation model that accounted for error in the location estimate process for tags. Given that the amount of error in location estimate for GPS and PTT tags varied significantly, we fit separate movement models for the two data types. In the case of the GPS data, we fit individual movement models with location error as fixed parameters with log(50) for 2D fixes and log(23.5) for 3D fixes to represent the differences in these two fix types. For PTT movement models, position uncertainty was modeled by including a prior distribution for each error class, represented by a normal distribution of the log(estimated error) for each location class (3, 2, 1, 0, A, B) based on Argos estimates (Douglas et al. 2012). Initial parameters were provided as the first location (latitude, longitude) for each individual along with a variance-covariance matrix. To aid in model fit, the retryFits option was set to 3000 (number of times to attempt to achieve convergence and valid variance estimates after the initial model fit), and attempts (the number of times likelihood optimization will be attempted in cases where the fit does not converge or is otherwise non-valid) was set to 2000. In order to propagate location error throughout the cumulative occupancy calculation process, 1000 simulations of each model for each individual were run.

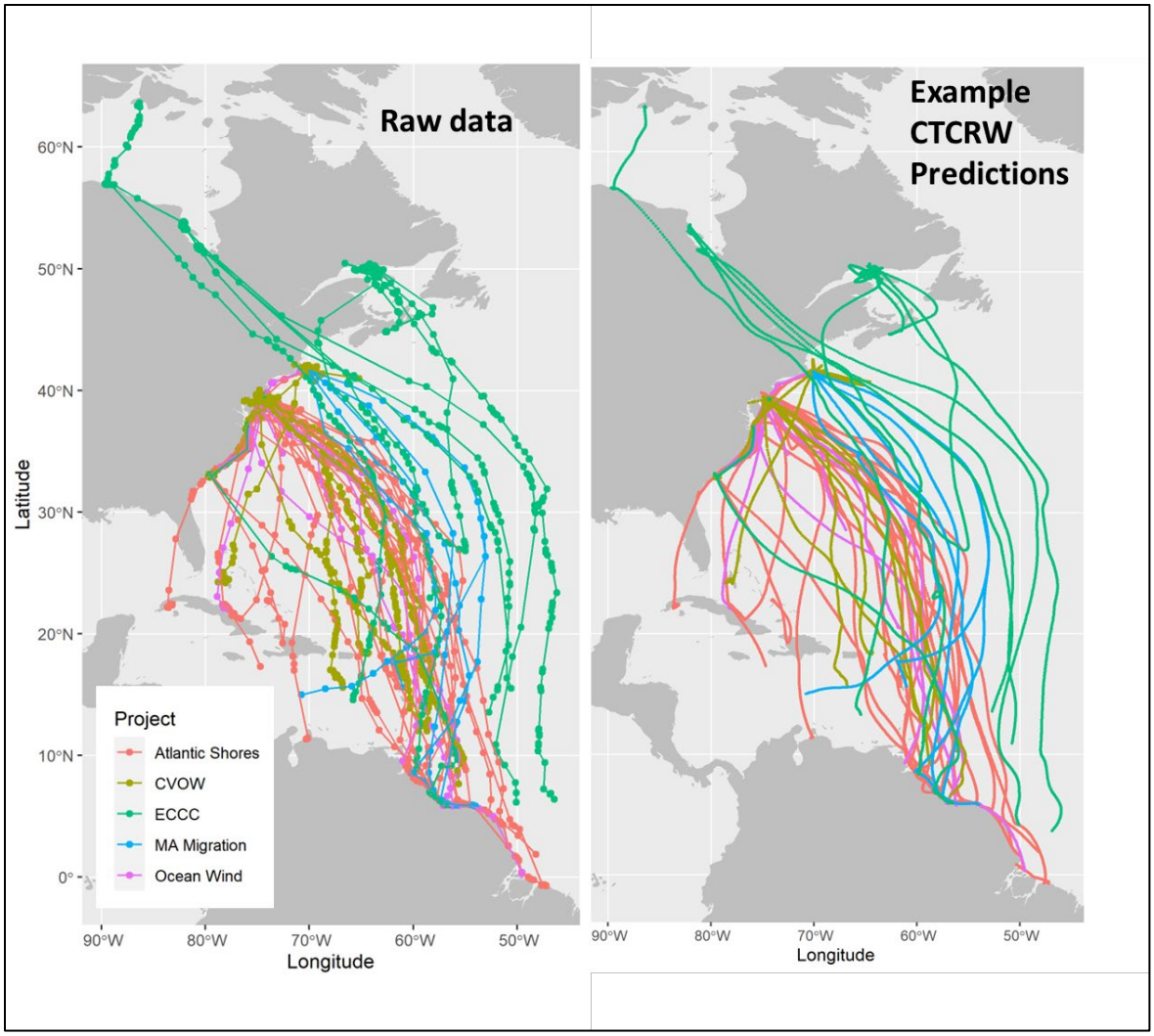

Figure 3. Raw red knot tracking data (fall migration only) used in continuous-time correlated random walk (CRCRW) models, and their predictions.
Raw data (left) and predictions at 15-min time intervals (right) are colored by Project (see Appendix B for more information). Model predictions are shown as an example of one of the 1000 simulated model outputs.

2.2.6 Calculation of Habitat Use

Occupancy was derived from the movement models and defined as the estimated proportion of tagged individuals present in each grid cell. "Cumulative use" (i.e., cumulative daily occupancy) was calculated from the number of days during which individuals crossed through a grid cell of the study area in any given month (Adams et al. 2022). A random sample of 1000 posterior estimates was drawn from the Motus model outputs (consistent with SCRAM 1.0.3), and the posterior number of individuals per grid cell was divided by the total number of tagged individuals in any given month, representing daily use (i.e., daily occupancy). Consistent with SCRAM 1.0.3, this rate was summed across days within each month (i.e., "cumulative use"). SCRAM 1.0.3 did not include the undetected middle months between first and last detection for a small number of individuals; we fixed this error in SCRAM 2, so that the number of tagged individuals remained consistent during the undetected middle months (Table 7). In the case of GPS/PTT models, a similar 1000 simulated tracks from model outputs were used. Given that these were 15-min predictions rather than estimates of daily locations, an initial step was added to first calculate the

proportion of time an individual spent in each cell daily. Then we followed the same process as for Motus data to calculate cumulative use.

The months containing cumulative use estimates differed slightly between SCRAM 2 and SCRAM 1.0.3. Only months with greater than five tracked individuals were used in the collision risk estimation, as was intended but not implemented for SCRAM 1.0.3. Therefore, the month of September no longer included a "cumulative use" Motus estimate for piping plovers. There were also no Motus-tagged red knots in December for either SCRAM 1.0.3 or SCRAM 2 (though in one location in the Adams et al. 2022 report, it was erroneously indicated otherwise). Likewise, we had only four red knots individuals with GPS/PTT data in December. However, more red knot tracking data from the updated Motus dataset (Loring et al. 2021) did allow for the addition of Motus models in July for that species (Table 7).

Table 7. Total number of tagged individuals per month in the data used to develop movement models for SCRAM 2.

Bolded values represent months where occupancy estimates were not used to inform collision risk model estimates, due to fewer than five tracked individuals within that month (consistent with the threshold designated for SCRAM 1.0.3). Models were fit to red knot Motus data, though occupancy predictions are presented only within the spatial extent of the study area and the temporal extent of the study period. For example, one red knot individual (tag 23596) was detected on 28 June 2017, but predictions for this month occurred outside (north of) the study area and thus were not included in the occupancy estimates used in SCRAM. Additionally, occupancy estimates are only presented for months with greater than five tracked individuals.

-	Piping Plover	Red Knot	Red Knot	Roseate Tern
Month	Motus	Motus	GPS/PTT	Motus
May	7	-	-	-
June	49	**1**	-	115
July	98	18	**4**	109
August	23	136	75	42
September	**4**	108	73	9
October	-	122	23	-
November	-	87	13	-
December	-	-	**4**	-

SCRAM 2 developed an ensemble of the Motus and satellite-based occupancy predictions by averaging model results from the two different data sources. Predictions of movement models from the satellite-based data extended across the full NES. However, estimates of Motus movements and collision risk were constrained to a study area of BOEM-funded Motus stations that were actively maintained during the study period. These Motus stations were deployed from Back Bay, Virginia, to Provincetown (Race Point) on Cape Cod, Massachusetts (Loring et al. 2018; Loring et al. 2019; Loring et al. 2021). Given the mean expected station detection range of 20 km, we included only grid cells from 20 km north of the Race Point Motus station at (42.2453°N, -70.2424°W) to 20 km south of the Back Bay Motus station (36.4914°N, -75.9171°W). Outside of these latitudes, other Motus stations were deployed by Motus network collaborators but operation during the study period was variable. Therefore, movement models were developed using all Motus detections – including detections from stations outside of the BOEM-funded study area – but occupancy values used for estimating collision risk were only transferred to the collision risk model for grid cells fully and partially located within this smaller area. Ensemble model

results represented the average of the Motus and satellite-based model outputs within this reduced Motus study area, and otherwise represented only satellite-based model outputs (e.g., on the northerly and southerly ends of the NES).

2.2.7 Movement Modeling Results

Altogether, the improved movement model performance in SCRAM 2 reduced the variability and uncertainty of model results described in SCRAM 1.0.3. Changes to the movement models implemented in SCRAM 2 had a smoothing effect on occupancy estimates as compared to SCRAM 1.0.3 (see example for Red Knots in Figure 4; mean and monthly cumulative daily occupancy estimates are presented by species in Figure 5 throughFigure7 and Appendix E through Appendix F). The general locations of high occupancy and low occupancy areas remained the same, but the highest highs and lowest lows from SCRAM 1.0.3 tended to be adjusted towards the median in SCRAM 2, and low-range occupancy values (closer to 0.01) were more frequent in SCRAM 2 across a greater breadth of grid cells (see example for red knots in Figure F-1). Across all months, SCRAM 2 movement model updates generally resulted in red knot and piping plover movements that more tightly adhered to the Atlantic Outer Continental Shelf than SCRAM 1.0.3 (Figure F-1). The resulting collision risk estimates derived from these cumulative use estimates are described below ("Collision Risk Modeling,").

In summary, improving the flexibility of the movement models to accommodate additional sources of movement data was fundamental to reducing estimated uncertainty. With the SCRAM 2 datasets, the more simplified (i.e. single-state) models fit better to Motus data than more complex (i.e. two-state) models. The challenge of achieving model convergence on Motus data was consistent with prior studies (Baldwin et al. 2018). Combined with erratic behaviors (e.g., brief northerly diversions amidst southerly movements), multi-day gaps between detections that were inherent to the Motus data may have contributed to the two-state model's difficulty separating migratory from staging movements. Future updates should continue to test further model adjustments in the sub-daily movements, as new tracking data become available.

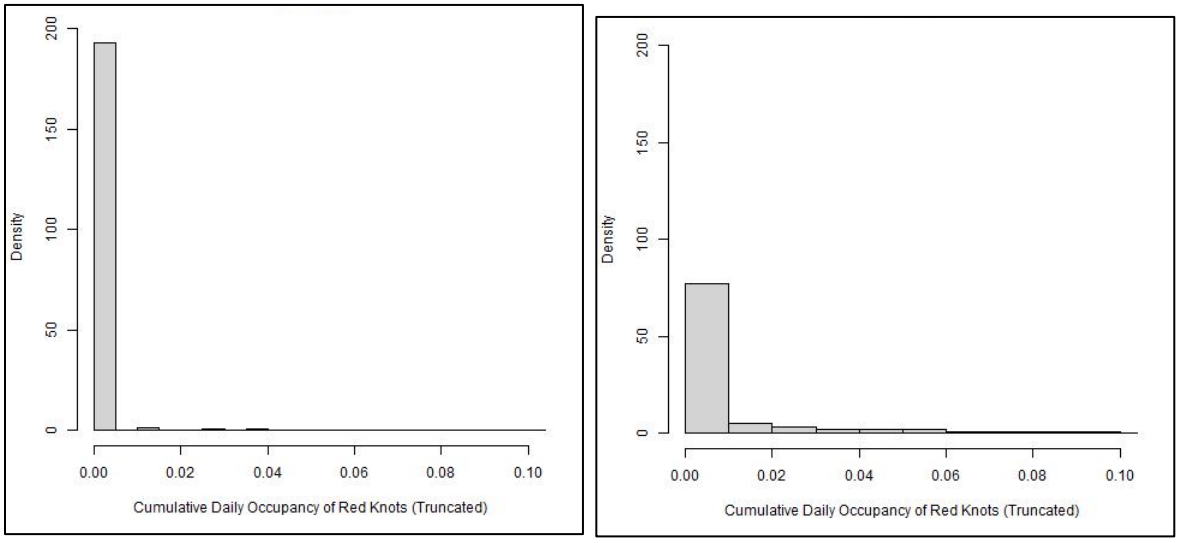

Figure 4. Comparison of cumulative use estimates for Red Knots between SCRAM versions.
For SCRAM 1.0.3 (left panel) and SCRAM 2 (right panel), the x-axis represents cumulative use (truncated to values < 0.10), and the y-axis ("Density") represents the number of estimates for each value, out of the total number of posterior estimates (i.e., 1000 samples for 12 months across 512 grid cells). Cumulative use estimates were more evenly dispersed across the study area in SCRAM 2 due to reduced variability and uncertainty in the results. Low-range values (closer to 0.01) were more frequent in SCRAM 2 across a greater breadth of grid cells.

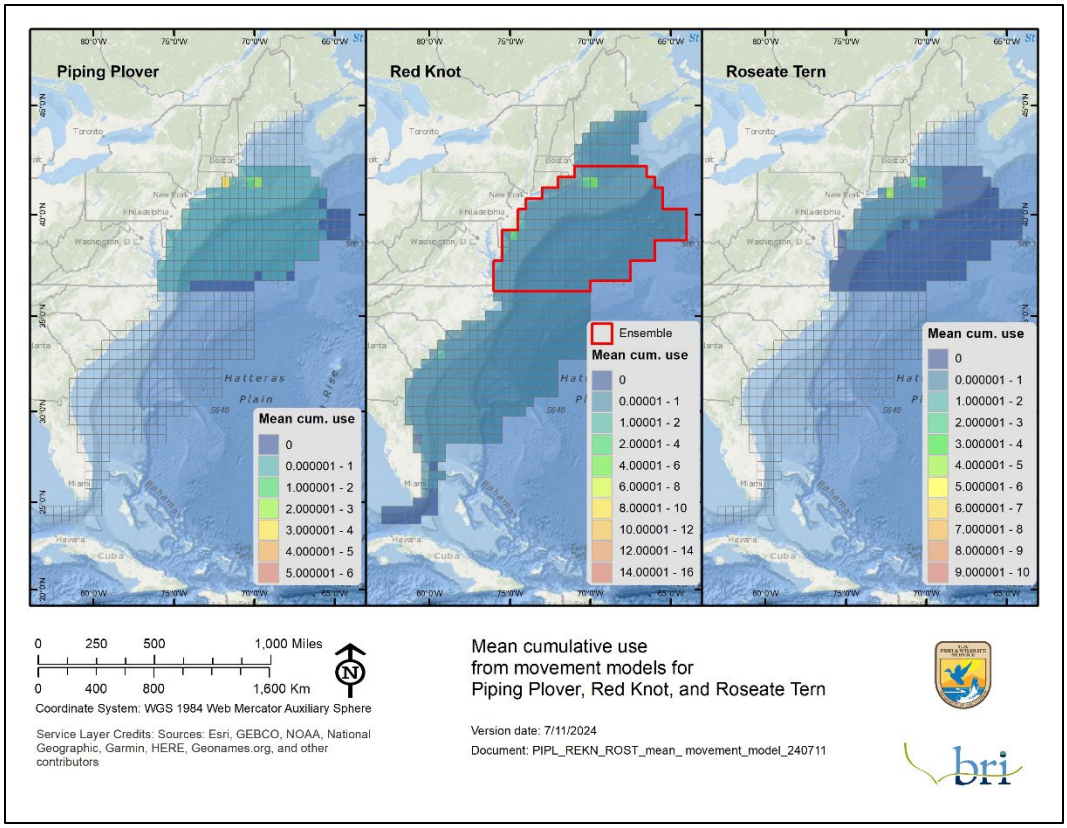

Figure 5. Cumulative use estimates averaged across months for the three study species. Estimates were based on single-state movement models using Motus (piping plover, red knots, roseate tern) and satellite-based data (red knots), and the number of tagged individuals in the study. The results of movement models from Motus and satellite-based data for red knots were combined in an ensemble model within the red study area; estimates outside the red study area were modeled from satellite-based data only. “Cumulative use” summed daily occupancy probabilities estimated via SCRAM for each month then averaged these values across all months with greater than five tracked individuals for a given species. Scale bars align with species-specific monthly estimates (Figure 6– Figure8).

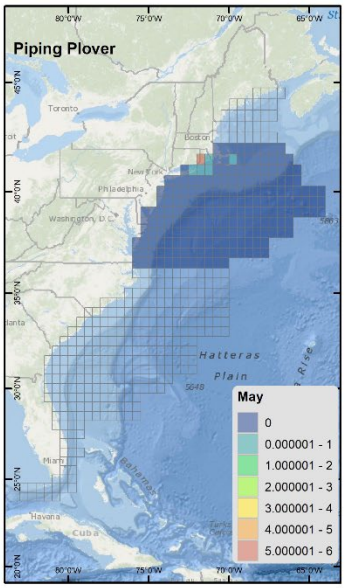

0 250 500 1,000 Miles

0 395 790 1,580 Km

Coordinate System: WGS 1984 Web Mercator Auxiliary Sphere

Service Layer Credits: Sources: Esri, GEBCO, NOAA, National Geographic, Garmin, HERE, Geonames.org, and other contributors

Monthly cumulative use from Motus movement models for Piping Plover

Version date: 7/12/2024

Document: PIPL_monthly_Motus_model_240711_1panel

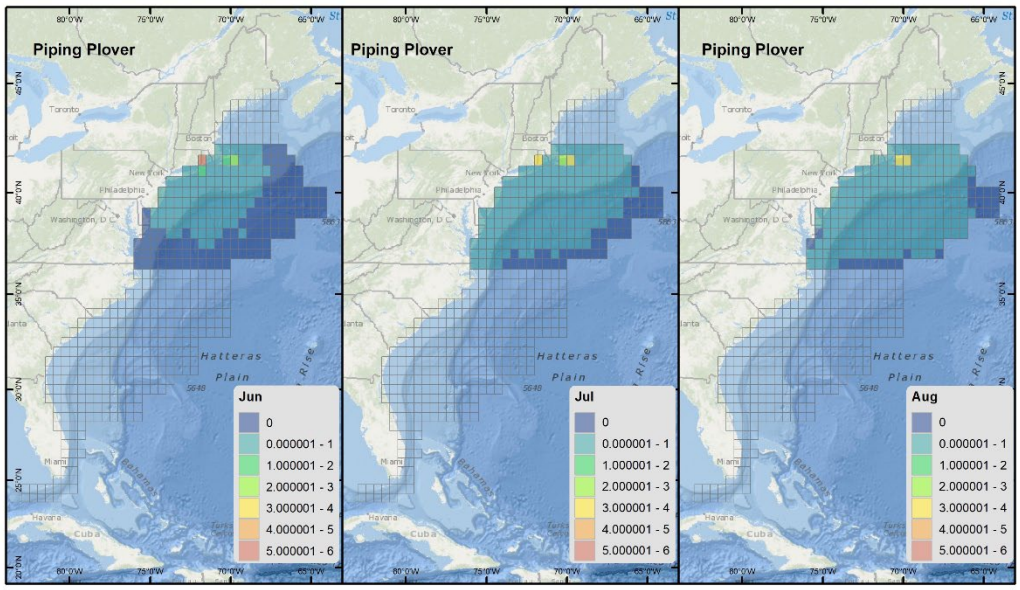

0 250 500 1,000 Miles

0 395 790 1,580 Km

Coordinate System: WGS 1984 Web Mercator Auxiliary Sphere

Service Layer Credits: Sources: Esri, GEBCO, NOAA, National Geographic, Garmin, HERE, Geonames.org, and other contributors

Monthly cumulative use from Motus movement models for Piping Plover

Version date: 7/12/2024

Document: PIPL_monthly_Motus_model_240711_3panel

)

Figure 6. Cumulative use estimates by month from the Motus movement models for piping plovers.
Estimates were based on single-state movement models using Motus data, and the number of tagged individuals in the study. “Cumulative use” summed daily occupancy probabilities estimated via SCRAM for each month with greater than five tracked individuals for a given species. Estimates covered May (top panel) and June-August (bottom panel) (see Table 7 for monthly sample sizes).

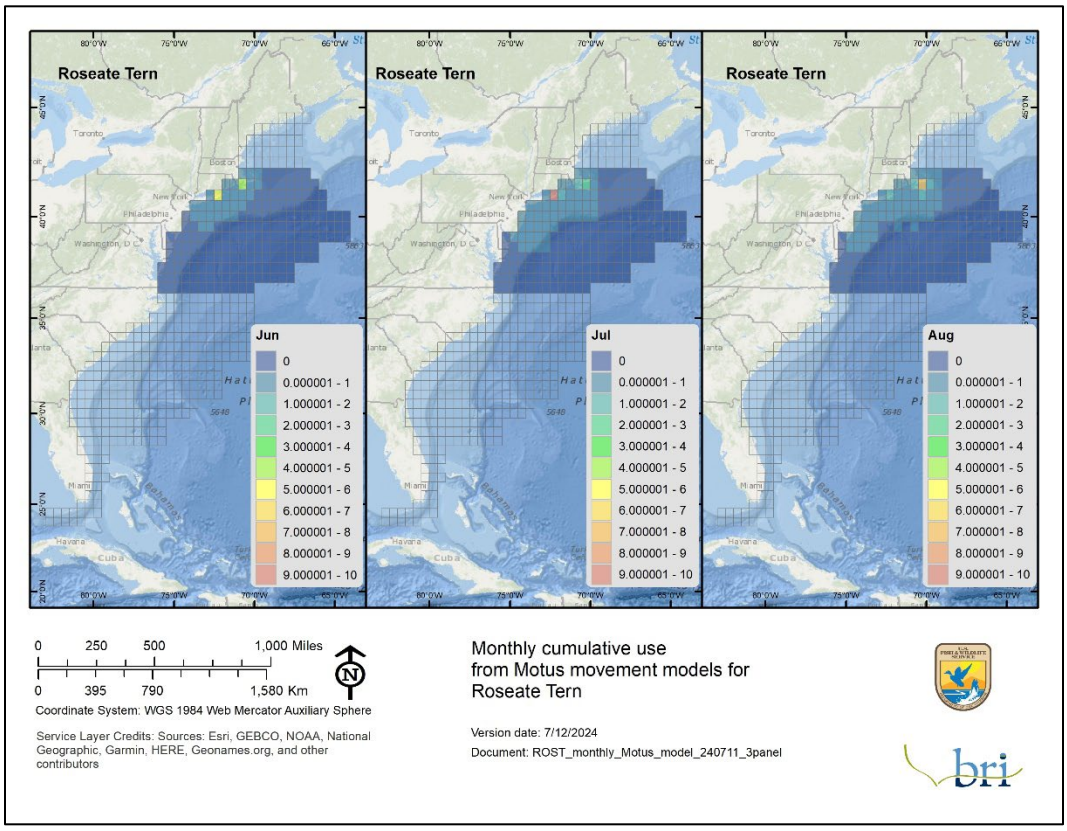

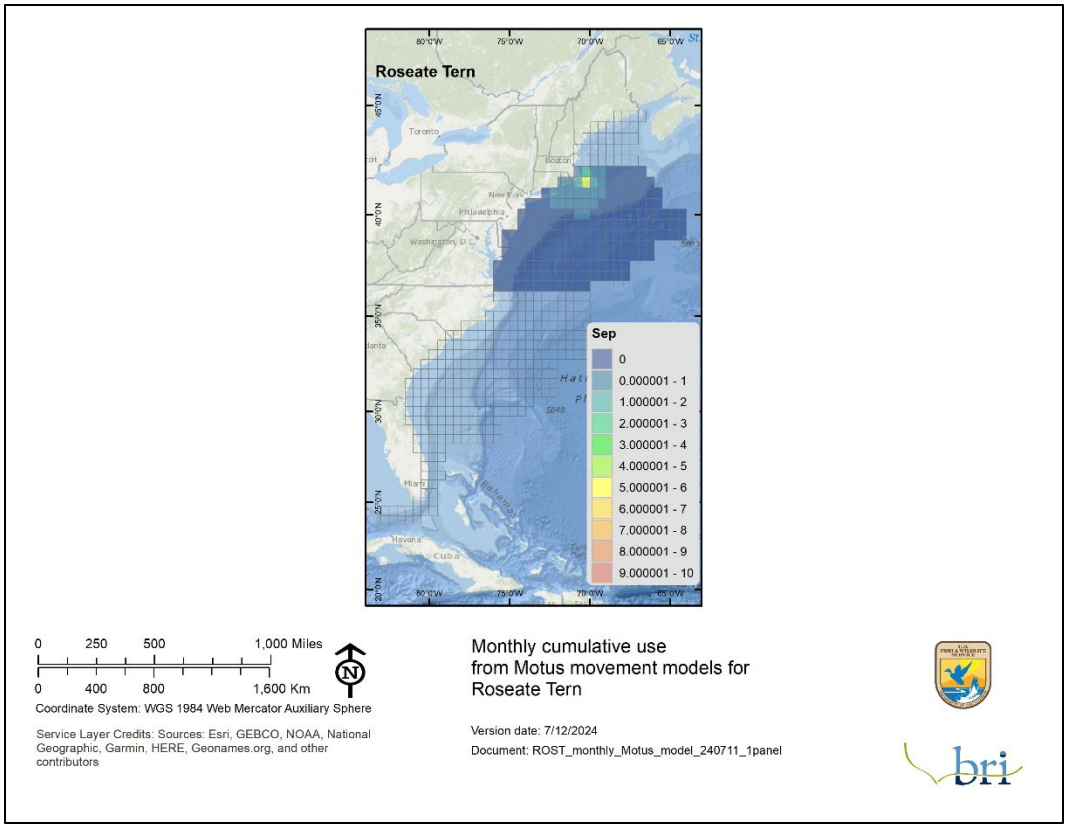

Figure 7. Cumulative use estimates by month from the Motus movement models for Roseate Terns.
Estimates were based on single-state movement models using Motus data, and the number of tagged individuals in the study. “Cumulative use” summed daily occupancy probabilities estimated via SCRAM for each month with greater than five tracked individuals for a given species. Estimates covered June–August (top panel) and September (bottom panel)for roseate terns (see Table 7 for monthly sample sizes).

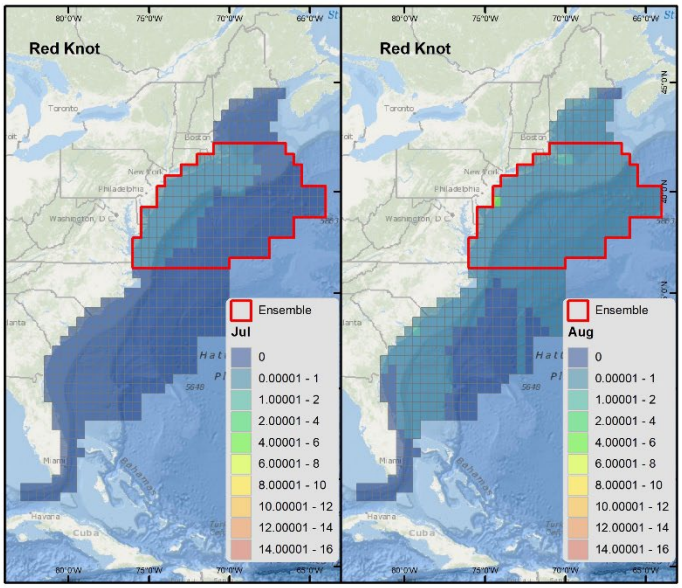

0 250 500 1,000 Miles

0 400 800 1,600 Km

Coordinate System: WGS 1984 Web Mercator Auxiliary Sphere

Service Layer Credits: Sources: Esri, GEBCO, NOAA, National Geographic, Garmin, HERE, Geonames.org, and other contributors

Monthly cumulative use
from ensemble movement models for
Motus and satellite-tracked Red Knot

Version date: 7/12/2024

Document: REKN_monthly_ensemble_model_240711_2panel

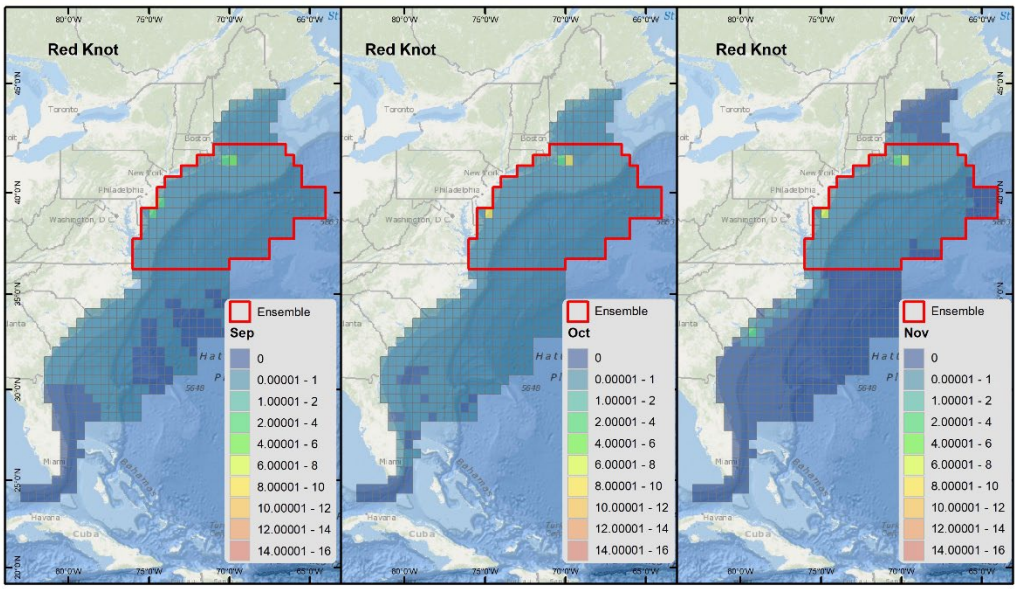

0 250 500 1,000 Miles

0 400 800 1,600 Km

Coordinate System: WGS 1984 Web Mercator Auxiliary Sphere

Service Layer Credits: Sources: Esri, GEBCO, NOAA, National Geographic, Garmin, HERE, Geonames.org, and other contributors

Monthly cumulative use
from ensemble movement model for
Motus and satellite-tracked Red Knot

Version date: 7/12/2024

Document: REKN_monthly_ensemble_model_240711_3panel

Figure 8. Cumulative use estimates by month from the ensemble model for Motus- and satellite-tracked red knots.
Estimates were based on single-state movement models using Motus- (within the red study area) and satellite-based data (within the red study area and elsewhere on the US Atlantic Outer Continental Shelf), and the number of tagged individuals in the study. "Cumulative use" summed daily occupancy probabilities estimated via SCRAM for each month with greater than five tracked individuals. Estimates covered July–August (top panel) and September–November (bottom panel)for Red Knots (see Table 7 for monthly sample sizes).

2.2.8 Analytical Assumptions of the Movement Models

Key assumptions of the updated movement models are listed as follows. The movement models assumed that:

1. Estimated behaviors represented an unbiased sample of fall migratory patterns for red knots and piping plovers, and an unbiased sample of breeding and post-breeding dispersal movement patterns for roseate terns.
2. Estimated behaviors represented an unbiased sample of offshore behaviors for the study species.
3. Environmental conditions during the tracking periods were representative of the study area.
4. Estimated pre-construction behaviors were representative of post-construction behaviors for the study species.
5. Habitat use estimates were proportional to the true population size of the study species.

Violation of these assumptions could lead to over- and/or under-estimates of exposure, depending on how sampling bias or measurement error impacted the estimates (see "Collision Risk Modeling," below). For a more complete list of assumptions and limitations relating to SCRAM, see Adams et al. (2022).

2.3 Flight Height Modeling for Red Knots

SCRAM 1.0.3 used flight height estimates from Motus tracking data for all three study species (Loring et al. 2021). The source of flight height estimates for piping plovers and roseate terns (as discussed in Adams et al. 2022) remained the same in SCRAM 2. However, the accuracy of this approach was challenging to validate, and flight height estimation uncertainty could not be propagated into the resulting flight height distribution. The inclusion of GPS tags in the SCRAM database for red knots presented an opportunity to use altitude estimates from these devices for new flight height distribution estimates in Phase 2. The consistent duty cycles of the GPS tags served to improve the accuracy of the SCRAM flight height estimates, as modeled from altitude fixes (i.e., measured heights at given coordinates). They also allowed for inclusion of different types of uncertainty into the final estimated flight height distributions. For these reasons, the ensemble approach used in the movement models was not extended to the flight heights from the new GPS data and old Motus data. Rather, the updated SCRAM 2 GPS flight height modeling replaced the SCRAM 1.0.3 Motus approach for red knots, due to the uncertainty propagation from the flight height measurement process and direct observation of flight heights from an accurate sensor.

2.3.1 Flight Height Data Management

Satellite telemetry data from 132 individuals with 6900 flight height observations (6658 with successful altitude measurements) were used to estimate the red knot offshore flight height distribution. Preparation for the development of flight height estimates from Lotek PinPoint GPS-Argos 75 transmitters (hereafter "GPS transmitters' or "GPS tags") included two key components: the correction of flight height values recorded on tags, and the determination of behavioral states for each record and individual, using the 2D position data. Raw altitude data were measured in meters and were referenced to the ellipsoid. To obtain

altitude measurements that referenced the surface of the earth, all altitudes were converted to altitude above the geoid (EGM 2008; Pavlis et al. 2012) by subtracting the difference between the ellipsoid-based altitude and the geoid at the location of the tag transmission. In most cases, this altitude above the geoid is considered synonymous with height above mean sea level, barring small scale fluctuations such as tidal height and sea surface height anomalies (Johnston et al. 2023). All altitudes used were measured over water, referenced to the height above the geoid. We assume the geoid is the reference used by offshore wind developers when estimating turbine height, but we are unclear if this is what all developers do. More detail on turbine height references would be useful for SCRAM in the future so we can incorporate this into the modeling process. Further corrections were required for GPS altitude measurements that were transmitted over land or in intertidal regions to obtain altitude measurements above ground level. Transmissions over land were considered to include any points within 50m of the shoreline (based on a 1:10m resolution land polygon obtained from Natural Earth[7]. To correct altitudes transmitted over land, a global relief grid-registered model (Amante and Eakins 2009) was subtracted from geoid-referenced altitudes to obtain flight altitude above ground level. As a result, the flight heights used in subsequent state space models were based on height above sea level or ground level, based on the geographic location of points over terrestrial or ocean environments.

Previous flight height estimation models have incorporated behavioral states to inform the measurement and uncertainty of flight height for different behaviors (Ross-Smith et al. 2016; Peschko et al. 2021; Johnston et al. 2023). Here, behavioral states were classified using Expectation-Maximization Binary Clustering with R Package "EMbC" (Version 2.0.4; Garriga et al. 2016), a Gaussian mixture model that uses speed and turning angle between GPS latitude/longitude fixes to classify the following four behavioral states: 1) high turning angle, high speed; 2) high turning angle, low speed; 3) low turning angle, high speed; and 4) low turning angle, low speed. There was also a delineation for points where no behavioral state was determined. The EMbC model was run for all points for all individuals, resulting in one behavioral state attribution for each transmission. Dawn/dusk times were used to determine if each observation occurred during day or night.

The raw altitudes estimated from GPS data included 6658 recorded altitudes, and 51% of the altitude values were below zero (range: -101m to 6894m; mean: 29.4m; standard deviation: 283.2m). Once corrections were made to obtain flight heights relative to the geoid (resulting in altitudes above mean sea level for flight heights over water) and relative to a digital elevation model (for flight heights over land), 6.2% of the altitudes were comprised of values below zero (range: -87.4m to 6926.6m; mean: 60.9m; standard deviation +/- 273.2m).

2.3.2 Flight Height Modeling Methods

We analyzed the corrected flight height data with a state-space modeling framework, which was developed for all flight heights that include both overland and overwater positions. This class of statistical model was useful for time series with multiple processes influencing the response variable (i.e., flight height). In this case, we followed a similar approach to Ross-Smith et al. (2016), who used GPS tracking data from lesser black-backed gulls (*Larus fuscus*) and great skuas (*Stercorarius skua*) to estimate flight height distributions for collision risk modeling. While these species have different flight behaviors from red knots, they share a key similarity in that these birds do not dive below the ocean surface. This similarity upholds many of the assumptions made by Ross-Smith et al. (2016). As such, the SCRAM

[7] Natural Earth: https://www.naturalearthdata.com/

flight height model has a similar structure to Ross-Smith et al. (2016), though the tags we used for this study had different flight height estimation processes and we incorporated different covariates.

The general form of the model differentiated the factors that influenced flight height into two components: the observation model and the process model. The models were linked: the observation model describes how flight height observations (obs_{it}) were related to true flight height (Z_{it}) as they varied across individual *i* and time step *t*. The observation model used information from satellite tags to quantify changes in uncertainty around the altitude measurements, and the process model explained variation in true flight height as a function of individual and environmental effects. Mathematically, the structure of this model is:

$$obs_{it} \sim N(Z_{it}, \sigma_{obs,it})$$

$$\log(Z_{it}) \sim N(\mu_{it}, \sigma_Z)$$

Where, $\sigma_{obs,it}$ is the standard deviation of the Gaussian uncertainty in the observation model, varied by individual and time. σ_Z is the standard deviation of the log-Gaussian process model and is constant across indices. The mean expectation of the process model, μ_{it}, is the component of that model that varies with *i* and *t*. The observation model is Gaussian with an expectation of Z_{it}, but the process model is log-Gaussian. This linkage allows uncertainty to be Gaussian in the measurement space but prevents true flight heights from including values below zero. Importantly this allows the error structure of the observation model to be consistent with the expected uncertainty in the GPS devices, as position uncertainty is often Gaussian (Péron et al. 2020), but vertical positions below the mean ocean height were almost certainly erroneous for this species. Thus, differentiating these effects into two models accommodated the multifaceted sources of variance in the flight height distributions of species measured through telemetry.

The observation model allowed variation in uncertainty through the variance parameter. Using a linear modeling framework, covariates to flight height estimation uncertainty were included:

$$\log(\sigma_{obs,it}) = \alpha_{obs} + \beta_{obs1} X_{obs1,it} + \beta_{obs2} X_{obs2,it}$$

Where, α_{obs} is the variance intercept and $\beta_{obs1}$and β_{obs2} are slope parameters that estimate the effect of covariates $X_{obs1,it}$and $X_{obs2,it}$. Using two covariates provided by Lotek (fix quality and cyclic redundancy check, CRC, respectively), we incorporated variation in the uncertainty of flight height estimates from this process into the observation model. Fix quality determined whether the measured point was an accurate three-dimensional ('3D') estimate or only a two-dimensional ('2D') estimate. 2D estimates did have estimated flight heights, but the position quality was expected to be lower. CRC identified if the 3D position had to be corrected. These covariates could influence the uncertainty in the altitude estimate.

The process model contained a log-linear model describing the relationship between the model's true flight height expectation and relevant covariates:

$$\mu_{it} = \alpha_Z + \beta_{ind,i} + \beta_{Z1} X_{Z1,it} + \beta_{Z2} X_{Z2,it} + \beta_{Z3} X_{Z3,it} + \beta_{Z4} X_{Z4,it} + \beta_{Z5} X_{Z5,it} + \beta_{Z6} X_{Z6,it}$$

$$\beta_{ind,i} \sim N(0, \sigma_{ind})$$

Where α_Z is the variance intercept, and the β_Z parameters are linear slope estimates that relate to the X_Z covariates. An individual random effect is included via $\beta_{ind,i}$, which is distributed as a zero-centered Gaussian with standard deviation σ_{ind}. These covariates are related to animal behavior, time of day, and distance to shore. β_{Z1} through β_{Z4} are categorical covariates representing movement states of animals

(states 2-5 [low speed/high turning angle, high/low, high/high, unknown] that are compared to the indexed state 1 [low/low]). Time of day and distance from shore are incorporated via β_{Z5} and β_{Z6}.

Uninformed Gaussian priors were used for all parameters except for σ_Z, which used an uninformed Gamma prior. The model was fit using NIMBLE, a Bayesian modeling framework in R (Michaud et al. 2021) and the model code is found in the SCRAM2 GitHub repository[8]. Hamiltonian Monte Carlo (HMC) was used for model likelihood estimation with a burn-in of 1000 and posterior draw of 1000 across three chains. Parameter convergence was assessed visually and using the Gelman-Rubin statistic ($\hat{r}$). All parameters and the model predicted true flights (Z_{it}) were below the $\hat{r}$ threshold of 1.1. Posterior data simulation was used to assess model fit, and the simulated data sets had similar moments. The model-generated data did have lower mean and standard deviation than the observations, but showed strong overall agreement with the original data and good evidence that model fit was appropriate.

2.3.3 Estimating Flight Height Distributions

The posterior estimates of all true flight heights that occurred over water were used to estimate the flight height distribution for red knots for SCRAM. The true flight heights had a different distribution than the corrected raw values with all values being greater than zero and lower mean and standard deviation (range: 2.3- 6926.5m; mean: 46m; median: 33.8; standard deviation: 176.5). We prioritized over-water flights to coincide with the SCRAM study area. We defined over-water as >50m from the coastline and selected flight heights from that subset of locations. For the 272 observations without flight height estimates, the model-predicted flight height estimates were used in this analysis. From these observations, 1000 posterior draws from a HMC chain were selected. For each draw, the true flight height estimates were compiled and the density of that distribution in 1m bins was calculated. The mean flight height distribution incorporated into SCRAM showed two modes: a peak below 10m and a peak at 40m (Figure 9, top). The uncertainty from these results was then propagated through to the CRM framework.

The flight height distribution estimated from this approach is considerably different than the distribution estimated in SCRAM 1.0.3 (Figure 9). Notably, the lack of uncertainty propagation in SCRAM 1.0.3 shows patchier and more accurate estimates of flight height density. Moreover, there are fewer low altitude detections and more high-altitude detections. However, the sums of probability density for the altitude range of a standard rotor swept zone (25–225m) were similar between the two methods (e.g., though the flight height distribution changed substantially between SCRAM versions, the resulting influence on collision risk estimates was minor). SCRAM 2 showed 53% and SCRAM 1.0.3 showed 55% of detections within the 25–225m range. While these overall values are similar note that Option 3 in the SCRAM collision risk model accounts for the specific flight heights relative to turbine blades. So collision probability likely will change for Option 3 specifically because SCRAM 2's flight heights have a lower mean and collision probability decreases as birds move away from the turbine nacelle.

2.3.4 Analytical Assumptions of the Flight Height Model for Red Knots

A more complete review of SCRAM's limitations and assumptions with flight height was included in Adams et al. (2022). The new flight height model for Red Knots assumes:

1. That tracked red knots are representative and unbiased sample of the *rufa* red knot population.
2. GPS altitude estimates are an unbiased estimator of *rufa* red knot flight height.
3. Individuals are similar in flight height behaviors in the sampled population.

[8] SCRAM2 GitHub repository: https://github.com/Biodiversity-Research-Institute/SCRAM2

4. GPS duty cycle is fine enough to capture overwater migratory flight heights.
5. GPS-measured altitude relative to the geoid is suitable for comparison to turbine height measurements, rather than measuring altitude relative to fine-scale oceanographic variability (e.g., sea surface height anomaly, tidal fluctuations).

In the above order, the consequences of violating these assumptions are:

1. Unclear; it depends on how sampling bias impacts the estimates.
2. Likely underestimating flight heights; Lato et al. (2022) suggest bias in altitude estimates that vary across transmitters and also tend to be lower than the true estimate. Future work on incorporating known biases into these models will be useful for assessing this effect.
3. Likely underestimating uncertainty; if significant variation exists across individuals then it should be accounted for directly in flight height distribution estimation.
4. Likely underestimating maximum flight heights; high altitude flights are likely relatively rare at the scale of the annual cycle, so we likely underestimate overwater flight heights with an infrequent duty cycle. A higher sampling frequency would allow us to better estimate the overwater flight heights.
5. Unclear; if tidal variation is significant then we could be overestimating flight heights because below 0 flight heights (geoid reference) are more likely. But this is unlikely to influence the estimate of animals within the rotor swept zone. If different developers are standardizing turbine heights on different reference points from the geoid, then our estimates would be biased until those references were identified and corrected.

2.3.5 Conclusions

The revised models for the red knot flight height distribution presented significant updates in SCRAM 2, though with caveats consistent with SCRAM 1.0.3. Spatial sampling bias was a significant limitation in both the Motus and satellite-based datasets, particularly from the lack of over-water movements during northbound migration south of the U.S. Mid-Atlantic. SCRAM 2 did not model spring migratory movements, due to lack of data, yet it assumed that observed flight heights were representative of the broader population. Therefore, any differences in flight heights that occurred early in the boreal spring remained underrepresented, presenting potential bias in the estimated flight height distribution. However, since SCRAM does not currently estimate collision risk for red knots during the spring, the effects of this potential bias are expected to be minimal. Individuals with more data points also contributed more to the population flight height distribution. This problem is common to most telemetry studies (Lindberg and Walker 2007, Girard et al. 2002; and other applications of these datasets in SCRAM). To ameliorate this issue, more satellite-based telemetry deployments are needed that place particular attention on distributing telemetry devices evenly across breeding and wintering populations.

The flight height estimation methods used for red knots in SCRAM 2 held several distinct advantages over SCRAM 1.0.3. Measurement uncertainty was estimated directly with the state-space framework, and propagated into the CRM, unlike the Motus flight height approach. Further, the SCRAM 2 method allowed for variance in uncertainty and filled in gaps in the flight height distribution profile by using environmental covariates to better estimate true altitude. Future work on flight height distributions for SCRAM should focus on incorporating measurement validation data into the models, quantifying uncertainty in the flight height estimates, accounting for variable differences in time between flight height observations and developing ecological models that better account for temporal autocorrelation in observations. If GPS-based altitude estimates become available for other focal species in SCRAM, we recommend similar flight height model updates to those implemented here for red knots.

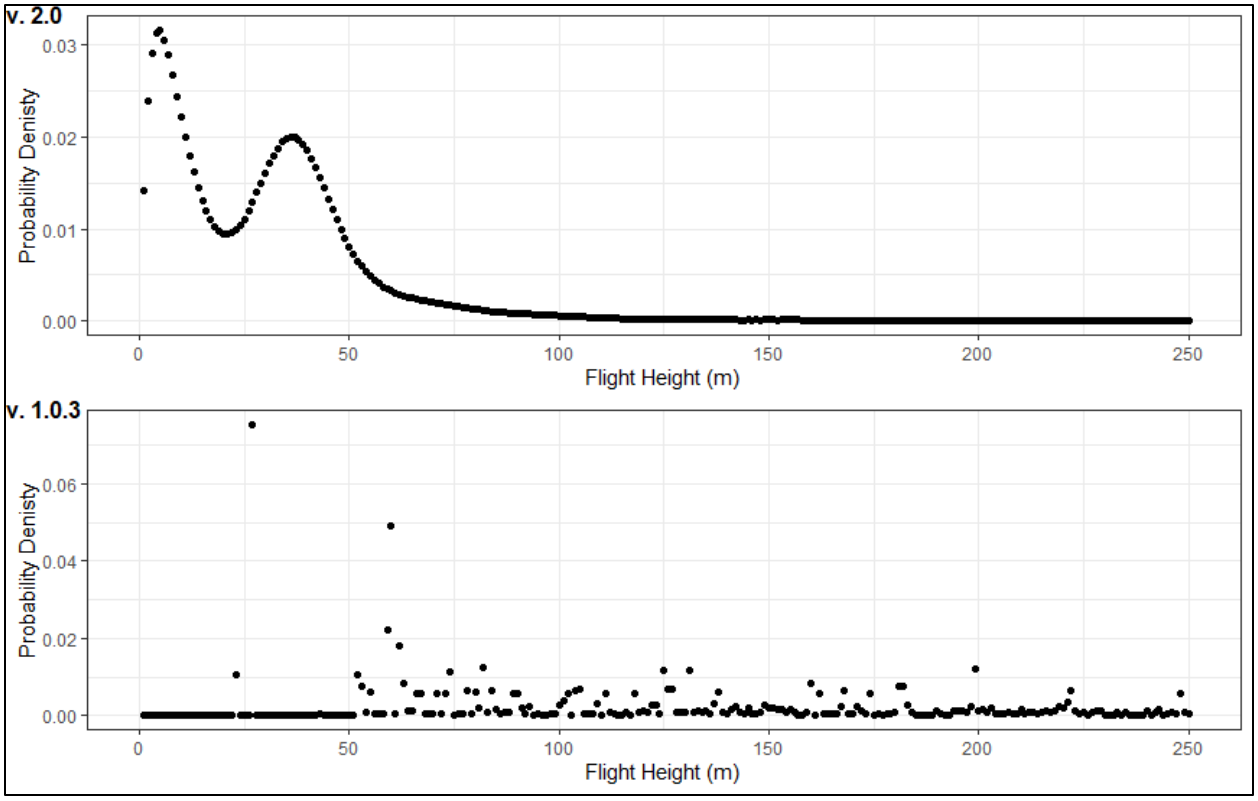

Figure 9. Comparison of flight height estimates for Red Knots between SCRAM versions. SCRAM 2 (top panel) uses a state space modeling framework to estimate flight heights from GPS transmitters deployed from 2020-2023. SCRAM 1.0.3 (bottom panel) used estimates from a movement model that used data from Motus tags to estimate the position of the animal. The mean estimate for the posterior draws (top) and bootstrapped estimates (bottom) is shown by 1m altitude bins.

2.4 Collision Risk Modeling

SCRAM 1.0.3's collision risk model (CRM) was based on McGregor et al. (2018) with some additional modifications (Adams et al. 2022), and could only be run via the RShiny web application. SCRAM 2's CRM codebase was converted using stochLAB (Caneco et al. 2022) to align with the most updated CRM used in the United Kingdom and utilize its error detection tools (Caneco et al. 2022), as well as to allow SCRAM to run in R separately from the web application (which better allowed for sensitivity analyses and other plans for further improvements). This code was repeatedly reviewed and several bug fixes were implemented since the McGregor et al. (2018) version of the stochCRM was published. Additionally, stochLAB code included several major improvements to accelerate runtime. As a result, the CRM in SCRAM 2, while functionally the same model structure as in SCRAM 1.0.3, ran substantially faster. Through this transition, bugs were fixed in the original SCRAM code as well as the stochLAB code. These bugs included a slight error in the calculation of turbine rotor heights (as noted in McGregor et al. 2018) and an incorrect default metric for chord pitch (which was in degrees rather than radians; G. Humphries pers. comm.) An additional bug encountered in the stochLAB R package (which did not affect the accuracy of results from the stochLAB RShiny interface) impacted Option 3 collision risk estimation. There was misalignment between altitude-specific collision risk and the flight height data, caused by insufficient sampling of the vertical component of the rotor swept zone. Essentially, avian flux was less likely to be counted at the fringes of the flight height range than it should be. The solution was to increase the vertical sampling rate for the collision model to ensure that flight height data were included from infrequently flown altitudes. In fixing this bug for SCRAM, we were able to increase the precision of

Option 3 estimations of the collision integral and flight height distribution. We allowed SCRAM to sample the rotor swept zone with a higher density of horizontal slices, which improved the altitude-specific collision estimates by combining the flux and collision integrals.

Finally, we adjusted the avoidance rate estimates for the basic model (Option 1 in SCRAM 1.0.3, renamed to Option 2 in SCRAM 2; see "Addition of a Band Annex 6 Module," below). In SCRAM 1.0.3, a single set of avoidance values per species was used for both collision risk estimation options. SCRAM 2 used slightly different values for the basic vs. extended model, as discussed in the "Morphometrics and Behavioral Data," above. Altogether, these changes to SCRAM 2 tended to result in lower collision risk estimates than those of SCRAM 1.0.3, all else being equal. The full code base for each version of SCRAM is available for comparison in GitHub[9].

2.4.1 Analytical Assumptions of the Collision Risk Models

The collision risk models assumed that:

1. Morphometric data were well-described by a Gaussian distribution and were representative of the populations at risk of collisions with offshore wind farms in the study area.
2. Birds were exposed to a turbine only once in a day, but they could be exposed to a turbine multiple times in a month.
3. The proportion of headwinds and tailwinds were equal at the wind farm, wind speeds were constant during operational periods, and other weather conditions (e.g., rain, fog, wind wake) did not influence collision risk.
4. Probability of collision was equal among turbines.
5. Birds did not adjust their behaviors to avoid wind farms altogether (i.e., macro-avoidance)

Violation of these assumptions could potentially result in:

6. Underestimates of collision risk for birds that flew slower than their species' assumed mean flight speed, or overestimates of collision risk for birds that flew faster than their assumed mean flight speed.
7. Underestimates of collision risk for species that transited a wind farm multiple times per day.
8. More variability in collision risk than estimated, due to real-world weather conditions at turbines.
9. Underestimates of collision risk for birds attracted to structures (e.g., for perching).
10. Overestimates of collision risk for birds that exhibited macro-avoidance.

2.5 Web Application

2.5.1 Addition of a Band Annex 6 Module

USFWS runs both SCRAM and the Band (2012) Annex 6 collision risk model for migrants as part of the process of assessing risk from offshore wind projects in the NES (P. Loring, pers. comm.). Both models require a pre-specified regional population size estimate. However, SCRAM uses movement model results to estimate the number of individuals from the regional population that may be exposed to a wind project (and thus may be at risk of collisions) at a given location. In contrast, the Band (2012) Annex 6

[9] The full code base for each version of SCRAM is available for comparison in GitHub (https://github.com/Biodiversity-Research-Institute/SCRAM and https://github.com/Biodiversity-ResearchInstitute/SCRAM2, respectively).

model for migrants assumes a uniform distribution of the migrant population across a pre-specified migratory corridor width. While corridor width can change with latitude, the assumption of a uniform distribution over that region is a key feature of the Band Annex 6 model, and is likely inaccurate for most species.

An implementation of the Band (2012) Annex 6 collision risk model for migrants has been added as a new module within the SCRAM RShiny tool to help improve USFWS risk assessment process, which previously utilized the Band (2012) collision risk spreadsheet (P. Loring, pers comm). This stochastic version of the Band CRM can be run alongside SCRAM, to help estimate uncertainty in results. Band results are now reported similarly to SCRAM (as a PDF report that includes all relevant inputs and outputs), making it easier to track inputs/outputs for each model run using both types of CRMs. The addition of this module allows for substantially improved ease of use, easier comparisons between results of models, and the implementation of a stochastic version of the Band (2012) model.

The Band (2012) Annex 6 migrant model was designed to be used with migrant species where information was lacking on their offshore movements. However, to create these estimates, assumptions must be made about the distribution of migrating animals. First, each individual in the migrating population has two opportunities for collision per year (one on the northbound migration and the other on the southbound migration). Second, migrants are evenly distributed across the expert-defined migratory corridor. Third, migrants could be avoiding the OCS entirely during certain times of year. The effects of these assumptions will vary by location, but more than one opportunity for collision is likely for migrants per migratory season due to non-linear migratory movements like reverse migration. Further, there does appear to be evidence that some species could be moving around, rather than through, the study area. More data from GPS transmitters will be useful for describing these patterns and determining appropriate adjustments to Band model assumptions.

The Band (2012) Annex 6 module in the SCRAM web application makes collision risk predictions for all months in which the focal species are assumed to be migrating through the study area (Table 4), and thus includes a slightly larger range of months than the SCRAM module, which is limited by the months in which there were sufficient tracking data to inform model predictions (Table 7). Additionally, the Band module is not limited to the spatial area in which Motus stations were being actively maintained during the tracking study (Loring et al. 2018; Loring et al. 2019). Thus, SCRAM and Band collision risk estimates encompass different spatial and temporal extents and are not directly comparable. However, the Annex 6 model provides a useful contrast with the SCRAM movement model results, and provides a check on assumptions in the collision risk estimates generated using movement models (see Adams et al. 2022 for further detail on these assumptions).

2.5.2 Other Updates

We removed the sensitivity analysis button and output from the web application for SCRAM 2. This functionality was not being utilized and a formal sensitivity analysis is planned for a later date. Since the improved computational efficiencies in the collision risk models (as described in “Collision Risk Modeling,” above) greatly reduced the time for the model to complete, the “cancel model” button was also removed and the range of allowable model iterations was increased from 100–10,000 (SCRAM 1.0.03) to 2,500–25,000 (SCRAM 2). As with SCRAM 1.0.3, at least 10,000 model iterations are recommended.

Lastly, SCRAM allows for two different collision risk estimation methods. The options in SCRAM 2 are calculated almost identically to SCRAM 1.0.3 (see “Morphometric and Behavioral Data,” above), but Option 1 has been renamed as Option 2 to align SCRAM nomenclature with that of Band (2012) and stochLAB (Caneco et al. 2022). Option 2 (formerly Option 1) uses general flight height data to run a Band Annex 6 model (not location-specific data), so we renamed it to bring this into alignment with

stochLAB options. SCRAM does not use location-specific flight-height data. Option 2 estimates the collision rate for the entire RSZ, whereas Option 3 estimates it in discrete increments of approximately 5 m or less. As stated in Adams et al. (2022), we generally recommend the use of Option 3 whenever possible, since it directly pairs flight height with altitude-specific turbine collision rates. Thus, if birds are more common at heights where collision probability is lower in the turbine RSZ, Option 3 accounts for the decreased collision risk while Option 2 would not.

2.6 User Manual and Code

The code for SCRAM 2 was substantially updated as described in the above sections of this report (and as summarized in Table 1). The user manual was also updated to match the revised web application[10].

3 Comparison of SCRAM 1.0.3 to SCRAM 2 Estimates of Collision Risk

Collision risk estimates varied between SCRAM 1.0.3 and SCRAM 2, for a variety of reasons that were not uniform by species nor location within the NES (Table 1). To illustrate some differences, we compared outputs of the movement models for Red Knots between SCRAM v. 1.0.3 and SCRAM v. 2.1.6. We used three locations that were arbitrarily selected within the Motus study area but outside of existing lease areas (Figure 10). We used the "Example wind farm input" available in each of the respective online tools and updated the centroid coordinates (i.e., Latitude and Longitude). These two files contained equivalent rotor and wind speed parameters for "Run 2", a 15 GW example turbine model, using the following conversion (Adams et al. 2022):

$$w = 60 * TSR * S/(2\,\pi r)$$

Where w is the rotations per minute, tip speed ratio (TSR) = 5.5, S is wind speed (m/s), and r is the rotor radius (m). We selected Option 3 ("slower but more precise") and otherwise relied on tool recommendations and defaults (e.g., a collision threshold of 1, using the recommended minimum iterations of 1,000 for SCRAM v. 1.0.3 and 10,000 for SCRAM v. 2.1.6). We reported the annual mean collisions for Run 2 (a 15 GW example turbine model).

The new collision risk estimates more often declined than increased for red knots from SCRAM 1.0.3 to SCRAM 2 (Table 8). These changes related to a combination of factors, including increased sample size, incorporation of GPS and Argos tracking data, improved model fit, the switch from two-state to one-state models, updates to the red knot monthly regional population size estimates, flight height estimates, and bug fixes (Table 1).

[10] As with SCRAM 1.0.3, the updated SCRAM 2 web application, model code, and user manual are available at and https://github.com/Biodiversity-Research-Institute/SCRAM2. All study products are also available via https://briwildlife.org/SCRAM/.

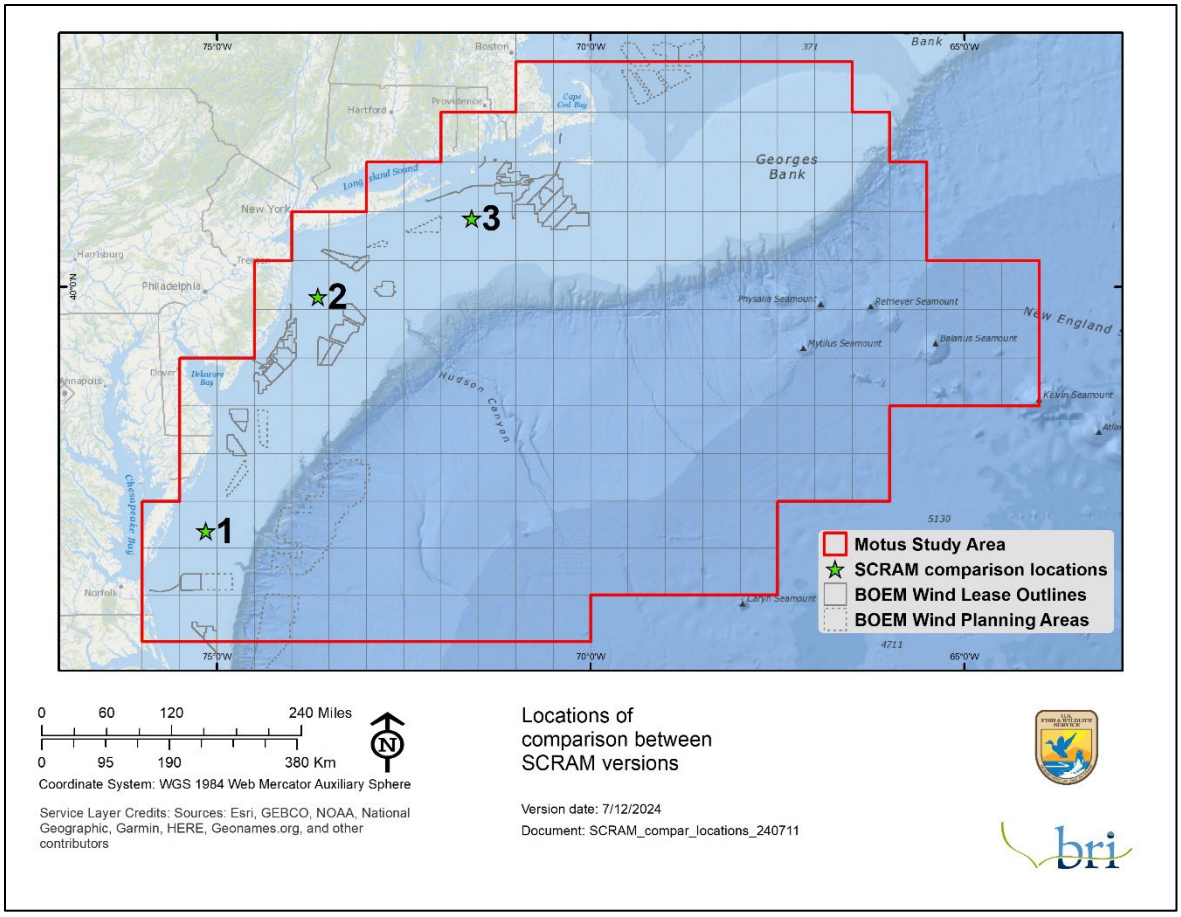

Figure 10. Locations selected for comparisons of collision risk estimates between SCRAM versions.
Location coordinates are presented in Table 8.

Table 8. Example collision estimates for Red Knots compared between SCRAM 1.0.3 and SCRAM v. 2.1.6.

Annual mean collisions were estimated at three locations in the study area, using a 15 GW example turbine model. Latitude and longitude are in decimal degrees.

Species	Location	Latitude	Longitude	SCRAM 1.0.3	SCRAM 2.1.6
Red Knot	1	37.45	-75.15	0.062	0.039
-	2	39.90	-73.65	0.035	0.063
-	3	40.70	-71.59	17.500	0.028

4 Future Work

SCRAM is a decision support tool that may be used to assess the relative risk of collisions (e.g., as compared among various project design envelopes; Adams et al. 2022), and may also inform future

research efforts. The limitations and analytical assumptions of the models provide insight into how data inputs may be improved to advance model development. For example, the most conspicuous information gap in SCRAM is the lack of spring migration data. Future tracking efforts (both Motus and satellite-based) should target full spring migration to inform northbound movements in SCRAM (i.e., through tagging efforts south of U.S. federal waters prior to spring movements). Additionally, the inclusion of satellite-based data in SCRAM 2 highlights the importance of tracking sub-daily movements to inform collision risk. Though sub-daily duty cycles in GPS data are recommended for future data collection, to inform both movement and flight height models, new Motus data sources may also help inform SCRAM development if they meet certain criteria. Such data would ideally include (1) high quality data filtering (e.g., to minimize false positives) and (2) adequate station coverage in the study area during the study period (i.e., including continued station maintenance to minimize downtime). Further development of the collision risk model to accommodate sub-daily movements would also benefit from data inputs on daily or sub-daily environmental and/or turbine operational conditions (e.g., average winds and/or turbine rotor speeds). Variations in these parameters over time are not currently built into any Band-type collision risk models. However, it may be a fruitful area of future model development.

Additionally, a recent meeting of the newly established international collision risk modeling workgroup in July 2024 suggested two potential priorities for future work:

- Development of guidance for the deployment of tracking devices on focal species (e.g., when, where, and how many tags should be deployed on each species to adequately sample the population of interest). In the United States, this guidance should be developed in collaboration with the Regional Wildlife Science Collaborative.
- Development of a database of wind turbine models and input parameters (e.g., tidal offsets as detailed in Band 2012, as well as turbine characteristics) to inform collision risk modeling.

Phase 3 of SCRAM (September 2024 to September 2026) is expected to include the following activities:

- Further updates to the regional population size estimates provided by the USFWS, based on the best available data.
- Continued updates to the structure of movement models and improved precision of movement modeling estimates.
- Incorporation of additional data into movement models (e.g., new species, new tracking technologies, and new datasets for species and tracking technologies already included in SCRAM, as available; e.g., Perkins 2024).
- Further development of the flight height modeling process as new data become available and methods are refined.
- Further consideration of approaches for estimating flight speed, as new data and methods become available.
- Re-examination of how uncertainty flows through the models and further sensitivity testing to 1) more clearly specify the assumptions in the SCRAM framework, and 2) identify key parameters driving model results to refine parameter estimation or inform further data collection.
- Update of the web application to apply a proportional adjustment to collision risk estimates for wind projects that are located in multiple grid cells within the NES study area (based on the percentage of the wind project located in each grid cell).
- Work with international collaborators to develop a common approach for obtaining biologically defensible cumulative effects estimates to meet regulatory needs.
- Continue to host and update the web application.
- Work with CRM experts in the UK to provide external review and feedback on the new version of SCRAM.

- Conduct additional outreach activities to help offshore wind stakeholders in the U.S. to better understand SCRAM and collision risk models generally.

5 Works Cited

Adams E, A Gilbert, P Loring, KA Williams. 2022. Transparent Modeling of Collision Risk for Three Federally Listed Bird Species in Relation to Offshore Wind Energy Development: Final Report. Washington, DC: U.S. Department of the Interior, Bureau of Ocean Energy Management Report No.: OCS Study BOEM 2022-071.

Amante C, Eakins BW. 2009. ETOPO1 1 Arc-Minute Global Relief Model: Procedures, Data Sources and Analysis. NOAA Technical Memorandum NESDIS NGDC-24 National Geophysical Data Center, NOAA. doi:10.7289/V5C8276M.

Auger-Méthé M, Newman K, Cole D, Empacher F, Gryba R, King AA, Leos-Barajas V, Mills Flemming J, Nielsen A, Petris G, et al. 2021. A guide to state–space modeling of ecological time series. Ecological Monographs. 91(4):e01470. doi:10.1002/ecm.1470.

Baldwin JW, Leap K, Finn JT, Smetzer JR. 2018. Bayesian state-space models reveal unobserved off-shore nocturnal migration from Motus data. Ecological Modelling. 386:38–46.

Band B. 2012. Using a collision risk model to assess bird collision risks for offshore windfarms. The Crown Estate as part of the Strategic Ornithological Support Services Programme, SOSS-02. 62 pp.

Caneco B, Humphries G, Cook AS, Masden E. 2022. Estimating bird collisions at offshore windfarms with stochLAB. https://hidef-aerial-surveying.github.io/stochLAB/.

Cook ASCP. 2021. Additional analysis to inform SNCB recommendations regarding collision risk modelling. BTO Research Report. 739:48.

Douglas DC, Weinzierl R, C. Davidson S, Kays R, Wikelski M, Bohrer G. 2012. Moderating Argos location errors in animal tracking data. Methods in Ecology and Evolution. 3(6):999–1007. doi:10.1111/j.2041-210X.2012.00245.x.

Garriga J, Palmer JRB, Oltra A, Bartumeus F. 2016. Expectation-Maximization Binary Clustering for Behavioural Annotation. PLOS ONE. 11(3):e0151984. doi:10.1371/journal.pone.0151984.

Gelman A, Rubin DB. 1992. Inference from iterative simulation using multiple sequences. Statistical science. 7(4):457–472.

Girard I, Ouellet J-P, Courtois R, Dussault C, Breton L. 2002. Effects of sampling effort based on GPS telemetry on home-range size estimations. The Journal of wildlife management.:1290–1300.

Johnson D, London J. 2018. crawl: an R package for fitting continuous-time correlated random walk models to animal movement data. https://doi.org/10.5281/zenodo.596464.

Johnson DS, London JM, Lea M-A, Durban JW. 2008. Continuous-time correlated random walk model for animal telemetry data. Ecology. 89(5):1208–1215.

Johnston DT, Thaxter CB, Boersch-Supan PH, Davies JG, Clewley GD, Green RMW, Shamoun-Baranes J, Cook ASCP, Burton NHK, Humphreys EM. 2023. Flight heights obtained from GPS versus altimeters influence estimates of collision risk with offshore wind turbines in Lesser Black-backed Gulls Larus fuscus. Mov Ecol. 11(1):66. doi:10.1186/s40462-023-00431-z.

Jonsen I. 2016. Joint estimation over multiple individuals improves behavioural state inference from animal movement data. Scientific reports. 6(1):20625.

Kéry M, Royle JA. 2016. Applied hierarchical modeling in ecology: analysis of distribution, abundance and species richness in R and BUGS. Volume 1, Prelude and static models. Boston, MA: Academic Press.

Lato KA, Stepanuk JEF, Heywood EI, Conners MG, Thorne LH. 2022. Assessing the accuracy of altitude estimates in avian biologging devices. PLOS ONE. 17(10):e0276098. doi:10.1371/journal.pone.0276098.

Lindberg MS, Walker J. 2007. Satellite telemetry in avian research and management: sample size considerations. Journal of Wildlife Management. 71(3):1002–1009. doi:10.2193/2005-696.

Loring P, Lenske A, McLaren J, Aikens M, Anderson A, Aubrey Y, Dalton E, Dey A, Friis C, Hamilton D, et al. 2021. Tracking Movements of Migratory Shorebirds in the US Atlantic Outer Continental Shelf Region. Sterling (VA): US Department of the Interior, Bureau of Ocean Energy Management. OCS Study BOEM 2021-008. 104 p.

Loring P, Paton P, McLaren J, Bai H, Janaswamy R, Goyert H, Griffin C, Sievert P. 2019. Tracking Offshore Occurrence of Common Terns, Endangered Roseate Terns, and Threatened Piping Plovers with VHF Arrays. Sterling, Virginia: US Department of the Interior, Bureau of Ocean Energy Management.

Loring PH, McLaren JD, Smith PA, Niles LJ, Koch SL, Goyert HF, Bai H. 2018. Tracking Movements of Threatened Migratory rufa Red Knots in U.S. Atlantic Outer Continental Shelf Waters. OCS Study BOEM 2018-046. U.S. Department of the Interior, Bureau of Ocean Energy Management, Sterling, VA. 145 pp.

Masden E. 2015. Developing an avian collision risk model to incorporate variability and uncertainty. Scottish Marine and Freshwater Science. 6(14):43. doi:10.7489/1659-1.

Michaud N, de Valpine P, Turek D, Paciorek CJ, Nguyen D. 2021. Sequential Monte Carlo methods in the nimble and nimbleSMC R packages. Journal of Statistical Software. 100:1–39.

Ozsanlav-Harris L, Inger R, Sherley R. 2023. Review of data used to calculate avoidance rates for collision risk modelling of seabirds. Joint Nature Conservation Committee. JNCC Report 732:60.

Pavlis NK, Holmes SA, Kenyon SC, Factor JK. 2012. The development and evaluation of the Earth Gravitational Model 2008 (EGM2008). Journal of Geophysical Research: Solid Earth. 117(B04406). doi:10.1029/2011JB008916. 10.1029/2011JB008916.

Perkins G. 2024. Migratory Bird Satellite Tracking Synthesis: Using cutting edge data to advance understanding of Red Knot migration and breeding patterns. Ninox Consulting Ltd. 62 pp.

Péron G, Calabrese JM, Duriez O, Fleming CH, García-Jiménez R, Johnston A, Lambertucci SA, Safi K, Shepard ELC. 2020. The challenges of estimating the distribution of flight heights from telemetry or altimetry data. Animal Biotelemetry. 8(1):5. doi:10.1186/s40317-020-00194-z.

Peschko V, Mendel B, Mercker M, Dierschke J, Garthe S. 2021. Northern gannets (*Morus bassanus*) are strongly affected by operating offshore wind farms during the breeding season. Journal of Environmental Management. 279:111509. doi:10.1016/j.jenvman.2020.111509.

Plummer M. 2017. JAGS Version 4.3.0 user manual. https://sourceforge.net/projects/mcmc-jags/files/Manuals/4.x/.

Plummer M. 2023. rjags: Bayesian graphical models using MCMC. R package version 4-14. Statistical software. https://CRAN.R-project.org/package=rjags.

R Core Team. 2023. R: A language and environment for statistical computing. R Foundation for Statistical Computing. https://www.R-project.org/.

Ross-Smith VH, Thaxter CB, Masden EA, Shamoun-Baranes J, Burton NHK, Wright LJ, Rehfisch MM, Johnston A. 2016. Modelling flight heights of lesser black-backed gulls and great skuas from GPS: a Bayesian approach. Journal of Applied Ecology. 53(6):1676–1685. doi:10.1111/1365-2664.12760.

Shimada T, Jones R, Limpus C, Hamann M. 2012. Improving data retention and home range estimates by data-driven screening. Mar Ecol Prog Ser. 457:171–180. doi:10.3354/meps09747.

Taylor PD, Crewe TL, Mackenzie SA, Lepage D, Aubry Y, Crysler Z, Francis CM, Guglielmo CG, Hamilton DJ, Holberton RL, et al. 2017. The Motus Wildlife Tracking System: A collaborative research network to enhance the understanding of wildlife movement. Avian Conservation and Ecology. 12(1). doi:10.5751/ACE-00953-120108.

Appendix A: Frequently Asked Questions (FAQ) for SCRAM 2

Q: Wow, SCRAM is working a lot faster now, what happened?

A: We integrated SCRAM with another offshore wind collision risk decision support tool (stochLAB; Caneco et al. 2022) that also uses the Band (2012) model as a basis for its estimates. The developers of stochLAB significantly improved the speed of the model runs and added QA/QC protocols as compared to the older model code on which SCRAM 1.0.3 was based. This change reduces the possibility of future errors and allows users to test multiple scenarios much faster.

Q: I'm seeing Option 2 and Option 3 listed for estimated collision risk, when before there was Option 1 and Option 3. Why the change?

A: The options are calculated almost exactly the same as before, but we have renamed Option 1 as Option 2 to make sure that SCRAM nomenclature is aligned with Band (2012) and stochLAB (Caneco et al. 2022). In Band and stochLAB, what is called Option 1 requires location-specific flight height data, while Option 2 uses general flight height data for the species. Since the latter case is what was originally called "Option 1" in SCRAM, we renamed this option to align with CRM nomenclature.

Additionally, we use very slightly different avoidance rate estimates for Option 2 (formerly Option 1) than were used in SCRAM 1.0.3; before, a single set of avoidance values per species were used for both collision risk estimation options. Values used in both Option 2 and Option 3 are taken from Table A2 in Cook (2021). However, as stated in Adams et al. (2022), we generally recommend the use of Option 3 whenever possible, which explicitly pairs the altitudes of bird activity with collision risk in the rotor swept zone. If birds tend to fly in the lower portion rotor swept zone where the chances of collision are lower, then their chances of collision should be estimated as such. We account for this distribution profile in Option 3, but not Option 2. In Option 2, we only look at overall use of the rotor swept zone and the average collision risk of the whole area.

Q: Why is the number of predicted collisions different between SCRAM 1.0.3 and 2?

A: Many changes were made to improve SCRAM between versions 1.0.3 and 2. First, the transition to the stochLAB code for the collision risk model helped us squash a few lingering bugs. Some of these changes seem to have generally decreased SCRAM 2 collision risk estimates relative to SCRAM 1.0.3. Second, we updated the movement models for all species; this included adding newer Motus data, implementing more stringent QA/QC procedures to filter out potentially erroneous detections in the tracking datasets for all three study species, after Loring et al. (2021), and eliminating the use of multiple movement states. We also incorporated data from multiple new transmitter types (GPS and PTT) for red knots. After these improvements, there were noticeable differences in the estimates of space use in the animals, though the general patterns were similar. In general, the highest and lowest occupancy values were smoothed out across the study area in SCRAM 2 as compared to SCRAM 1.0.3. Lastly, the regional population size estimates were updated on both an overall and monthly basis, which tended to decrease estimated collision risk. The net change in collision risk varied by species and location.

Q: What movement data are now included in SCRAM?

SCRAM 2 movement models are based on data from Motus tags (Piping plover n=107, roseate tern n=134, red knot n=240), GPS transmitters (red knot n=81), and PTT transmitters (red knot n=25). The Motus data are all from BOEM-funded tracking studies conducted in 2015-2017 (Loring et al. 2018; Loring et al. 2019; Loring et al. 2021). GPS and PTT data are from six different studies conducted in

2020-2023, as discussed in the main text and in Appendix C. SCRAM 1.0.3 included only Motus data, including a much smaller Motus dataset for red knots than is included in SCRAM 2.

Due to the coastal locations of Motus stations in 2015-2017, Motus detections in the dataset tend to be somewhat clustered towards the coastline, and there is substantial uncertainty in occupancy estimates for grid cells located well offshore (despite substantial improvements in movement models in SCRAM 2, which reduced this uncertainty from SCRAM 1.0.3). For red knots, GPS and PTT transmitters incorporated into SCRAM 2 provide location data for both coastal and offshore regions with substantially higher precision than Motus technology, improving resulting occupancy models.

Flight height models in SCRAM 1.0.3 were based solely on Motus data (Loring et al. 2018; Loring et al. 2019). For SCRAM 2, red knot flight height models are now based on GPS tracking data (n=132 individuals). Future updates to SCRAM are expected to continue to incorporate additional tracking datasets (as they become available) into both movement models and flight height models.

Q: It sounds like there were a lot of changes to the Motus movement models, what happened there?

A: It started with an update to the red knot tracking dataset, to incorporate newer Motus data into SCRAM 2. The movement model didn't fit the data properly, so we simplified the model to improve convergence. For consistency, we applied a similar approach and improvements to the piping plover and roseate tern datasets. The greatest change simplified the models from two-state behavioral models to one-state models. Previously we adjusted the collision estimates to only include occupancy from birds in a migratory movement state. However, following changes to the underlying red knot dataset that added data and improved QA/QC (e.g., data filtering procedures), the model could no longer reliably differentiate two movement states. This means that collision risk estimates for SCRAM 2 may be higher in some nearshore grid cells and lower in offshore grid cells as compared to SCRAM 1.0.3. Future model development is expected to revisit a two-state model, as new tracking data become available.

Q: Why did you add the Band Annex 6 models to the SCRAM web application?

A: We added functionality to run a stochastic version of the Band (2012) model (specifically Band Annex 6, the collision risk model for migrants) in the SCRAM web application. Band (2012) Annex 6 uses nearly the same underlying collision risk model as SCRAM, but estimates "flux," or the number of animals that are present to potentially collide with a turbine, based on range-wide estimates of migratory corridor width. Essentially, the Band migratory model (i.e., Annex 6) assumes animals are evenly distributed across the width of the user-designated migratory corridor. In contrast, SCRAM's movement modeling approach estimates the occupancy to be higher in places that more animals moved through, and lower where fewer animals occurred (based on individual tracking data). A random distribution of animals, as in the Band migrant model, isn't often a reasonable assumption, but it can be helpful for making approximate collision risk estimates where other data are lacking. By allowing users to contrast the two models, it can more easily be seen how certain assumptions play out in the collision risk estimates, and will better allow those differences to inform conservation decision making. Including the Band (2012) Annex 6 collision risk model in the tool will also simplify the process of running both models for the same wind energy facilities, ensure consistent reporting of data inputs and outputs between the two types of models, and facilitate the use of a stochastic, rather than deterministic, version of the Band model.

Q: Anything else we should know about?

A: Yep, there are a few other noteworthy changes in SCRAM 2, including:

- We are now limiting SCRAM's Motus model output to a smaller geographic area where there was consistent Motus station coverage during the tracking studies that make up our movement

dataset. This area ranges approximately from northern Cape Cod to the Virginia-North Carolina border. If you ask SCRAM for a movement model-based collision risk estimate in the NES outside of that geographic area, you will only get one for red knots, and it will be 100% based on satellite tracking data (not Motus tags). The Band Annex 6 model will also provide collision risk predictions throughout the NES study area. We hope to expand the geographic area to which we can make confident predictions using Motus data in future iterations of SCRAM, but that will require new data and better coverage.

- SCRAM produces monthly collision risk estimates for a slightly different subset of month/species combinations than before. This is because we 1) added new Motus data and GPS/PTT data to our red knot models, 2) incorporated new Motus data for red knots and implemented additional quality control filtering to remove potentially erroneous data points for all three species, and 3) removed occupancy and collision estimates for piping plovers in September, when only 4 individuals were detected (below the sample size threshold of 5).
- We updated the monthly regional population size estimates of birds thought to be present in the NES study area that could be available to collide with turbines. These updates were based on the best available science from the USFWS and aligned the numbers in SCRAM 2 with those being used in the most recent Band (2012) model runs. In general, these updates tended to decrease monthly regional population size estimates, as USFWS refined their estimates of when animals were moving through the NES during fall migration.
- We updated the avoidance rates for all three species to average the values recommended by Cook (2021) and Ozsanlav-Harris et al. (2023). These two reports used similar (but not identical) datasets from Europe to estimate avoidance rates of offshore wind turbines by gulls and terns, and developed differing estimates of avoidance rates. Upon review, neither analysis seems like it was a clear improvement over the other, and thus we chose to average the avoidance rates from the two reports (SCRAM 1 avoidance rates were based solely on values from the Cook report, and were lower than the averaged values from the two reports included in SCRAM 2).

Appendix B: Red Knot GPS and PTT Tag Deployments

Table B-1. Red knot GPS and PTT tag deployments between August 2020-August 2023 considered for potential inclusion in SCRAM.

Information on each tag includes project, deployment site, location (state/province, country) and date deployed. Table indicates the number of locations (locs, n) and days (n) of movement data available for each individual following data cleaning. Bolded individuals are those used in final movement models for fall migration. Individuals were excluded from modeling for a variety of reasons, including tag duration and tag deployment date (e.g., whether the tag was operational during potential overwater migration periods and whether there were enough tags operational to conduct modeling for a given migration season). For more information, see the “Data Inputs - Satellite Telemetry” section of the report. Tags were funded by five projects: Atlantic Shores Offshore Wind, U.S. Fish and Wildlife Service, Ocean Wind Offshore Wind, Environment and Climate Chance Canada (ECCC), and Coastal Virginia Offshore Wind (CVOW). Tags were primarily deployed at migratory staging sites in New Jersey including North Brigantine Natural Area (NBRIG), Thompson’s Beach (THOMPS), Norbury’s Beach (NORBURYC), Avalon Beach (AVALON), Stone Harbor (STOHARB), Fortescue Fish and Wildlife Management Area (FORTESCU), Moores Beach (MOORES), Kimble’s Beach (KIMBLESO), and Two Mile Beach (TWOMILE), as well as on Monomoy, Massachusetts (MONOMOY), and at two wintering sites in Brazil including Lagao do Peixe National Park (PEIXE) and Pesca (PESCA).

Tag ID	Tag Type	Project	Deploy Site	State/Province	Country	Deploy Date	Locs (n)	Days (n)
204351	**GPS**	**Atlantic Shores**	**NBRIG**	**New Jersey**	**USA**	**8/22/2020**	**67**	**15**
204352	**GPS**	**Atlantic Shores**	**NBRIG**	**New Jersey**	**USA**	**8/13/2020**	**72**	**17**
204353	GPS	Atlantic Shores	NBRIG	New Jersey	USA	8/24/2020	0	0
204354	GPS	Atlantic Shores	NBRIG	New Jersey	USA	8/24/2020	0	0
204355	GPS	Atlantic Shores	NBRIG	New Jersey	USA	8/24/2020	0	0
204356	GPS	Atlantic Shores	NBRIG	New Jersey	USA	8/24/2020	0	0
204357	**GPS**	**Atlantic Shores**	**NBRIG**	**New Jersey**	**USA**	**8/13/2020**	**71**	**17**
204358	GPS	Atlantic Shores	NBRIG	New Jersey	USA	8/24/2020	0	0
204359	**GPS**	**Atlantic Shores**	**NBRIG**	**New Jersey**	**USA**	**8/22/2020**	**68**	**16**
204360	GPS	Atlantic Shores	NBRIG	New Jersey	USA	8/24/2020	0	0
204361	**GPS**	**Atlantic Shores**	**NBRIG**	**New Jersey**	**USA**	**8/13/2020**	**79**	**17**
204362	GPS	Atlantic Shores	NBRIG	New Jersey	USA	8/13/2020	4	1
204363	GPS	Atlantic Shores	NBRIG	New Jersey	USA	8/24/2020	0	0
204364	**GPS**	**Atlantic Shores**	**NBRIG**	**New Jersey**	**USA**	**8/22/2020**	**61**	**13**
204365	GPS	Atlantic Shores	NBRIG	New Jersey	USA	8/24/2020	0	0
204366	GPS	Atlantic Shores	NBRIG	New Jersey	USA	8/24/2020	0	0
204367	GPS	Atlantic Shores	NBRIG	New Jersey	USA	8/24/2020	0	0
204368	GPS	Atlantic Shores	NBRIG	New Jersey	USA	8/24/2020	0	0
204369	**GPS**	**Atlantic Shores**	**NBRIG**	**New Jersey**	**USA**	**8/22/2020**	**68**	**15**
204370	**GPS**	**Atlantic Shores**	**NBRIG**	**New Jersey**	**USA**	**8/13/2020**	**50**	**15**
204371	**GPS**	**Atlantic Shores**	**NBRIG**	**New Jersey**	**USA**	**8/22/2020**	**75**	**16**
204372	GPS	Atlantic Shores	NBRIG	New Jersey	USA	8/24/2020	0	0
204373	GPS	Atlantic Shores	NBRIG	New Jersey	USA	8/24/2020	0	0
204374	GPS	Atlantic Shores	NBRIG	New Jersey	USA	8/24/2020	0	0
204375	**GPS**	**Atlantic Shores**	**NBRIG**	**New Jersey**	**USA**	**8/22/2020**	**69**	**15**
204376	GPS	Atlantic Shores	NBRIG	New Jersey	USA	8/24/2020	0	0
204377	GPS	Atlantic Shores	NBRIG	New Jersey	USA	8/24/2020	0	0
204378	GPS	Atlantic Shores	NBRIG	New Jersey	USA	8/24/2020	0	0
204379	GPS	Atlantic Shores	NBRIG	New Jersey	USA	8/24/2020	0	0
213827	GPS	USFWS Spring Mig.	THOMPS	New Jersey	USA	5/26/2021	0	0
213828	GPS	USFWS Spring Mig.	NORBURYC	New Jersey	USA	5/25/2021	56	80
213829	GPS	USFWS Spring Mig.	THOMPS	New Jersey	USA	5/19/2021	8	8
213830	GPS	USFWS Spring Mig.	THOMPS	New Jersey	USA	5/19/2021	0	0

Tag ID	Tag Type	Project	Deploy Site	State/Province	Country	Deploy Date	Locs (n)	Days (n)
213831	GPS	USFWS Spring Mig.	NORBURYC	New Jersey	USA	5/25/2021	19	21
213832	GPS	USFWS Spring Mig.	THOMPS	New Jersey	USA	5/19/2021	19	20
213833	GPS	USFWS Spring Mig.	THOMPS	New Jersey	USA	5/19/2021	7	8
213834	GPS	USFWS Spring Mig.	NORBURYC	New Jersey	USA	5/25/2021	0	0
213835	GPS	USFWS Spring Mig.	NORBURYC	New Jersey	USA	5/25/2021	0	0
213836	GPS	USFWS Spring Mig.	THOMPS	New Jersey	USA	5/26/2021	0	0
213837	GPS	USFWS Spring Mig.	THOMPS	New Jersey	USA	5/19/2021	0	0
213838	GPS	USFWS Spring Mig.	THOMPS	New Jersey	USA	5/19/2021	0	0
213839	GPS	USFWS Spring Mig.	THOMPS	New Jersey	USA	5/19/2021	4	4
213840	GPS	USFWS Spring Mig.	THOMPS	New Jersey	USA	5/19/2021	0	0
213841	GPS	USFWS Spring Mig.	THOMPS	New Jersey	USA	5/26/2021	14	13
213842	GPS	USFWS Spring Mig.	THOMPS	New Jersey	USA	5/19/2021	0	0
221837	GPS	Ocean Wind	AVALON	New Jersey	USA	10/20/2021	0	0
221838	**GPS**	**Ocean Wind**	**NBRIG**	**New Jersey**	**USA**	**9/8/2021**	**10**	**9**
221839	GPS	Ocean Wind	AVALON	New Jersey	USA	10/20/2021	0	0
221840	GPS	Ocean Wind	AVALON	New Jersey	USA	10/27/2021	0	0
221841	**GPS**	**Ocean Wind**	**AVALON**	**New Jersey**	**USA**	**10/27/2021**	**82**	**18**
221842	**GPS**	**Ocean Wind**	**NBRIG**	**New Jersey**	**USA**	**9/8/2021**	**98**	**21**
221843	**GPS**	**Ocean Wind**	**AVALON**	**New Jersey**	**USA**	**10/27/2021**	**52**	**12**
221844	**GPS**	**Ocean Wind**	**STOHARB**	**New Jersey**	**USA**	**11/10/2021**	**27**	**7**
221845	**GPS**	**Ocean Wind**	**STOHARB**	**New Jersey**	**USA**	**11/10/2021**	**17**	**3**
221846	GPS	Ocean Wind	AVALON	New Jersey	USA	10/27/2021	40	9
221847	GPS	Ocean Wind	STOHARB	New Jersey	USA	11/10/2021	0	0
221848	**GPS**	**Ocean Wind**	**NBRIG**	**New Jersey**	**USA**	**9/8/2021**	**26**	**27**
221849	**GPS**	**Ocean Wind**	**NBRIG**	**New Jersey**	**USA**	**9/8/2021**	**50**	**11**
221850	**GPS**	**Ocean Wind**	**STOHARB**	**New Jersey**	**USA**	**11/10/2021**	**74**	**18**
221851	**GPS**	**Ocean Wind**	**NBRIG**	**New Jersey**	**USA**	**9/8/2021**	**32**	**32**
221852	**GPS**	**Ocean Wind**	**AVALON**	**New Jersey**	**USA**	**10/27/2021**	**46**	**10**
221853	GPS	Ocean Wind	AVALON	New Jersey	USA	10/20/2021	0	0
221854	GPS	Ocean Wind	STOHARB	New Jersey	USA	11/10/2021	0	0
221855	GPS	Ocean Wind	AVALON	New Jersey	USA	10/20/2021	0	0
221856	GPS	Ocean Wind	STOHARB	New Jersey	USA	11/10/2021	2	0
221857	GPS	Ocean Wind	AVALON	New Jersey	USA	10/20/2021	0	0

Tag ID	Tag Type	Project	Deploy Site	State/Province	Country	Deploy Date	Locs (n)	Days (n)
221858	GPS	Ocean Wind	STOHARB	New Jersey	USA	11/10/2021	0	0
221859	GPS	Ocean Wind	AVALON	New Jersey	USA	10/20/2021	0	0
221860	**GPS**	**Ocean Wind**	**STOHARB**	**New Jersey**	**USA**	**11/10/2021**	**99**	**23**
221861	GPS	Ocean Wind	AVALON	New Jersey	USA	10/20/2021	0	0
221862	GPS	Ocean Wind	AVALON	New Jersey	USA	10/20/2021	0	0
221863	**GPS**	**Ocean Wind**	**STOHARB**	**New Jersey**	**USA**	**11/10/2021**	**42**	**10**
221864	GPS	Ocean Wind	AVALON	New Jersey	USA	10/20/2021	0	0
221865	GPS	Ocean Wind	AVALON	New Jersey	USA	10/20/2021	0	0
221866	**GPS**	**Ocean Wind**	**STOHARB**	**New Jersey**	**USA**	**11/10/2021**	**127**	**28**
221867	**GPS**	**Ocean Wind**	**AVALON**	**New Jersey**	**USA**	**10/27/2021**	**60**	**14**
221868	GPS	Ocean Wind	AVALON	New Jersey	USA	10/27/2021	0	0
224072	GPS	Atlantic Shores	NBRIG	New Jersey	USA	8/20/2021	12	5
224073	**GPS**	**Atlantic Shores**	**NBRIG**	**New Jersey**	**USA**	**8/25/2021**	**84**	**21**
224074	GPS	Atlantic Shores	NBRIG	New Jersey	USA	8/23/2021	0	0
224075	**GPS**	**Atlantic Shores**	**NBRIG**	**New Jersey**	**USA**	**8/25/2021**	**118**	**31**
224076	**GPS**	**Atlantic Shores**	**NBRIG**	**New Jersey**	**USA**	**8/25/2021**	**52**	**13**
224077	**GPS**	**Atlantic Shores**	**NBRIG**	**New Jersey**	**USA**	**8/20/2021**	**46**	**12**
224078	**GPS**	**Atlantic Shores**	**NBRIG**	**New Jersey**	**USA**	**8/20/2021**	**56**	**14**
224079	**GPS**	**Atlantic Shores**	**NBRIG**	**New Jersey**	**USA**	**8/20/2021**	**43**	**11**
224080	**GPS**	**Atlantic Shores**	**NBRIG**	**New Jersey**	**USA**	**8/20/2021**	**121**	**30**
224081	**GPS**	**Atlantic Shores**	**NBRIG**	**New Jersey**	**USA**	**8/23/2021**	**32**	**8**
224082	**GPS**	**Atlantic Shores**	**NBRIG**	**New Jersey**	**USA**	**8/20/2021**	**132**	**33**
224083	**GPS**	**Atlantic Shores**	**NBRIG**	**New Jersey**	**USA**	**8/20/2021**	**44**	**12**
224085	**GPS**	**Atlantic Shores**	**NBRIG**	**New Jersey**	**USA**	**8/20/2021**	**106**	**27**
224086	GPS	Atlantic Shores	NBRIG	New Jersey	USA	8/25/2021	72	20
224087	**GPS**	**Atlantic Shores**	**NBRIG**	**New Jersey**	**USA**	**8/23/2021**	**84**	**21**
224088	**GPS**	**Atlantic Shores**	**NBRIG**	**New Jersey**	**USA**	**8/25/2021**	**124**	**31**
224089	**GPS**	**Atlantic Shores**	**NBRIG**	**New Jersey**	**USA**	**8/25/2021**	**83**	**21**
224090	GPS	Atlantic Shores	NBRIG	New Jersey	USA	8/23/2021	0	0
224091	**GPS**	**Atlantic Shores**	**NBRIG**	**New Jersey**	**USA**	**8/25/2021**	**16**	**4**
224092	**GPS**	**Atlantic Shores**	**NBRIG**	**New Jersey**	**USA**	**8/23/2021**	**20**	**5**
224093	**GPS**	**Atlantic Shores**	**NBRIG**	**New Jersey**	**USA**	**8/20/2021**	**22**	**6**
224094	**GPS**	**Atlantic Shores**	**NBRIG**	**New Jersey**	**USA**	**8/20/2021**	**36**	**10**

Tag ID	Tag Type	Project	Deploy Site	State/Province	Country	Deploy Date	Locs (n)	Days (n)
224095	**GPS**	**Atlantic Shores**	**NBRIG**	**New Jersey**	**USA**	**8/20/2021**	**46**	**12**
224096	**GPS**	**Atlantic Shores**	**NBRIG**	**New Jersey**	**USA**	**8/20/2021**	**24**	**6**
224097	**GPS**	**Atlantic Shores**	**NBRIG**	**New Jersey**	**USA**	**8/20/2021**	**65**	**17**
224098	**GPS**	**Atlantic Shores**	**NBRIG**	**New Jersey**	**USA**	**8/25/2021**	**120**	**31**
224099	**GPS**	**Atlantic Shores**	**NBRIG**	**New Jersey**	**USA**	**8/23/2021**	**87**	**22**
224100	**GPS**	**Atlantic Shores**	**NBRIG**	**New Jersey**	**USA**	**8/23/2021**	**8**	**2**
224101	GPS	Atlantic Shores	NBRIG	New Jersey	USA	8/20/2021	50	12
224102	**GPS**	**Atlantic Shores**	**NBRIG**	**New Jersey**	**USA**	**8/25/2021**	**68**	**17**
224103	**GPS**	**Atlantic Shores**	**NBRIG**	**New Jersey**	**USA**	**8/20/2021**	**31**	**8**
230299	GPS	ECCC	FORTESCU	New Jersey	USA	5/25/2022	60	73
230300	GPS	ECCC	KIMBLESO	New Jersey	USA	5/16/2022	12	13
230301	GPS	ECCC	MOORES	New Jersey	USA	5/21/2022	13	14
230302	GPS	ECCC	MOORES	New Jersey	USA	5/21/2022	15	15
230303	GPS	ECCC	MOORES	New Jersey	USA	5/21/2022	12	11
230304	GPS	ECCC	MOORES	New Jersey	USA	5/21/2022	16	15
230305	GPS	ECCC	KIMBLESO	New Jersey	USA	5/16/2022	14	28
230306	GPS	ECCC	FORTESCU	New Jersey	USA	5/25/2022	46	45
230307	GPS	ECCC	FORTESCU	New Jersey	USA	5/25/2022	11	10
230308	GPS	ECCC	FORTESCU	New Jersey	USA	5/25/2022	82	82
230309	GPS	ECCC	MOORES	New Jersey	USA	5/21/2022	24	23
230310	GPS	ECCC	FORTESCU	New Jersey	USA	5/25/2022	18	71
230311	GPS	ECCC	FORTESCU	New Jersey	USA	5/25/2022	9	9
230312	GPS	ECCC	FORTESCU	New Jersey	USA	5/25/2022	68	74
230313	GPS	ECCC	KIMBLESO	New Jersey	USA	5/16/2022	0	0
230314	GPS	ECCC	FORTESCU	New Jersey	USA	5/25/2022	8	7
230315	GPS	ECCC	MOORES	New Jersey	USA	5/21/2022	16	16
230316	GPS	ECCC	KIMBLESO	New Jersey	USA	5/16/2022	14	16
230317	GPS	ECCC	FORTESCU	New Jersey	USA	5/25/2022	49	82
230318	GPS	ECCC	KIMBLESO	New Jersey	USA	5/16/2022	14	16
230319	GPS	ECCC	MOORES	New Jersey	USA	5/21/2022	12	13
230320	GPS	ECCC	MOORES	New Jersey	USA	5/21/2022	9	9
232980	PTT	ECCC	MOORES	New Jersey	USA	5/21/2022	80	7
232981	**PTT**	**ECCC**	**MOORES**	**New Jersey**	**USA**	**5/21/2022**	**1583**	**115**

Tag ID	Tag Type	Project	Deploy Site	State/Province	Country	Deploy Date	Locs (n)	Days (n)
232982	**PTT**	**ECCC**	**MOORES**	**New Jersey**	**USA**	**5/16/2023**	**723**	**138**
232984	PTT	ECCC	KIMBLESO	New Jersey	USA	5/16/2022	0	0
232985	PTT	ECCC	KIMBLESO	New Jersey	USA	5/16/2022	1962	89
232986	PTT	ECCC	KIMBLESO	New Jersey	USA	5/16/2022	1035	58
233781	**GPS**	**Atlantic Shores**	**NBRIG**	**New Jersey**	**USA**	**8/18/2022**	**124**	**27**
233918	**GPS**	**Ocean Wind**	**STOHARB**	**New Jersey**	**USA**	**9/28/2022**	**122**	**26**
233919	**GPS**	**Ocean Wind**	**NBRIG**	**New Jersey**	**USA**	**8/18/2022**	**110**	**24**
233920	GPS	Ocean Wind	STOHARB	New Jersey	USA	9/28/2022	9	2
233921	**GPS**	**Ocean Wind**	**TWOMILE**	**New Jersey**	**USA**	**9/1/2022**	**124**	**26**
233922	**GPS**	**Ocean Wind**	**STOHARB**	**New Jersey**	**USA**	**9/28/2022**	**54**	**12**
233923	**GPS**	**Ocean Wind**	**NBRIG**	**New Jersey**	**USA**	**8/18/2022**	**90**	**20**
233924	GPS	Ocean Wind	STOHARB	New Jersey	USA	9/28/2022	6	1
233925	**GPS**	**Ocean Wind**	**STOHARB**	**New Jersey**	**USA**	**9/28/2022**	**22**	**4**
233926	**GPS**	**Ocean Wind**	**NBRIG**	**New Jersey**	**USA**	**8/18/2022**	**108**	**24**
233927	**GPS**	**Ocean Wind**	**TWOMILE**	**New Jersey**	**USA**	**9/1/2022**	**90**	**20**
233928	**GPS**	**Ocean Wind**	**NBRIG**	**New Jersey**	**USA**	**8/18/2022**	**126**	**27**
233929	**GPS**	**Ocean Wind**	**STOHARB**	**New Jersey**	**USA**	**9/28/2022**	**18**	**3**
233930	**GPS**	**Ocean Wind**	**TWOMILE**	**New Jersey**	**USA**	**9/1/2022**	**62**	**13**
233931	**GPS**	**Ocean Wind**	**STOHARB**	**New Jersey**	**USA**	**9/28/2022**	**118**	**26**
233932	**GPS**	**Ocean Wind**	**TWOMILE**	**New Jersey**	**USA**	**9/1/2022**	**22**	**4**
234177	**GPS**	**Ocean Wind**	**STOHARB**	**New Jersey**	**USA**	**9/28/2022**	**107**	**23**
234178	**GPS**	**Ocean Wind**	**STOHARB**	**New Jersey**	**USA**	**9/28/2022**	**124**	**26**
234179	GPS	Ocean Wind	STOHARB	New Jersey	USA	9/28/2022	57	20
234180	**GPS**	**Ocean Wind**	**STOHARB**	**New Jersey**	**USA**	**9/28/2022**	**120**	**25**
234181	**GPS**	**Ocean Wind**	**NBRIG**	**New Jersey**	**USA**	**8/18/2022**	**126**	**26**
234182	**GPS**	**Ocean Wind**	**NBRIG**	**New Jersey**	**USA**	**8/18/2022**	**110**	**25**
234183	**GPS**	**Ocean Wind**	**STOHARB**	**New Jersey**	**USA**	**9/28/2022**	**117**	**25**
234184	**GPS**	**Ocean Wind**	**STOHARB**	**New Jersey**	**USA**	**9/28/2022**	**16**	**3**
234185	**GPS**	**Ocean Wind**	**TWOMILE**	**New Jersey**	**USA**	**9/1/2022**	**21**	**4**
234186	GPS	Ocean Wind	STOHARB	New Jersey	USA	9/28/2022	0	0
234187	GPS	Ocean Wind	STOHARB	New Jersey	USA	9/28/2022	92	22
234189	**GPS**	**Ocean Wind**	**NBRIG**	**New Jersey**	**USA**	**8/18/2022**	**64**	**13**
234190	GPS	Ocean Wind	STOHARB	New Jersey	USA	9/28/2022	6	1

Tag ID	Tag Type	Project	Deploy Site	State/Province	Country	Deploy Date	Locs (n)	Days (n)
234191	**GPS**	**Ocean Wind**	**NBRIG**	**New Jersey**	**USA**	**8/18/2022**	**60**	**12**
234233	GPS	ECCC	MOORES	New Jersey	USA	5/28/2022	21	59
234234	GPS	ECCC	MOORES	New Jersey	USA	5/28/2022	10	9
234235	GPS	ECCC	MOORES	New Jersey	USA	5/28/2022	24	24
234236	GPS	ECCC	MOORES	New Jersey	USA	5/28/2022	80	80
234237	GPS	ECCC	FORTESCU	New Jersey	USA	5/30/2022	12	11
234238	GPS	ECCC	FORTESCU	New Jersey	USA	5/30/2022	16	15
234239	GPS	ECCC	FORTESCU	New Jersey	USA	5/30/2022	7	6
234240	GPS	ECCC	FORTESCU	New Jersey	USA	5/30/2022	5	223
234370	**PTT**	**CVOW**	**MONOMOY**	**Massachusetts**	**USA**	**8/26/2022**	**801**	**110**
234371	**PTT**	**CVOW**	**NBRIG**	**New Jersey**	**USA**	**8/15/2023**	**835**	**70**
234372	**PTT**	**CVOW**	**MONOMOY**	**Massachusetts**	**USA**	**8/26/2022**	**195**	**64**
234373	**PTT**	**CVOW**	**MONOMOY**	**Massachusetts**	**USA**	**8/26/2022**	**70**	**111**
234374	**PTT**	**CVOW**	**NBRIG**	**New Jersey**	**USA**	**8/15/2023**	**312**	**24**
234375	**PTT**	**CVOW**	**NBRIG**	**New Jersey**	**USA**	**8/15/2023**	**676**	**52**
234376	**PTT**	**CVOW**	**NBRIG**	**New Jersey**	**USA**	**8/15/2023**	**292**	**65**
234377	**PTT**	**CVOW**	**MONOMOY**	**Massachusetts**	**USA**	**8/26/2022**	**246**	**65**
234378	**PTT**	**CVOW**	**NBRIG**	**New Jersey**	**USA**	**8/15/2023**	**214**	**22**
234379	**PTT**	**CVOW**	**MONOMOY**	**Massachusetts**	**USA**	**8/26/2022**	**75**	**89**
234380	**PTT**	**CVOW**	**NBRIG**	**New Jersey**	**USA**	**8/15/2023**	**208**	**17**
234381	**PTT**	**CVOW**	**NBRIG**	**New Jersey**	**USA**	**8/15/2023**	**825**	**77**
234382	**PTT**	**CVOW**	**NBRIG**	**New Jersey**	**USA**	**8/15/2023**	**408**	**32**
234383	**PTT**	**CVOW**	**MONOMOY**	**Massachusetts**	**USA**	**8/26/2022**	**18**	**9**
234384	**PTT**	**CVOW**	**MONOMOY**	**Massachusetts**	**USA**	**8/26/2022**	**104**	**21**
236444	**GPS**	**Fall MA Migration**	**MONOMOY**	**Massachusetts**	**USA**	**8/26/2022**	**131**	**30**
236445	**GPS**	**Fall MA Migration**	**MONOMOY**	**Massachusetts**	**USA**	**8/26/2022**	**84**	**19**
236446	**GPS**	**Fall MA Migration**	**MONOMOY**	**Massachusetts**	**USA**	**8/26/2022**	**28**	**6**
236447	**GPS**	**Fall MA Migration**	**MONOMOY**	**Massachusetts**	**USA**	**8/26/2022**	**73**	**16**
236448	GPS	Fall MA Migration	NBRIG	New Jersey	USA	5/15/2023	27	13
236449	GPS	Fall MA Migration	NBRIG	New Jersey	USA	5/14/2023	90	44
236450	**GPS**	**Fall MA Migration**	**MONOMOY**	**Massachusetts**	**USA**	**8/26/2022**	**132**	**30**
236451	**GPS**	**Fall MA Migration**	**MONOMOY**	**Massachusetts**	**USA**	**8/26/2022**	**128**	**28**
236452	GPS	Fall MA Migration	NBRIG	New Jersey	USA	5/17/2023	28	14

Tag ID	Tag Type	Project	Deploy Site	State/Province	Country	Deploy Date	Locs (n)	Days (n)
236453	GPS	Fall MA Migration	NBRIG	New Jersey	USA	5/16/2023	34	17
238539	PTT	ECCC	PESCA	Rio Grande do Sul	Brazil	4/21/2023	0	0
238541	PTT	ECCC	MOORES	New Jersey	USA	4/16/2023	0	0
238542	**PTT**	**ECCC**	**NBRIG**	**New Jersey**	**USA**	**8/15/2023**	**36**	**4**
238543	PTT	ECCC	MOORES	New Jersey	USA	5/16/2023	35	4
238544	**PTT**	**ECCC**	**MOORES**	**New Jersey**	**USA**	**5/14/2023**	**1273**	**126**
238545	PTT	ECCC	PESCA	Rio Grande do Sul	Brazil	4/21/2023	0	0
238546	**PTT**	**ECCC**	**MOORES**	**New Jersey**	**USA**	**5/16/2023**	**1262**	**90**
238547	PTT	ECCC	PESCA	Rio Grande do Sul	Brazil	4/21/2023	0	0
238548	PTT	ECCC	PESCA	Rio Grande do Sul	Brazil	4/21/2023	0	0
238550	PTT	ECCC	PESCA	Rio Grande do Sul	Brazil	4/21/2023	0	0
238551	PTT	ECCC	PESCA	Rio Grande do Sul	Brazil	4/21/2023	0	0
238553	PTT	ECCC	PESCA	Rio Grande do Sul	Brazil	4/21/2023	0	0
240155	PTT	ECCC	PEIXE	Rio Grande do Sul	Brazil	4/10/2023	187	174
240156	PTT	ECCC	MOORES	New Jersey	USA	5/16/2023	292	95
240157	PTT	ECCC	PEIXE	Rio Grande do Sul	Brazil	4/10/2023	17	8
240158	PTT	ECCC	PEIXE	Rio Grande do Sul	Brazil	4/10/2023	468	67
240159	PTT	ECCC	PEIXE	Rio Grande do Sul	Brazil	4/10/2023	643	92
240160	PTT	ECCC	PEIXE	Rio Grande do Sul	Brazil	4/10/2023	12	111
240161	PTT	ECCC	MOORES	New Jersey	USA	5/16/2023	933	91
240162	PTT	ECCC	PEIXE	Rio Grande do Sul	Brazil	4/10/2023	130	146
240163	PTT	ECCC	PEIXE	Rio Grande do Sul	Brazil	4/11/2023	15	4
240164	PTT	ECCC	PEIXE	Rio Grande do Sul	Brazil	4/10/2023	1188	166
240165	PTT	ECCC	PEIXE	Rio Grande do Sul	Brazil	4/10/2023	63	67
240166	PTT	ECCC	PEIXE	Rio Grande do Sul	Brazil	4/10/2023	17	35
240167	**PTT**	**ECCC**	**PEIXE**	**Rio Grande do Sul**	**Brazil**	**4/10/2023**	**2020**	**177**
240168	**PTT**	**ECCC**	**MOORES**	**New Jersey**	**USA**	**5/16/2023**	**1361**	**122**
240169	PTT	ECCC	MOORES	New Jersey	USA	5/16/2023	0	0
241166	PTT	ECCC	PEIXE	Rio Grande do Sul	Brazil	4/8/2023	261	86
241167	**PTT**	**ECCC**	**PEIXE**	**Rio Grande do Sul**	**Brazil**	**4/8/2023**	**784**	**131**
242570	**PTT**	**ECCC**	**EASTPIT**	**New Jersey**	**USA**	**5/19/2023**	**1029**	**137**
242571	PTT	ECCC	EASTPIT	New Jersey	USA	5/19/2023	47	9
242573	PTT	ECCC	MOORES	New Jersey	USA	4/8/2023	40	58

Tag ID	Tag Type	Project	Deploy Site	State/Province	Country	Deploy Date	Locs (n)	Days (n)
242574	PTT	ECCC	MOORES	New Jersey	USA	4/8/2023	1296	143
242575	PTT	ECCC	NBRIG	New Jersey	USA	8/15/2023	0	0
242576	PTT	ECCC	NBRIG	New Jersey	USA	8/15/2023	0	0
242577	PTT	ECCC	EASTPIT	New Jersey	USA	5/19/2023	164	42
242578	PTT	ECCC	NBRIG	New Jersey	USA	8/15/2023	0	0
242580	**PTT**	**ECCC**	**EASTPIT**	**New Jersey**	**USA**	**5/19/2023**	**1556**	**137**
242582	PTT	ECCC	NBRIG	New Jersey	USA	5/19/2023	0	0
242583	PTT	ECCC	MOORES	New Jersey	USA	5/16/2023	0	0

.

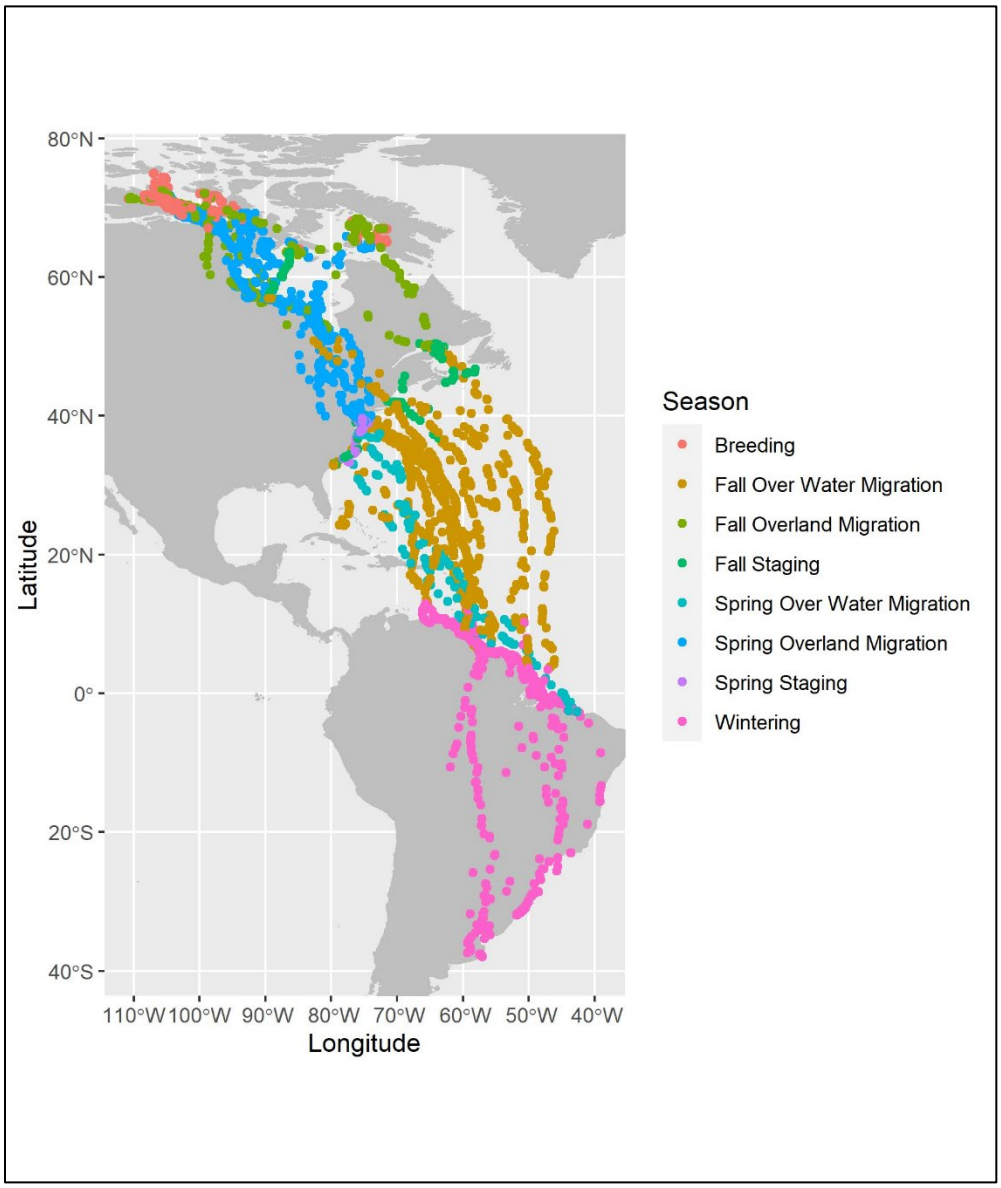

Figure B-1. Breakdown of red knot PTT tracking data by season.
Fall Staging and Fall Over Water Migration were included in fall movement modeling for SCRAM purposes.

Appendix C: Estimated Monthly Numbers of Rufa Red Knots Crossing "Migration Fronts" in the Mid-Atlantic (Massachusetts to Virginia)

U.S. Fish and Wildlife Service, 2023

Estimated Monthly Numbers of Rufa Red Knots Crossing "Migration Fronts" in the Mid-Atlantic (Massachusetts to Virginia)

This document lays out the biological basis for use of the Band (2012) model by the U.S. Fish and Wildlife Service (Service) to estimate collision risk of the federally listed (threatened) rufa red knot (*Calidris cantutus rufa*) for proposed wind energy development on the Outer Continental Shelf (OCS) offshore the mid-Atlantic States from Massachusetts to Virginia. As shown in Table 1, this assessment considers birds from three of the four rufa red knot recovery units: Southeast U.S./Caribbean (SEC), Northern Coast of South America (NCSA), and Southern. See USFWS (2014, 2020, 2023) for the geographic range of these populations and background information on the species and offshore wind.

Model Assumptions

Band (2012) does not contemplate a species that may be resident in the wind farm area in some seasons and migrating through in other seasons. Stage B of the Band basic model (*i.e.*, for resident birds) requires an estimate of observed bird density on an area basis. This information is currently unavailable for rufa red knots in the mid-Atlantic OCS during any month. In addition, far greater numbers of rufa red knots are present in the mid-Atlantic during the migration seasons than during winter or summer. For these reasons, we use Band Annex 6, for birds on migration. Under Annex 6, Band (2012) assumes that the entire bird population passes through a migratory corridor exactly twice each year. Annex 6 involves measuring the width of the corridor at the latitude of the wind farm (*i.e.*, along a "migratory front," which is an imaginary line passing through the wind development area and extending to the western and eastern edges of the migratory corridor used by the species). Our application of the Band (2012) model was reviewed by an independent expert who concurred with our approach (Cook pers. comm. 2023). However, there are several significant caveats associated with use of Annex C, as discussed below.

Consistent with Annex C, our model inputs are deliberately calibrated to count each bird only once during the northbound (NB) and once during the southbound (SB) migration seasons. However, in addition to migration flights, seasonally resident rufa red knots are also known to make regional flights, some of which cross the OCS. Seasonally resident birds occurring in the mid-Atlantic may include nonbreeding adults during the breeding season, juveniles at any time of year, birds on extended stopover or staging visits, and birds during the early part of the wintering season (see USFWS 2023). Rufa red knots have also been documented making regional flights opposite the main migration trajectory (*i.e.*, south in spring, north in fall), a phenomenon known as reverse migration that is likely an attempt to find optimal food or other conditions for the stopover period (USFWS 2014, Hunter pers. comm. 2022, Sanders pers. comm. 2023, Perkins 2023). The prevalence of regional movements is reflected in available tracking data, summarized by USFWS (2023).

Rufa red knots are known to move considerable distances within their wintering regions during the core winter months, and may also depart the mid-Atlantic on late-season migration flights toward wintering destinations farther south (Burger *et al.* 2012, USFWS 2014, Perkins 2023). As shown in Table 2, Ebird data from the past 10 years from Massachusetts to Virginia average 42 rufa red knot records (>311 birds) in December and 52 records (>397 birds) in January per year. In addition, rufa red knots occur along the mid-Atlantic in June, with an average of 139 records (>1,710 birds) per year, which includes late-migrating breeding birds, as well as over-summering juveniles and nonbreeding adults. Due to the limitations associated with Ebird data, the actual number of rufa red knots knots

wintering or summering in the mid-Atlantic is highly uncertain, and we have little information on the frequency with which these seasonally resident birds may cross the OCS.

Conversely, the majority of NB rufa red knots are likely to cross the migration front over land and not over the OCS. A growing body of evidence indicates that a substantial portion of NB rufa red knots depart from the U.S. Atlantic Coast (Florida to Delaware Bay) on a northwest trajectory to their final stopover areas along Hudson Bay in Canada. Some birds do continue along the Atlantic Coast north of Delaware Bay, and some of those birds may cross the OCS. However, the overland route does appear to be the predominant flyway for this leg of the northbound migration (USFWS 2014, USFWS 2021, Loring *et al.* 2021, Perkins 2023, unpublished satellite data) and this route entirely avoids the OCS.

In summary, the assumptions necessary to use Band (2012), Annex C, cannot account for: (1) more than two crossings of the migratory front per year by migrating birds (*e.g.*, as may be associated with juveniles or instances of reverse migration); (2) crossings of the migratory front by birds summering or wintering in the mid-Atlantic; or (3) avoidance of the OCS by the majority of NB migrants.

Reproductive Output and Nonbreeding Birds

Research has documented a variety of behaviors among juveniles and nonbreeding adults.

- All juveniles of the Tierra del Fuego wintering area are thought to remain in the Southern Hemisphere during their first year of life, possibly moving to northern South America (Niles *et al.* 2008). (Tierra del Fuego supports the vast majority of the Southern recovery unit during the winter months (USFWS 2020, Castellino and González pers. comm. 2023)).
- Some nonbreeding birds of both age classes remain south of the mid-Atlantic (USFWS, 2014, Martínez-Curci *et al.* 2020, Perkins 2023).
- Some nonbreeding birds may pass through the mid-Atlantic once in spring and spend the breeding season on (adults) or just south of (juveniles) the breeding grounds (USFWS 2014, Smith pers. comm. 2023, Perkins 2023).
- Some birds may remain resident in the mid-Atlantic for prolonged periods (Burger *et al.* 2012, Loring *et al.* 2018, Perkins 2023) and may make multiple regional flights.

Given high uncertainty around the use of the OCS airspace by nonbreeding birds, we include them in our migration passage population estimates *except* for juveniles from the Southern population. For the rest, we assume they all cross the mid-Atlantic once during the NB migration window and once during the SB migration window. All of these assumptions are associated with high uncertainty.

Table 3 shows information and assumptions underpinning our estimation of the number of breeding birds and the addition of young of the year (YOY) to the SB migration population. Modeling by Schwarzer (2011) found that the Florida population was stable at around 8.75 percent juveniles among wintering birds. Available data suggest the three populations considered in this analysis are currently stable. Thus, we assume 8.75 percent of the total wintering birds are juveniles. We have no estimate of the number of nonbreeding adults in a typical year, or their distribution across the species' nonbreeding range. To account for nonbreeding adults, we round our estimate of nonbreeding birds up to 10 percent, and exclude all these nonbreeding birds (juveniles and adults) from our calculation of chicks fledged per pair. Because all three rufa red knot populations are apparently stable, we assume annual mortality balances reproduction and we do not add any YOY to the wintering population totals.

Table 1. Current estimates of rufa red knot abundance by recovery unit

Recovery Unit	Abundance Estimate	Certainty	Basis	Source
SEC[1]	15,500	Moderate	mark/resight model (2011 data) + stable isotope analysis	Lyons *et al.* 2017
NCSA	31,065	Moderate	2019 aerial count	Mizrahi 2020
Southern[2]	14,484	High	2021-23 average count	Castellino and González pers. comm. 2023, Castellino 2023, Norambuena *et al.* 2023, Norambuena *et al.* 2022, Matus 2021
Subtotal	*61,049*			
Western[3]	5,500	Low	best professional estimate	Newstead pers. comm. 2019, 2020
Total	**66,549**			

[1] Includes an estimated 10,400 birds in the Southeastern U.S. and 5,100 birds in the Caribbean.
[2] The 2022 and 23 estimates include ground surveys of Patagonia, which varied in geographic coverage and methodology, and which were not conducted in 2021.
[3] Birds from the Western unit are known to occur in the mid-Atlantic during migration, but the predominant flyway for these birds is through the midcontinent (Newstead *et al.* 2013, Perkins 2023). Thus, we consider them discountable in our assessment of wind energy development on the OCS and omit them from further calculations.

Table 2. Ebird data by State* and month, June 2013 through May 2023

	MA	RI	CT	NY	NJ	DE	MD	VA		MA	RI	CT	NY	NJ	DE	MD	VA	
*cumulative total # of birds***									% of total	*cumulative total # of records****								% of total
Jan	112	0	0	2,188	1,184	9	47	425	0.2%	6	0	0	294	128	3	47	37	1.8%
Feb	11	0	12	418	147	0	1	72	0.0%	6	0	12	113	36	0	1	23	0.7%
Mar	0	4	0	180	79	7	0	24	0.0%	0	4	0	47	23	4	0	10	0.3%
Apr	2	7	0	110	897	88	2	241	0.1%	1	7	0	48	113	19	1	28	0.8%
May	3,320	807	281	21,133	825,966	401,589	2,380	22,831	77.5%	384	145	104	1,232	5,594	2,458	281	857	38.4%
Jun	1,204	520	120	5,784	3,298	1,880	702	3,596	1.0%	152	100	34	534	237	136	74	125	4.8%
Jul	22,844	277	28	3,655	8,177	756	195	5,514	2.5%	743	100	7	501	256	160	63	133	6.8%
Aug	86,546	1,452	193	13,237	40,856	551	394	13,537	9.5%	2,385	300	138	1,044	962	96	73	389	18.7%
Sep	46,514	1,089	97	7,908	19,244	340	159	2,567	4.7%	1,995	225	70	698	864	71	53	259	14.7%
Oct	10,969	118	17	4,165	32,048	21	120	997	2.9%	471	46	9	461	1,295	12	43	73	8.4%
Nov	3,011	25	6	4,298	11,917	9	51	130	1.2%	70	13	6	429	315	2	22	44	3.1%
Dec	12	3	2	1,292	1,329	0	20	449	0.2%	11	3	2	203	128	0	20	52	1.5%
*annual average # of birds***									total	*annual average # of records****								total
Jan	11	0	0	219	118	1	5	43	397	1	0	0	29	13	0	5	4	52
Feb	1	0	1	42	15	0	0	7	66	1	0	1	11	4	0	0	2	19
Mar	0	0	0	18	8	1	0	2	29	0	0	0	5	2	0	0	1	9
Apr	0	1	0	11	90	9	0	24	135	0	1	0	5	11	2	0	3	22
May	332	81	28	2,113	82,597	40,159	238	2,283	127,831	38	15	10	123	559	246	28	86	1,106
Jun	120	52	12	578	330	188	70	360	1,710	15	10	3	53	24	14	7	13	139
Jul	2,284	28	3	366	818	76	20	551	4,145	74	10	1	50	26	16	6	13	196
Aug	8,655	145	19	1,324	4,086	55	39	1,354	15,677	239	30	14	104	96	10	7	39	539
Sep	4,651	109	10	791	1,924	34	16	257	7,792	200	23	7	70	86	7	5	26	424
Oct	1,097	12	2	417	3,205	2	12	100	4,846	47	5	1	46	130	1	4	7	241
Nov	301	3	1	430	1,192	1	5	13	1,945	7	1	1	43	32	0	2	4	90
Dec	1	0	0	129	133	0	2	45	311	1	0	0	20	13	0	2	5	42
total	17,455	430	76	6,437	94,514	40,525	407	5,038	164,882	622	94	38	560	995	296	68	203	2,877

*Only records falling within the Study Area defined by Adams *et al.* (2022), Figure 2 are included.
**Bird numbers exclude 1,075 records for which the number of rufa red knots was not recorded.
***Numbers of both birds and records likely include duplicate reports of the same birds. Conversely, these data reflect those times and places that bird watchers were active, which does not cover all times and places rufa red knots occur.

Table 3. Data sources and assumptions to estimate the southbound population size

Population Segment	Method/Assumptions	Value	Sources
# of Southern juveniles	8.75% of Southern population *[14,484 * 0.0875]*	1,267	Table 1, Schwarzer 2011
# of NB birds expected to occur in the mid-Atlantic	(SEC + NCSA + Southern) – Southern juveniles *[61,049 - 1,267]*	59,782	Table 1, Niles *et al.* 2008, USFWS 2014, Perkins 2023
# of breeding birds expected to produce offspring that will migrate south through the mid-Atlantic	90% of (SEC + NCSA + Southern) *[61,049 * 0.9]*	54,944 (27,472 breeding pairs)	Smith pers. comm. 2023, Perkins 2023, Martínez-Curci *et al.* 2020, Schwarzer 2011
Annual # of YOY expected to migrate south through the mid-Atlantic	0.5 chicks per pair *[27,472 * 0.5]*	13,736	Smith pers. comm. 2023 and considering ASMFC 2022, Tucker 2019, Wilson and Morrison 2018
Total # of southbound birds expected to occur in the mid-Atlantic	NB migrants + YOY *[59,782 + 13,736]*	73,518	

Table 4. Numbers of rufa red knot mid-Atlantic crossings,* by month, for input to Band (2012), Annex 6

Month	# Crossings	Basis
January	0	
February	0	
March	0	
April	0	
May	59,782	100% of NB. (Any NB flights in April and June are attributed to May.)
June	1,470	2% of SB.
July	11,028	15% of SB.
August	29,407	40% of SB.
September	14,704	20% of SB.
October	11,028	15% of SB.
November	3,676	5% of SB.
December	2,206	3% of SB. (Any SB flights in January are attributed to December.)

*Annex C considers only two migratory flights per year (*i.e.*, one NB and one SB). Allocations of the NB and SB population totals across the months are based on consideration of Ebird 2023; Perkins 2023; and Barrett and Harkness 2023.

REFERENCES

Literature Cited

Adams EM, Gilbert A, Loring P, Williams, KA (Biodiversity Research Institute, Portland, ME and U.S. Fish and Wildlife Service, Charlestown, RI). 2022. Transparent Modeling of Collision Risk for Three Federally_-Listed Bird Species in Relation to Offshore Wind Energy Development: Final Report. Washington, DC: U.S. Department of the Interior, Bureau of Ocean Energy Management. Contract No.: M19PG00023. https://briloon.shinyapps.io/SCRAM/_w_76fb2514/SCRAM_manual_v103_031723.pdf [Accessed September 28, 2023]

Atlantic States Marine Fisheries Commission [ASMFC]. 2022. Revision to the Framework for Adaptive Management of Horseshoe Crab Harvest in the Delaware Bay Inclusive of Red Knot Conservation. Accepted for Management Use by the Horseshoe Crab Management Board January 26, 2022. Arlington, Virginia. 230 pp. http://www.asmfc.org/uploads/file/63d41dc32021ARM_FrameworkRevisionAndPeerReviewReport_Jan2022.pdf [Accessed April 6, 2023]

Band, B. 2012. Using a Collision Risk Model to Assess Bird Collision Risks for Offshore Wind Farms. Report by British Trust for Ornithology for The Crown Estate. Thetford, Norfolk, United Kingdom. 62 pp. https://tethys.pnnl.gov/publications/using-collision-risk-model-assess-bird-collision-risks-offshore-wind-farms [Accessed April 8, 2023]

Barrett, A. and J. Harkness. 2023. Shorebird Report: 2023 Summer/Fall Season Edwin B. Forsythe National Wildlife Refuge. U.S. Fish and Wildlife Service, Oceanville, New Jersey. 25 pp.

Burger, J, LJ Niles, RR Porter, AD Dey, S Koch, C Gordon. 2012. Using a shore bird (red knot) fitted with geolocators to evaluate a conceptual risk model focusing on offshore wind. Renewable Energy 43(2012):370-377.

Castellino, M. 2023. Results of the Red Knot (subspecies rufa) Surveys from Winter 2022: Census of Key Sites in South America. Western Hemisphere Shorebird Reserve Network. https://whsrn.org/red-knot-survey-2022/ [Accessed October 24, 2023]

eBird 2023. Basic Dataset. Version: EBD_relFeb-2023. Cornell Lab of Ornithology, Ithaca, New York. February 2023. https://ebird.org/ [Accessed April 4, 2023]

Loring PH, McLaren JD, Smith PA, Niles LJ, Koch SL, Goyert HF, and Bai H. 2018. Tracking movements of threatened migratory rufa Red Knots in U.S. Atlantic Outer Continental Shelf Waters. Sterling (VA): US Department of the Interior, Bureau of Ocean Energy Management. OCS Study BOEM 2018-046. 145 pp. https://espis.boem.gov/Final%20Reports/BOEM_2018-046.pdf [Accessed April 6, 2023]

Lyons, J.E., B. Winn, T. Teyes, and K.S. Kalasz. 2017. Post-Breeding Migration and Connectivity of Red Knots in the Western Atlantic. The Journal of Wildlife Management 82(Supplement 1):1-14.

Martínez-Curci, NS, JP Isacch, VL D'Amico, P Rojas, and GS Castresana. To migrate or not: drivers of over-summering in a long-distance migratory shorebird. Journal of Avian Biology. doi: 10.1111/jav.02401

Matus, R. 2021. Results of the 2021 Aerial Census at Bahía Lomas, Chile. Centro de Rehabilitación de Aves Leñadura. Guest author for the Western Hemisphere Shorebird Reserve Network. https://whsrn.org/results-of-the-2021-aerial-census-at-bahia-lomas-chile/ [Accessed April 6, 2023]

Mizrahi, D.S. 2020. Aerial Surveys for Shorebirds Wintering along Northern South America's Atlantic Coast with an emphasis on Semipalmated Sandpipers and Red Knots – Phase 2. Report to National Fish and Wildlife Foundation, Project # 59145. New Jersey Audubon Society, Cape May Court House, New Jersey. 26 pp.

Newstead, D.J., L.J. Niles, R.R. Porter, A.D. Dey, J. Burger, and O.N. Fitzsimmons. 2013. Geolocation reveals mid-continent migratory routes and Texas wintering areas of red knots Calidris canutus rufa. Wader Study Group Bulletin 120(1):53-59.

Niles, L.J., H.P. Sitters, A.D. Dey, P.W. Atkinson, A.J. Baker, K.A. Bennett, R. Carmona, K.E. Clark, N.A. Clark, C. Espoz, P.M. González, B.A. Harrington, D.E. Hernández, K.S. Kalasz, R.G. Lathrop, R.N. Matus, C.D.T. Minton, R.I.G. Morrison, M.K. Peck, W. Pitts, R.A. Robinson, and I. Serrano. 2008. Status of the red knot (*Calidris canutus rufa*) in the Western Hemisphere. Studies in Avian Biology 36:1-185.

Norambuena, HV, R Matus, A Larrea, and C Espoz. 2022. Censos aéreos de aves playeras en el santuario de la naturaleza Bahía Lomas, Enero 2022. Centro Bahía Lomas, Universidad Santo Tomás, Punta Arenas, Región de Magallanes, Chile. 20 pp.

Norambuena, HV, R Matus, A Larrea, and C Espoz. 2023. Censos aéreos de aves playeras en el santuario de la naturaleza Bahía Lomas, Enero 2023. Centro Bahía Lomas, Universidad Santo Tomás, Punta Arenas, Región de Magallanes, Chile. 16 pp.

Perkins, G. 2023. Geolocator Project Coordinator: Using geolocator tracking data to advance understanding of Red Knot migration habits. EC Contract No: 3000738325. Prepared For: Environment and Climate Change Canada, and the United States Fish and Wildlife Service by Ninox Consulting Ltd., Smithers, British Columbia, Canda. 36 pp. + Appendices.

Schwarzer, A.C. 2011. Demographic rates and energetics of red knots wintering in Florida. University of Florida, Gainesville, Florida, USA.

Tucker, AM. 2019. Stopover ecology and population dynamics of migratory shorebirds. A dissertation submitted to the Graduate Faculty of Auburn University in partial fulfillment of the requirements for the Degree of Doctor of Philosophy. 185 pp.

U.S. Fish and Wildlife Service [USFWS]. 2014. Rufa red knot background information and threats assessment. Supplement to Endangered and Threatened Wildlife and Plants; Final Threatened Status for the Rufa Red Knot (*Calidris canutus rufa*) [Docket No. FWS–R5–ES–2013–0097; RIN AY17]. Pleasantville, New Jersey. 376 pp. + Appendices. https://www.regulations.gov/document/FWS-R5-ES-2013-0097-0703 [Accessed April 6, 2023]

U.S. Fish and Wildlife Service. 2020. Species status assessment report for the rufa red knot (*Calidris canutus rufa*). Version 1.1. Ecological Services New Jersey Field Office, Galloway, New Jersey. https://ecos.fws.gov/ServCat/DownloadFile/187781 [Accessed April 6, 2023]

U.S. Fish and Wildlife Service [USFWS]. 2021. Rufa Red Knot (*Calidris canutus rufa*) 5-Year Review: Summary and Evaluation. U.S. Fish and Wildlife Service, New Jersey Field Office, Galloway, New Jersey. 35 pp. https://ecos.fws.gov/docs/tess/species_nonpublish/3624.pdf [Accessed April 5, 2023]

U.S. Fish and Wildlife Service. 2023. Draft Biological Opinion on the Effects of the Atlantic Shores Offshore Wind South Energy Projects, Offshore Atlantic City, New Jersey on Three Federally Listed Species. New Jersey Field Office, Galloway, New Jersey. 83 pp.

Wilson, S. and R.I.G. Morrison. October 2018. Appendix 1. Proportions of juvenile, sub-adult and adult birds in populations of Red Knot. Unpublished data. Committee on the Status of Endangered Wildlife in Canada, Ottawa, Canada. 2 pp.

Personal Communications

Castellino, M. and P. González. Emails of June 9 and 13, 2023. Western Hemisphere Shorebird Reserve Network Executive Office Manomet, Massachusetts and Fundación Inalafquen, Argentina.

Cook, A. 2023. Principal Ecologist – Offshore Renewable Energy. Email of June 6, 2023. British Trust for Ornithology, Thetford, Norfolk, United Kingdom.

Hunter, C. 2022. Regional Refuge Biologist. Email of July 6, 2022.U.S. Fish and Wildlife Service, National wildlife Refuge System, Division of Strategic Resource Management, Atlanta, Georgia.

Newstead, D. 2020. Manager, Coastal Waterbird Program. Emails of March 6 and June 3, 2020. Coastal Bend Bays and Estuaries Program. Corpus Christi, Texas.

Newstead, D. 2019. Manager, Coastal Waterbird Program. Email of October 3, 2019. Coastal Bend Bays and Estuaries Program. Corpus Christi, Texas.

Sanders, F. 2023. Coastal Bird Conservation Project Supervisor. Email of August 9, 2023. South Carolina Department of Natural Resources, McClellanville, South Carolina.

Smith, P. 2023. Research Scientist. Email of October 16, 2023. Wildlife Research Division, Environment and Climate Change Canada, Ottawa, Ontario, Canada.

Appendix D. Templates for Wind Farm Data and Operations Data

Wind farm data and operations data should be provided by developers in the Constructions and Operations Plan for each proposed wind energy project (Tables D1-D2). Additional details may be found in the case studies sections of Adams et al. (2022) and in the "Wind Turbine Input Data" section of this report.

Table D-1. Wind farm data needed to run SCRAM.

In the case of a project design envelope, parameters for each turbine model under consideration should be provided in each Run column (e.g., Run 1, Run 2, add columns as needed).

Parameter	Parameter definitions	Run 1	Run 2
Num_Turbines	The number of installed turbines	-	-
TurbineModel_MW	The turbine model option or MW rating of the turbine. In SCRAM, this is purely for labeling purposes only and does not affect the results.	-	-
Num_Blades	The number of installed blades on each turbine	-	-
RotorRadius_m	The radius (meters) of the rotor from blade tip to middle of the rotor nacelle (axis of rotation)	-	-
RotorRadiusSD_m	The standard deviation of the rotor radius (meters). We recommend setting this value to 0.	-	-
HubHeightAdd_m	The distance between mean sea level at the wind farm centroid and the lower blade tip (meters), also referred to as the air gap. From this value the hub height is calculated and presented in the output. Note: the air gap at highest astronomical tide (HAT) can be provided as an alternative to mean sea level, but depending on the degree of tidal variation at the wind farm location, this may lead to overestimates of collision risk.	-	-
HubHeightAddSD_m	The standard deviation of the air gap (meters). We recommend setting this value to 0.	-	-
BladeWidth_m	The max. turbine blade width (meters).	-	-
BladeWidthSD_m	The standard deviation of the turbine blade width (meters). We recommend setting this value to 0.	-	-
RotorSpeed_rpm	The average annual number of turbine rotations per minute when turbine is active. Non-operational time (due to maintenance downtime and low wind speeds) is accounted for elsewhere in the model	-	-
RotorSpeedSD_rpm	The standard deviation of turbine rotations per minute. We recommend setting this value to 0 unless data can be obtained on the variation in RPMs due to wind speed or other environmental conditions.	-	-
Pitch	The average angle of the blade (degrees) relative to the rotational plane of the blades while the turbine is spinning.	-	-
PitchSD	The standard deviation in pitch (degrees).	-	-
WFWidth_km	Wind farm width (km). If the wind farm is not square, use (length + width)/2 of the wind farm or total perimeter length/4 if an irregular shape.	-	-
Latitude	Latitude (decimal degrees) of wind farm centroid	-	-
Longitude	Longitude (decimal degrees) of wind farm centroid	-	-

Table D-2. Wind farm operations data needed to run SCRAM.

Op = Wind availability, the maximum amount of time turbines can be operational/month depending on wind speeds and cut-in and cut-out speeds of the turbine. OpMean = Mean time that turbines will not be operational ("down time"), assumed to be independent of "MonthOp" – i.e., total operation = MonthOp*(1 – MonthOpMean). OpSD = standard deviation of mean operational time.

Month	Op	OpMean	OpSD
Jan	-	-	-
Feb	-	-	-
Mar	-	-	-
Apr	-	-	-
May	-	-	-
Jun	-	-	-
Jul	-	-	-
Aug	-	-	-
Sep	-	-	-
Oct	-	-	-
Nov	-	-	-
Dec	-	-	-

Appendix E. Motus-Only and Satellite-Only Maps of Red Knot Use

We used the ensemble of Motus and satellite based movement models for red knots to estimate cumulative use (i.e., cumulative daily occupancy probability) in the SCRAM 2 collision risk models (see main text). Estimates of cumulative use from the Motus and satellite based movement models (i.e., prior to combining them in the ensemble) are presented here (Figures E-1 and E-2). Ensemble maps are presented in the main text, though the ensemble map of mean cumulative use (Figure 5) is reproduced here for comparison to Motus- and satellite-based estimates (Figure E-1).

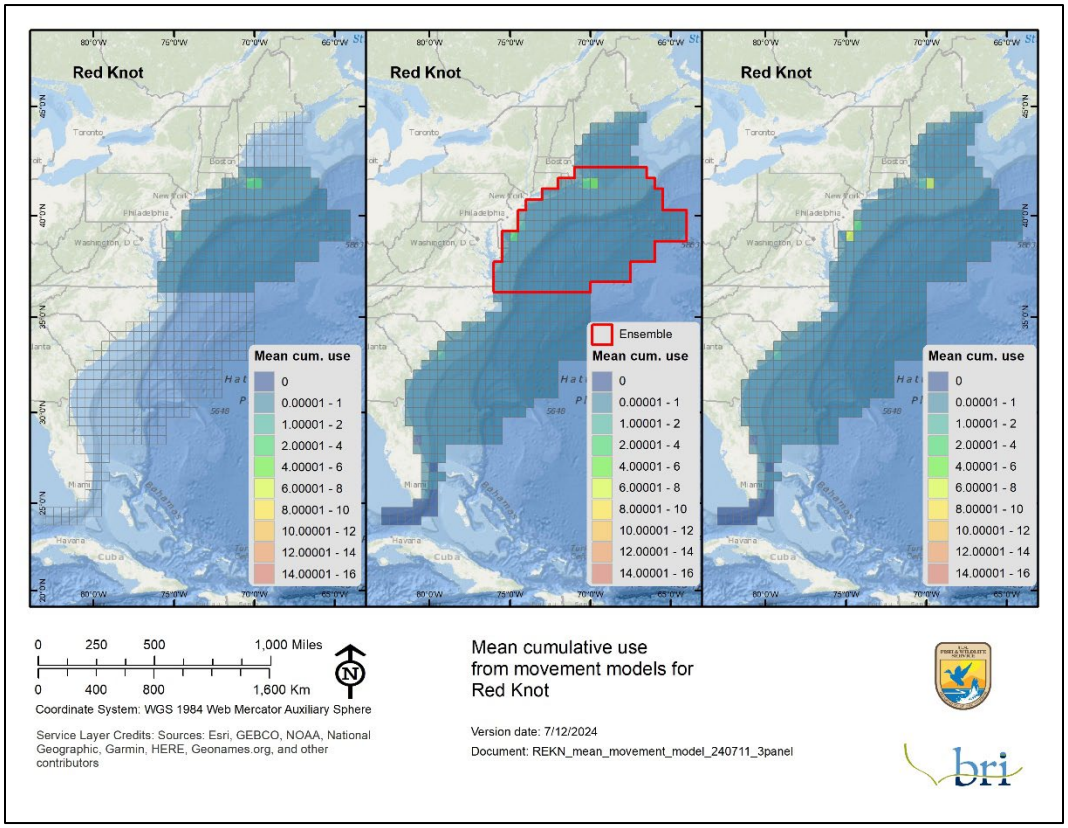

Figure E-1. Cumulative use estimates from movement models for Motus- and satellite-tracked red knots, averaged across months.
Estimates were based on single-state movement models using Motus (left panel) and satellite-based data (right panel), and the number of tagged individuals in the study. The results of movement models from Motus and satellite-based data for red knots were combined in an ensemble model within the red study area (center panel); estimates outside the red study area were modeled from satellite-based data only. “Cumulative use” summed daily occupancy probabilities estimated via SCRAM for each month then averaged these values across all months with greater than five tracked individuals for a given species. Scale bars align with monthly estimates for red knots (Figure E-2 and Figure E-3).

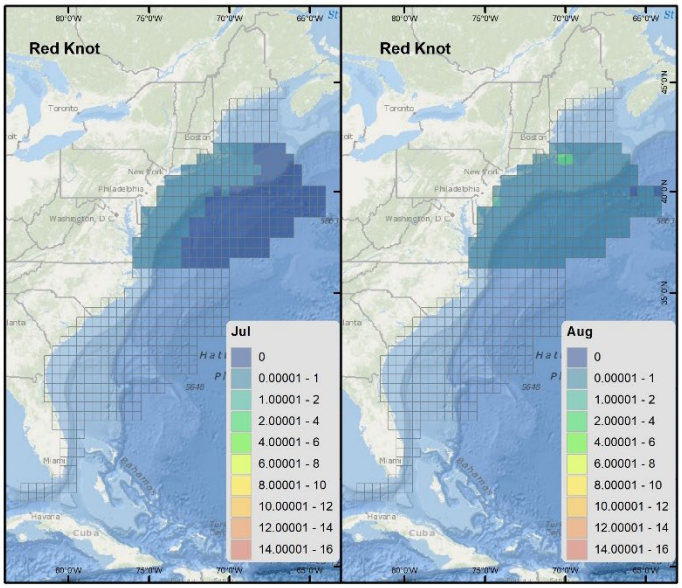

0 250 500 1,000 Miles

0 400 800 1,600 Km

Coordinate System: WGS 1984 Web Mercator Auxiliary Sphere

Service Layer Credits: Sources: Esri, GEBCO, NOAA, National Geographic, Garmin, HERE, Geonames.org, and other contributors

Monthly cumulative use from Motus movement models for Red Knot

Version date: 7/12/2024

Document: REKN_monthly_Motus_model_240711_2panel

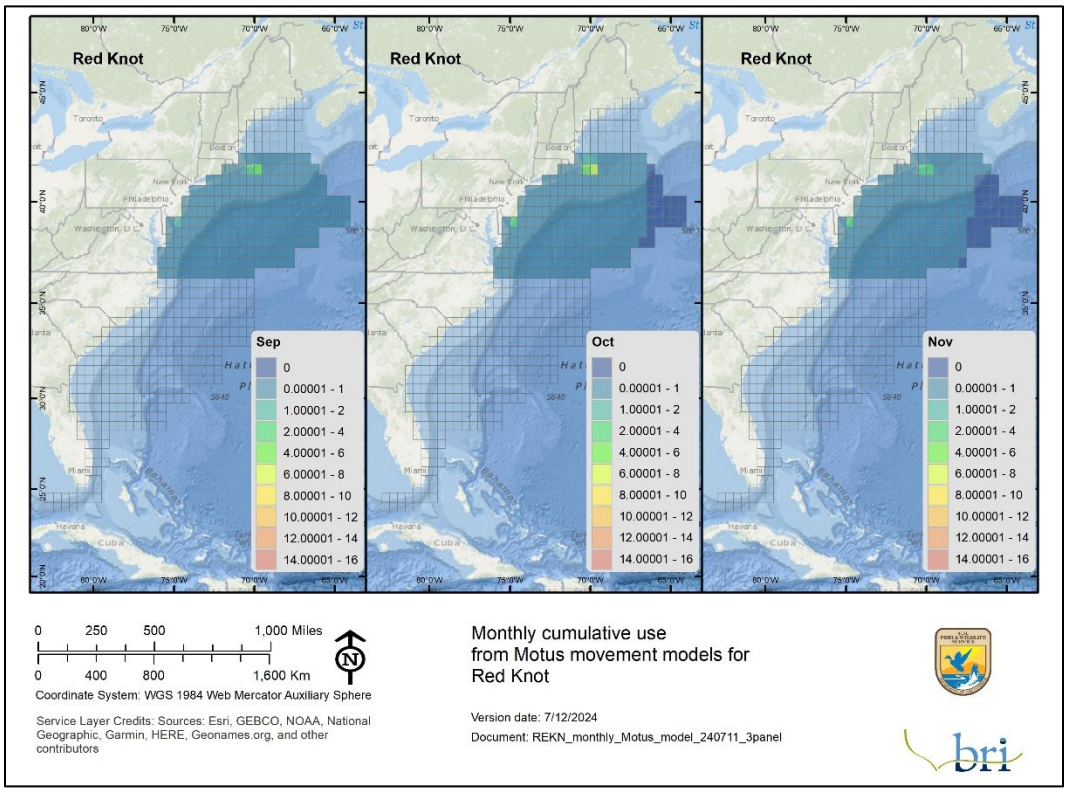

Figure E-2. Cumulative use estimates by month from the Motus movement models for red knots. Estimates were based on single-state movement models using Motus data, and the number of tagged individuals in the study. “Cumulative use” summed daily occupancy probabilities estimated via SCRAM for each month with greater than five tracked individuals for a given species. Estimates covered July–August (top panel) and September–November (bottom panel) (see Table 7 for monthly sample sizes).

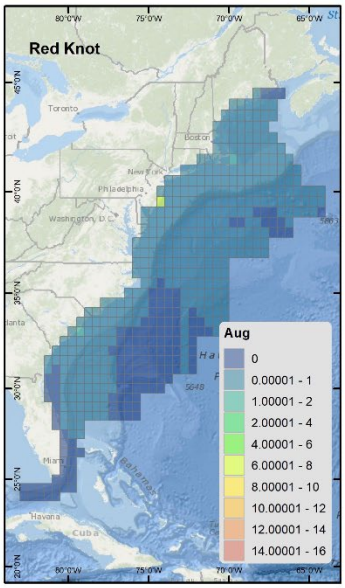

0 250 500 1,000 Miles

0 400 800 1,600 Km

Coordinate System: WGS 1984 Web Mercator Auxiliary Sphere

Service Layer Credits: Sources: Esri, GEBCO, NOAA, National Geographic, Garmin, HERE, Geonames.org, and other contributors

Monthly cumulative use
from movement models for satellite-tracked
Red Knot

Version date: 7/11/2024

Document: REKN_mean_monthly_satellite_model_240711_1panel

bri

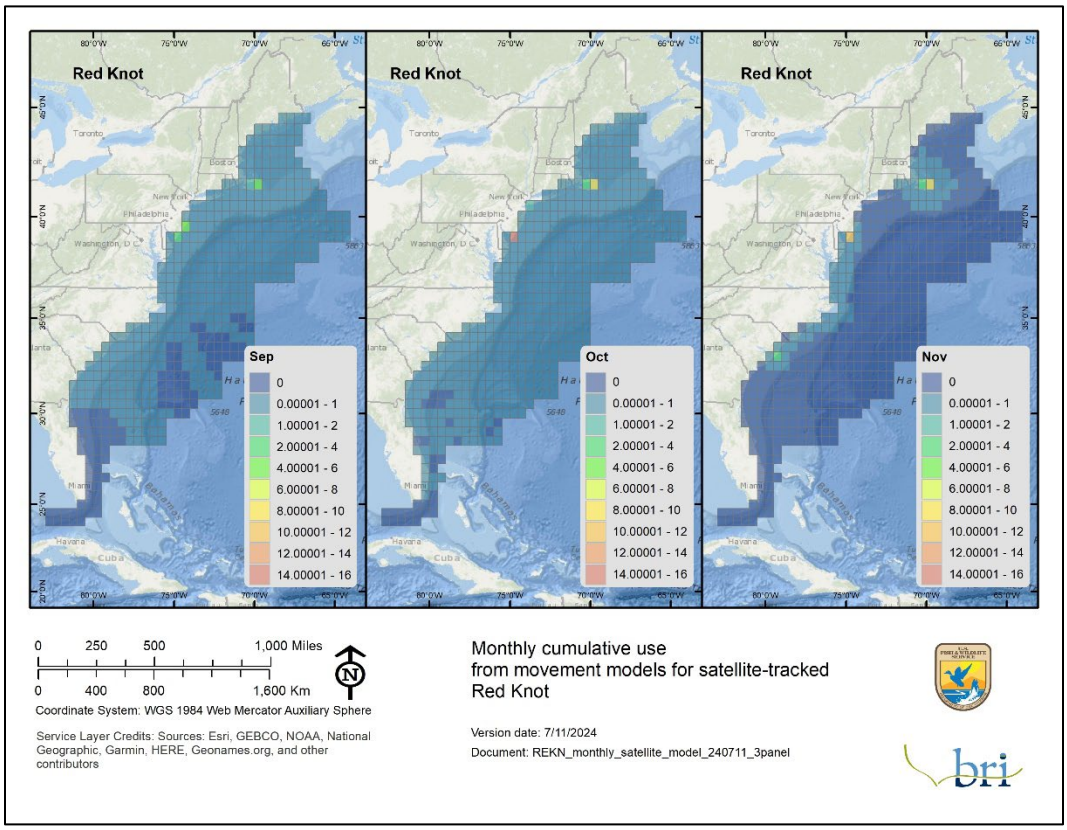

Figure E-3. Cumulative use estimates from the movement models for satellite-tracked Red Knots. Estimates were based on single-state movement models using satellite-based data, and the number of tagged individuals in the study. “Cumulative use” summed daily occupancy probabilities estimated via SCRAM for each month with greater than five tracked individuals for the given species. Estimates covered August (top panel) and September–November (bottom panel) (see Table 7 for monthly sample sizes).

Appendix F. Octile Maps of Cumulative Daily Occupancy

Figures in the main text used a standardized scale for each species, to enable comparison of relative use among grid cells and months. Maps included in the Adams et al. (2022) report, as well as in the SCRAM web application, used octiles to visualize the data instead; in this case, each color represented 12.5% of the range in values for that species. This display choice enabled the visual identification of subtle changes in patterns of relative use among grid cells within a given time period, but did not allow for comparison of relative use among months. We included octile maps here (Figure F-1) as another way of visualizing the same cumulative daily occupancy data, and for comparison with Adams et al. (2022).

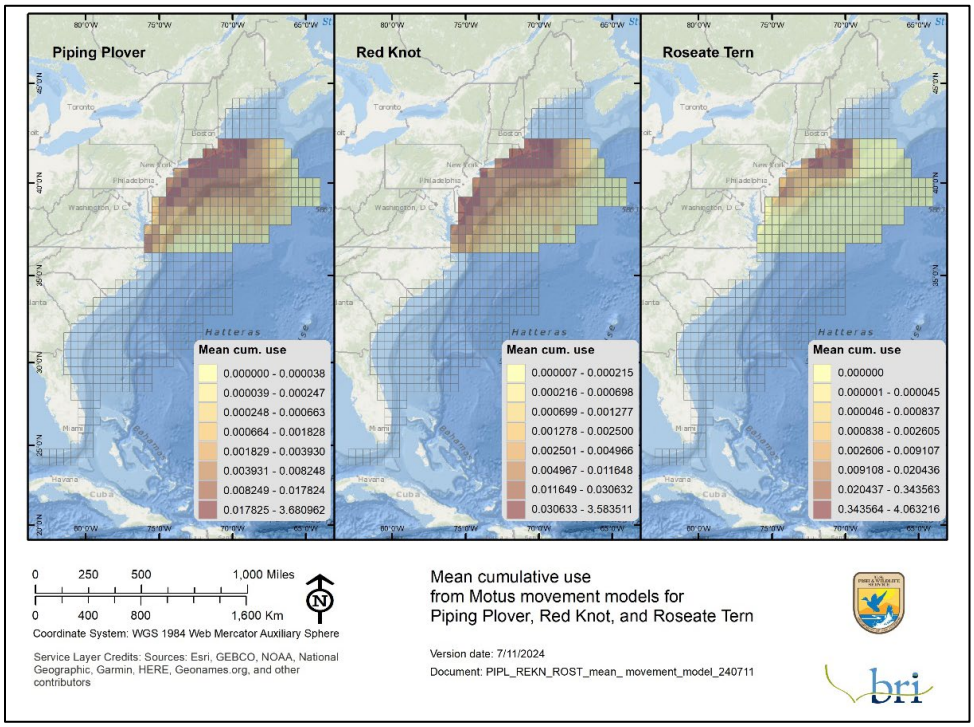

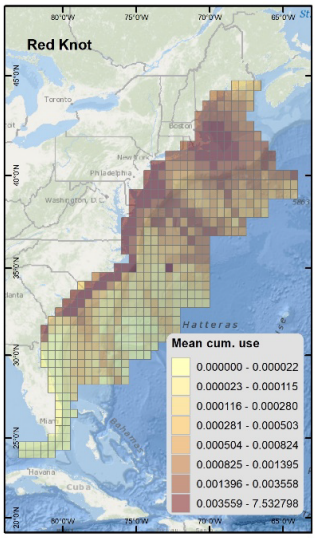

0 250 500 1,000 Miles

0 400 800 1,600 Km

Coordinate System: WGS 1984 Web Mercator Auxiliary Sphere

Service Layer Credits: Sources: Esri, GEBCO, NOAA, National Geographic, Garmin, HERE, Geonames.org, and other contributors

Mean cumulative use
from movement models for satellite-tracked
Red Knot

Version date: 7/11/2024

Document: REKN_mean_monthly_satellite_model_240711_1panel

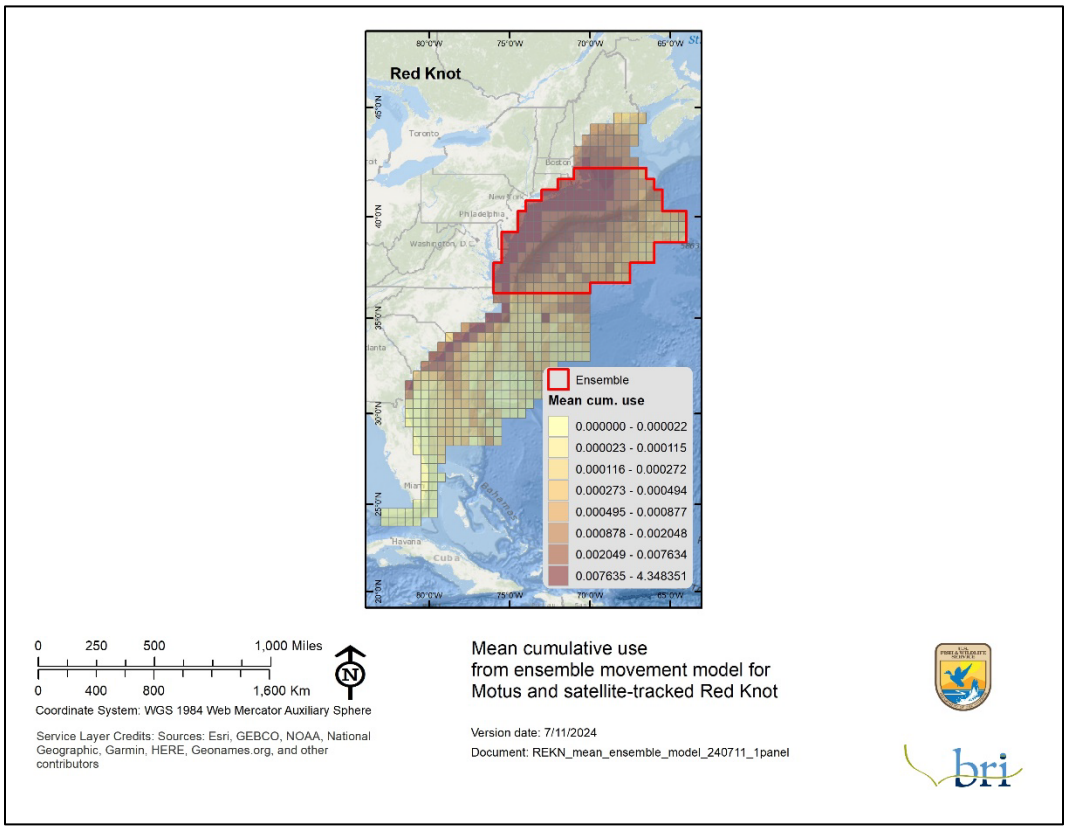

Figure F-1. Mean cumulative use estimates averaged across months using Motus and satellite-tracked data.
Movement model results are presented for Motus movement data (top panel; piping plovers at left, red knots middle, roseate terns at right); satellite-tracking data (middle panel; red knots); and the ensemble model that includes both motus and satellite-tracking data (bottom panel; red knots).

U.S. Department of the Interior (DOI)
DOI protects and manages the Nation's natural resources and cultural heritage; provides scientific and other information about those resources; and honors the Nation's trust responsibilities or special commitments to American Indians, Alaska Natives, and affiliated island communities.

Bureau of Ocean Energy Management (BOEM)
BOEM's mission is to manage development of U.S. Outer Continental Shelf energy and mineral resources in an environmentally and economically responsible way.

BOEM Environmental Studies Program
The mission of the Environmental Studies Program is to provide the information needed to predict, assess, and manage impacts from offshore energy and marine mineral exploration, development, and production activities on human, marine, and coastal environments. The proposal, selection, research, review, collaboration, production, and dissemination of each of BOEM's Environmental Studies follows the DOI Code of Scientific and Scholarly Conduct, in support of a culture of scientific and professional integrity, as set out in the DOI Departmental Manual (305 DM 3).